APPLICATION OF ROBUSTNESS ANALYSIS TO LARGE GEODETIC NETWORKS

P. VANICEK
P. ONG
E. J. KRAKIWSKY
M. R. CRAYMER

March 1996

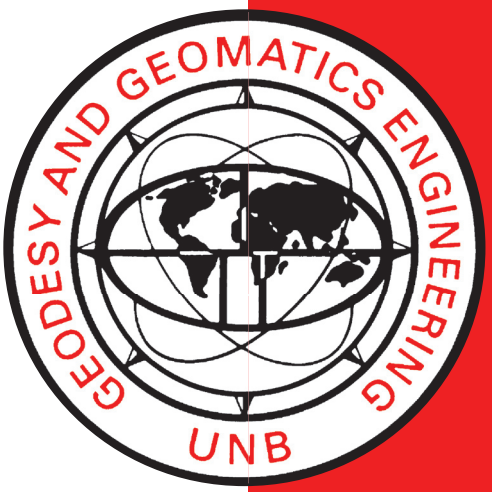

TECHNICAL REPORT
NO. 180

PREFACE

In order to make our extensive series of technical reports more readily available, we have scanned the old master copies and produced electronic versions in Portable Document Format. The quality of the images varies depending on the quality of the originals. The images have not been converted to searchable text.

APPLICATION OF ROBUSTNESS ANALYSIS TO LARGE GEODETIC NETWORKS

Petr Vaníček, Peng Ong
Department of Geodesy and Geomatics Engineering
University of New Brunswick

Edward J. Krakiwsky
Department of Geomatics Engineering
The University of Calgary

Michael R. Craymer
Geodetic Survey Division
Geomatics Canada

Department of Geodesy and Geomatics Engineering
University of New Brunswick
P.O. Box 4400
Fredericton, N.B.
Canada
E3B 5A3

March 1996

Preface

This technical report is a reproduction of a final contract report prepared for the Geodetic Survey Division, Geomatics Canada, by Petr Vaníček[1], Peng Ong[1], Edward J. Krakiwsky[2], and Michael R. Craymer[3], and submitted on 8 February 1996.

As with any copyrighted material, permission to reprint or quote extensively from this report must be received from the authors. The citation to this work should appear as follows:

Vaníček, P., P. Ong, E.J. Krakiwsky, and M.R. Craymer (1996). *Application of Robustness Analysis to Large Geodetic Networks.* Final contract report for the Geodetic Survey Division of Geomatics Canada, Department of Geodesy and Geomatics Engineering Technical Report No. 180, University of New Brunswick, Fredericton, New Brunswick, Canada, 75 pp.

1 Department of Geodesy and Geomatics Engineering, University of New Brunswick, P.O. Box 4400, Fredericton, N.B., Canada E3B 5A3

2 Department of Geomatics Engineering, The University of Calgary, 2500 University Drive N.W., Calgary, Alberta, Canada T2N 1N4

3 Geodetic Survey Division, Geomatics Canada, 615 Booth Street, Ottawa, Ontario, Canada K1A 0E9

EXECUTIVE SUMMARY

In this report we have addressed three more or less independent problems in robustness analysis: finding a more economical algorithm for searching for the most influential observations (chapter 2), finding a more satisfactory definition of the neighborhood in which strain measures are evaluated (chapter 3) and finding a technique for network classification that would take into account both the precision (random error contribution) and accuracy (potential systematic error or bias contribution) in point positions. These are discussed separately below.

Search for the Most Influential Observation

Application of robustness analysis to large geodetic networks requires a modification of the original method of determining robustness. When searching for the potential observation bias that most influences a point, the coordinate biases at all points in the network were being computed for every potential observation bias. This involves too much computational effort which is usually unnecessary. The same criticism also applies to the conventional method of reliability analysis if such is to be considered.

To overcome this problem, we have proposed two methods of limiting the search for the most influential observation biases. The recommended method is based on limiting the search to only those observations between points which are within 3 connection levels of the point of interest. This method consistently provides the most reliable and efficient results and is recommended for universal use. One can expect about an order of magnitude saving in computational effort for a 100 point network resulting from this limited search algorithm. Moreover, the computational saving increases as the size of the network increases. Similar increases can also be expected for reliability analysis.

A problem with limiting the search for potential observation biases in any way is that it is no longer possible to remove the block rotation of the entire network from the estimates of the differential rotations. For each observation bias a different block rotation of network is produced and must be removed. In the original algorithm, each block rotation is approximated by the average of the differential rotations at all points in the network. When we are not computing differential rotations at all points it is no longer possible to estimate the block rotations and the individual differential rotations become datum dependent.

Strain Neighbourhood Definition

The other problem we have addressed is the one arising from dealing with long observation ties, such as long GPS and VLBI baselines. Using points linked with the point of interest by such long ties in the neighbourhood needed to compute strain tends to adversely affect the estimates of robustness. The problem is that strain, by definition, represents a differential quantity. Using long ties tends to smooth (average) out the robustness across the network. What is required for the strain computation in robustness is a more local definition of the neighbourhood in order to properly describe the differential behaviour. To attenuate the effect of these long ties, alternate methods of defining the local neighbourhood for the strain computation have been suggested.

The method investigated in depth in this contract is that based on Delaunay triangulation. This method was chosen mainly because of its popularity for defining spatial adjacency in a wide variety of GIS and cartographic applications. The local Delaunay neighbourhood for a point is defined by those points which are directly connected to it by the sides of the Delaunay triangles (Delaunay ties). However, the method still has a difficulty dealing with points on the border of the network and with gaps in the distribution of points within the network. The first problem is that Delaunay

triangulation always forms a convex boundary around the network which often results in very long ties when the actual periphery of the network is not convex. The second problem frequently arises when the network is of a looping or traversing design. This again results in some long ties across the gaps in the network. To avoid this situation, we simply omit the long ties manually.

As a result of these problems, comparisons between results based on strain neighbourhood defined in terms of observation ties and Delaunay ties do not show good agreement. There were still large disagreements even when the long Delaunay ties on the network periphery were omitted. These were mainly due to the relatively long ties across the gaps within the network. Consequently, we do not recommend using the Delaunay method by itself.

As an alternative approach we recommend instead to investigate the use of an inverse distance weighting scheme, which is also popular in contouring applications. This could be used together with any of the methods for defining the local strain neighbourhood, including those based on observation ties, Delaunay ties or n closest points. A number of different weighting functions should be investigated and implemented in the NETAN software for all of the neighbourhood options. This would reduce most of the differences we presently see between the results caused by the different neighbourhood definitions.

Criteria for the Classification of Robustness

Traditionally, networks have been classified using only the size of the confidence regions. However, the confidence regions only provide a measure of precision and cannot be used to determine whether also a specified accuracy has been met, as often assumed by the user.

To properly characterize the total possible error in the estimated positions, it is necessary to provide a measure of both precision and accuracy. For classification purposes, single number absolute and relative measures are needed for both precision and accuracy. Although absolute measures of both precision and accuracy are inherently dependent on the choice of datum constraints, the relative measures may or may not be. Datum independent relative measures—such as relative confidence regions and robustness measures—should be used whenever possible to facilitate the objective comparison and classification of networks.

The classification of precision and accuracy measures can also be treated either separately for each point (out-of-context of the others) or simultaneously as a group (in-context). The later requires the use of a modified significance level as described in Krakiwsky et al. (1994).

For consistency and simplicity similar kinds of measures should be used to characterize precision and accuracy. For accuracy, the largest absolute and relative measures should be chosen at each point from among all those induced by all the potential observation biases (i.e., the worst case estimate of the average bias). Testing of the suggested measures with simulated and real data is needed in order to recommend which is the most appropriate for classification purposes.

Finally, precision and accuracy should ideally be characterized in a joint manner. One possible method of representing the total possible error in an estimated position is to vectorially combine the semi-axes of the confidence region with the coordinate bias vector for each potential observation bias. The largest such vector at each point would represent the worst average absolute and relative error. This idea should be further investigated and thoroughly tested.

CONTENTS

1. INTRODUCTION

1.1 Background

The collaboration between the Geodetic Survey of Canada and the Universities of New Brunswick and Calgary resulted in the development of "robustness analysis", a new technique for the assessment of the accuracy of geodetic networks (see Vaníček et al., 1990 and Krakiwsky et al., 1993). Traditional confidence regions only provide an assessment of the effect of random errors (precision) of the network. Robustness analysis complements this by providing a complete assessment of the effect of possible systematic biases (accuracy) that may escape the usual statistical tests for outliers.

Robustness is defined as the ability of the network to resist deformations induced by undetected blunders, or biases, as determined from "internal reliability analysis". The "geometrical strength analysis" technique is used instead of "external reliability" in order to provide a more meaningful description of the network strength. This also makes robustness invariant with respect to datum selection. Robustness is expressed in terms of three independent deformation parameters at each point; namely, robustness in scale, robustness in shear (local change in shape) and robustness in rotation (twisting). It should be emphasized that the full description of a deformation induced by blunders cannot be achieved with fewer than three independent parameters.

Our experience with robustness analysis has shown that it is a very powerful technique capable of providing a detailed point-by-point assessment of the strength of a network in terms of its ability to resist the negative effect of biases. Nevertheless, a few problems remained, which limit the application of robustness analysis in practice. The objective of the research described here has been to address the two remaining problems we had been aware of.

The first problem with the robustness analysis has been its heavy computational requirements, which rendered it unsuitable for application to larger networks of more than about 100 points. This was due primarily to the use of internal reliability which examines the effect of each observation's undetectable bias on each and every point in the network, even if the point is at the opposite end of a very long network. Yet we knew from theoretical considerations, as well as from experience, that the effect is limited to a fairly small neighbourhood of the observation. The same problem also applies to external reliability and our solutions here apply equally well there.

The other significant problem encountered during the last robustness contract, was the effect of long observational ties that span relatively large parts of the network. Such cases are typical of GPS surveys. These long ties have an unwarranted smoothing effect on the overall plot of robustness parameters. This smoothing is not only unwarranted, it is also wrong! Strain, as a mathematical technique for depicting deformations, is a differential technique, and thus local by its very nature.

A practical application of robustness analysis to larger geodetic networks required further development aimed at making the algorithm much faster. The main idea to have been investigated and numerically tested was to examine the effect of each observation bias on only those network points which are within a certain number of "connection levels". Points on the first connection level are those directly connected by the observation; points on the second connection level are those directly connected by observations to the points on the first connection level, etc. The number of connection levels required to adequately represent strain was to be investigated.

An alternative but similar idea is to limit the search for the most influential observation to points that highly correlated with those points directly connected by the observation. The correlations are determined from the covariance matrix of the adjusted coordinates. The required minimum correlation level that correctly represents the strain was investigated.

A correction of the problem of robustness parameter smoothing was to be sought among the ways of defining the "local strain neighbourhood" of each point of interest, comprising the points for which the robustness parameters are to be estimated. Various methods of defining the local neighbourhood were to be investigated in this context.

Finally, it was recommended by Vaníček et al. (1990) and Krakiwsky et al. (1993) that any new standards for geodetic networks should include not only an assessment of precision by means of confidence regions, but also an assessment of accuracy by means of robustness analysis. This report supports and complements the current development being conducted by the Geodetic Survey of Canada by recommending criteria for station classification from the robustness point of view.

1.2 Statement of work

The contract called for the following tasks to be performed:

1. Development and testing of more efficient algorithms for computing point robustness measures in large networks (e.g., of the order of 1000 or more points) and the selection and implementation (in the NETAN software) of the most appropriate one(s);

2. Development of technique(s) to handle long observational ties in the strain computation algorithm for quantifying local robustness measures;

3. Development of method(s) of station classification in terms of robustness for use in any new survey standards for geodetic networks.

1.3 Solution

We have noticed in previous work that observational errors that potentially affect points the most (i.e., the "most influential observations") are generally within a few connection levels of the affected points for several networks examined. This does not constitute a proof that this is always going to be the case; pathological situations could occur where observations further away will have the dominant effect. But it is not possible to produce an efficient technique completely impervious to all pathological cases. We found that searching only to the 3rd connection level was sufficient in the overwhelming majority of the cases we have dealt with and that it is much more computationally efficient than the original search among all observations.

We have also designed and tested an alternative approach to the search for the most "influential observations". In this approach, the potential influential observations are sought only among the observations connecting points which show a correlation with the point of interest that reaches a specified level (in absolute value). The correlations are obtained from the covariance matrix of the adjusted coordinates. The main problem with this approach is that the minimum correlation level required to give correct results varies greatly from network to network. The idea of using the covariance matrix has some merits however and should be further investigated, perhaps in terms of the entire projection matrix transforming the observations (and their biases) into the parameters, i.e., the adjusted coordinates.

It should be noted that both of these methods can be applied not only to robustness analysis, but also to the more traditional reliability analysis where one is interested in determining the maximum external reliability at each point (i.e., the quadratic forms of displacements at each point). The same general conclusions about the methods would apply there also.

The existing software, NETAN (Craymer et al., 1987), that analyses robustness, has been deployed mostly in the mode where the local neighbourhood of the point of interest (for the computation of point robustness parameters) is defined as comprising all the points tied to the point of interest by observations. It is in this mode, that the above described smoothing problem with long observation ties is encountered. Another method of defining the local 'strain neighbourhood' is available in NETAN: the neighbourhood around each point of interest can be defined as consisting of all the points within a specified radius. It was found, however, that this mode does not work very satisfactorily when analysing real networks, where we often encounter a widely varying point density (Craymer et al., 1987). In order to provide a more general method of handling long observation ties we have tested a new method of defining the local neighbourhood in terms of ties obtained from a Delaunay triangulation of the network points. Other methods are also recommended for further investigation, such as using the closest point in each quadrant, sextant or octant around the point of interest, or using an inverse-distance weighting scheme with any of these methods.

The 3rd item in the Statement of work in section 1.2 is understood to mean that the central issues and parameters related to using robustness analysis are to be identified, discussed, interpreted, and then assessed as to their appropriateness for inclusion into standards for geodetic networks. The pertinent issues to be addressed are the following: concepts of precision and accuracy, characterisation of precision (random error component), characterisation of accuracy (systematic error or bias component) and joint characterisation of precision and accuracy (total error).

The specified target accuracy is understood to consist of the total error (random and systematic) as opposed to just the random error, as is currently the practice. This means that the present practice of specifying only confidence ellipses (or ellipsoids) deals with only random errors and thus only relates to the precision of the results. This procedure neither defines the accuracy, nor guarantees the repeatability of a set of coordinate values for a station coordinates, or the coordinate differences between a pair of stations.

2. SEARCH FOR THE MOST INFLUENTIAL OBSERVATIONS

2.1 Background

In the original program NETAN, all the observations are considered when searching for the most influential one – the observation that causes the maximum deformation in the sense of one of the three robustness parameters – when the effect is being determined for each point in the network. In this contract we have added two new options that allow the user to limit this search to either (i) observations within a certain number of connection levels, or (ii) observations at points which are correlated with the point of interest beyond a prescribed limit.

The definition of a "connection level" is illustrated in Figure 2.1. Points that are directly connected by an observation are considered to be on the first connection level with respect to that observation. Points directly connected to the points on the first connection level are considered to be on the second connection level, and so on. To determine the required maximum connection level (and the minimum required correlation level), we have examined the connection levels for the most influential observations at each point in a variety of networks. Each of these will be discussed separately in the following sections.

For the correlation approach, we use the maximum of the correlations between the point of interest and the points connected by the observation being considered. The observation is included in the search for the most influential one at the point of interest if this maximum correlation exceeds some specified level. The maximum correlation, obtained from the covariance matrix of the adjusted coordinates, is defined as the largest, in an absolute sense, of all the correlations among the coordinate components between the two points. Thus we have to search among 18 correlations in the 3D case and among 8 correlations in the 2D case. For example, consider the problem of determining whether an observation connecting points #4 and #5 should be included in the search for the most influential observation at point #1 in 3 dimensions. Given the following covariances between points #1 and #4 and points #1 and #5,

$$\sigma_{x_1x_4} = -0.85\,, \quad \sigma_{x_1y_4} = 0.77, \quad \sigma_{x_1z_4} = -0.91\,,$$
$$\sigma_{y_1x_4} = 0.63\,, \quad \sigma_{y_1y_4} = 0.83, \quad \sigma_{y_1z_4} = 0.68\,,$$
$$\sigma_{z_1x_4} = 0.69\,, \quad \sigma_{z_1y_4} = -0.72, \quad \sigma_{z_1z_4} = 0.89\,,$$

$$\sigma_{x_1x_5} = -0.77\,, \quad \sigma_{x_1y_5} = 0.85, \quad \sigma_{x_1z_5} = -0.86\,,$$
$$\sigma_{y_1x_5} = 0.81\,, \quad \sigma_{y_1y_5} = 0.91, \quad \sigma_{y_1z_5} = 0.72\,,$$
$$\sigma_{z_1x_5} = 0.93\,, \quad \sigma_{z_1y_5} = -0.73, \quad \sigma_{z_1z_5} = 0.68\,,$$

the maximum correlation (in an absolute sense) between the point of interest (point #1) and the observation connecting points #4 and #5 is taken to be 0.93. The observation is then included in the search for the most influential observation for point #1 when this maximum correlation exceeds some prescribed limit.

In these tests, the differential rotations, representing robustness in twist, are not corrected by removing the mean network-wide value, representing the spurious implied rotation of the entire network, for each observation bias (see Krakiwsky et al., 1993). This is because the average value cannot be determined when dealing with only a subset of all observations (limiting the propagation of observation biases to a reduced search area). The new twist values will therefore not be datum dependent. For some networks, using this datum dependent twist parameter results

in the identification of "most influential observation" at some points, which are different form the original ones.

For all of the tests the same Type I and Type II error levels have been used, resulting in a noncentrality parameter of λ=3.61 (see Krakiwsky et al., 1993) being used for all networks. Robustness values for other noncentrality parameters can be easily found by simply rescaling them by λ_{new} / 3.61, where λ_{new} is the new noncentrality parameter.

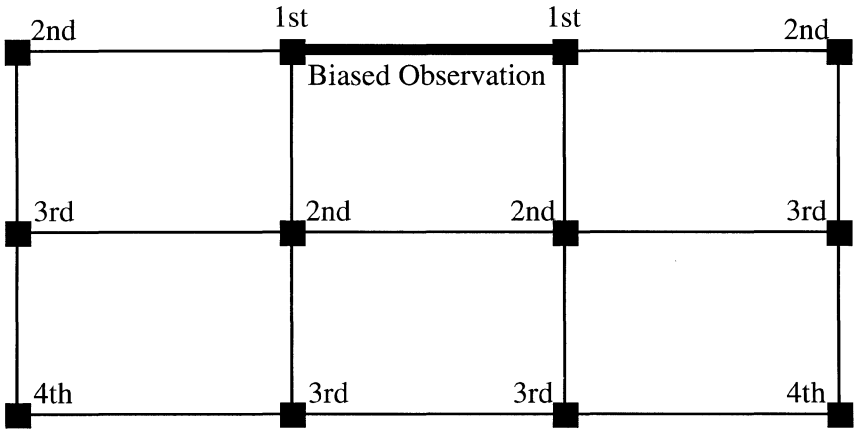

FIGURE 2.1: Connection levels relative to potentially biased observation for a grid-type network.

2.2 HOACS2D Network

The HOACS2D network, shown in Figure 2.2, is a simulated example of a standard terrestrial chain-type network consisting of 11 points with 38 direction, 19 distance and 1 azimuth (constraint) observations. The total degrees of freedom of the adjustment is 27.

The correct robustness measures, computed using the network-wide search for the most influential observations, are given in Table 2.1 and in Figure 2.3. In Table 2.2, the most influential observation producing the maximum robustness measures in twist, shear and scale at each point is given together with the number of connections from the point of interest. The largest (absolute value) correlation between each point of interest and the points associated with the most influential observation, is also shown in Table 2.2. Histograms of the distribution of the connection and correlation levels for all the most influential observations are given in Figures 2.4 and 2.5, respectively.

From Table 2.2 and Figure 2.4 we see that it is necessary to search up to the third connection (for robustness in twist) in order to capture all the "most influential observations". When limiting the search to the 3rd connection level, we find that for all of the points in the network it is required to search a total of 515 observations, as compared to 638 when searching the entire network; a reduction of 20%. We note that the percentage of reduction increases with the size of the network; the relatively modest saving of 20% encountered here is due to the small size of the network and would not be very interesting in practice.

For the correlation method, we see from Table 2.2 and Figure 2.5 that it is necessary to search observations that have a correlation level with respect to the point of interest of at least 90% (again for robustness in twist at point #2). We note that when the most influential observation is directly connected to the point of interest – first connection level – the correlation is identified as equal to 1. When limiting the search to the 90% and higher correlation level, it is required to search a total of 438 observations for all of the observations, which results in computational saving of 31%.

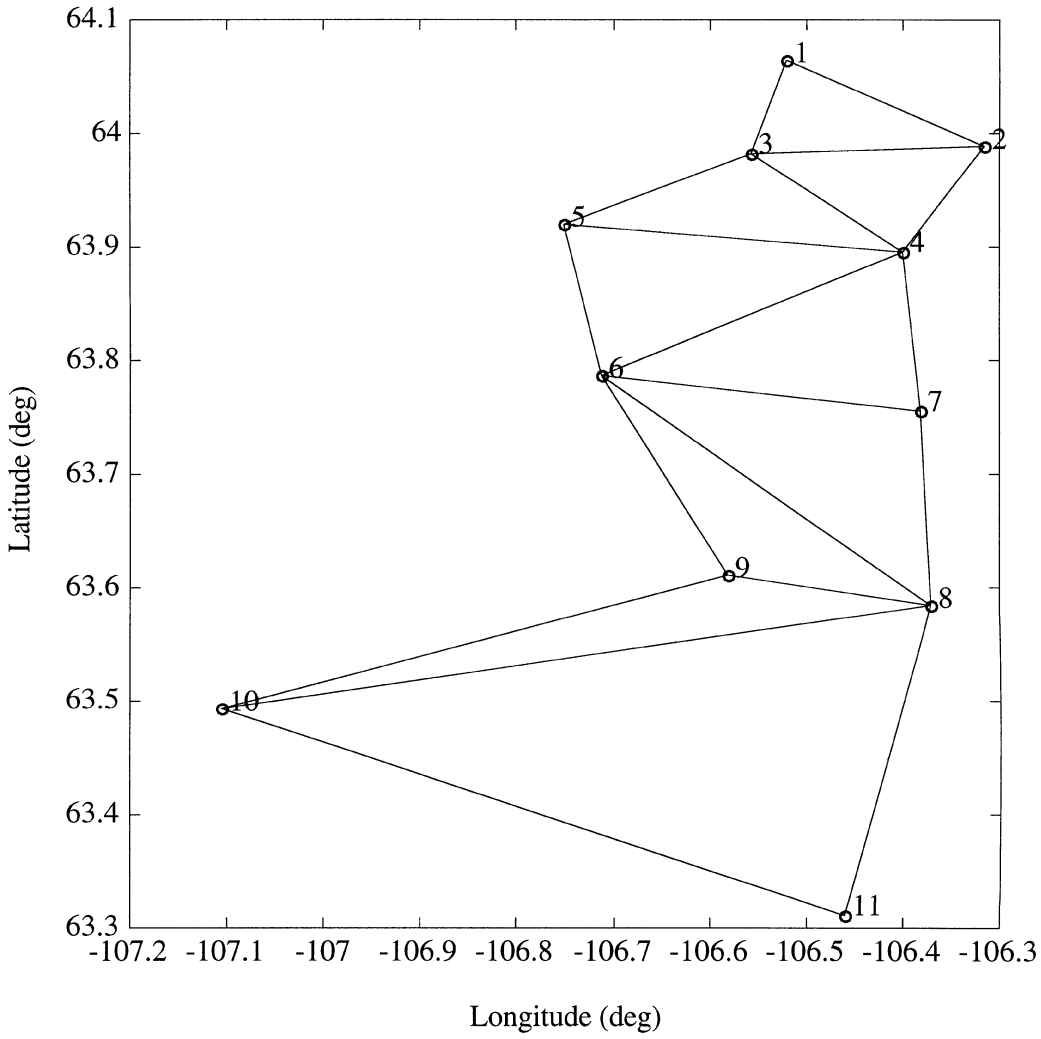

FIGURE 2.2: HOACS2D simulated 2D horizontal network with observations ties.

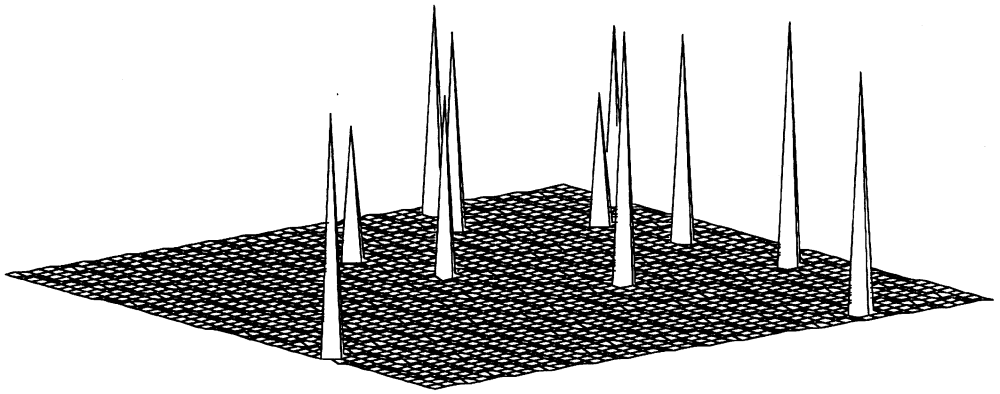

Max Twist Strain = 9.18 ppm, Point # 9

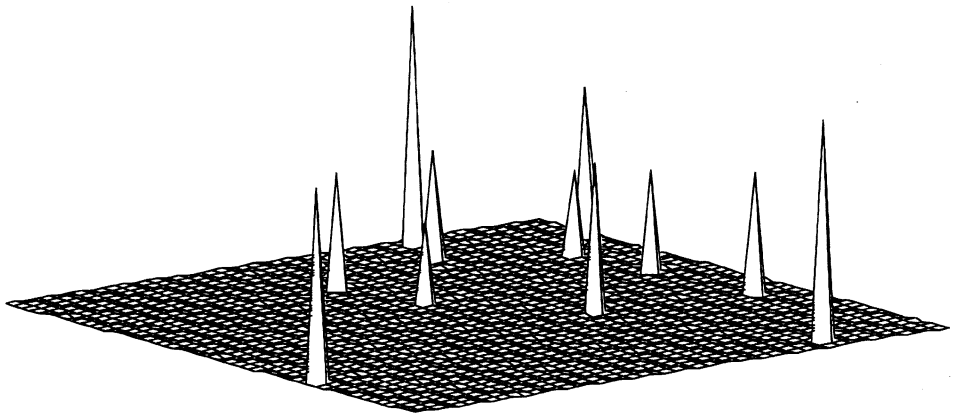

Max Shear Strain = 5.94 ppm, Point # 1

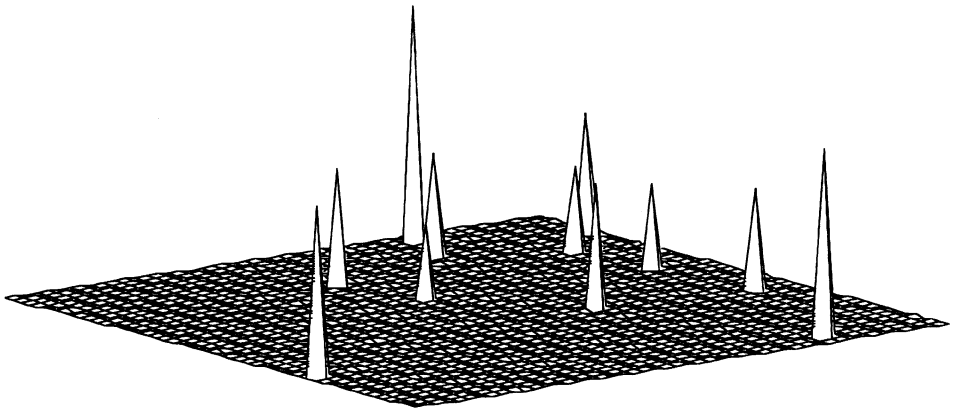

Max Scale Strain = 12.67 ppm, Point # 1

FIGURE 2.3: Surface plots of robustness in twist (top), shear (middle) and scale (bottom) for HOACS2D network. View is from SW.

TABLE 2.1: Robustness measures (ppm) for HOACS2D network.

Point	Twist	Shear	Scale
1	-7.6	**5.9**	**12.7**
2	6.5	3.7	6.3
3	7.2	2.7	5.5
4	4.8	2.1	4.7
5	4.8	2.9	6.3
6	6.5	2.0	4.2
7	7.6	2.5	4.5
8	8.8	3.0	5.4
9	**9.2**	3.7	6.7
10	8.9	4.8	9.2
11	8.8	5.5	10.1

TABLE 2.2: Most influential observations for HOACS2D network.

	Robustness in								
	Twist			Shear			Scale		
Point	Obs	Conn	Corr	Obs	Conn	Corr	Obs	Conn	Corr
1	6	1	1.00	6	1	1.00	40	1	1.00
2	17	**3**	**0.90**	7	1	1.00	41	1	1.00
3	17	2	0.95	44	1	1.00	40	1	1.00
4	17	2	0.98	45	1	1.00	45	1	1.00
5	17	1	1.00	48	1	1.00	48	1	1.00
6	21	1	1.00	52	2	0.99	52	2	0.99
7	21	2	0.99	22	2	0.99	52	1	1.00
8	21	2	0.98	34	2	**0.98**	56	2	0.99
9	21	2	0.98	32	1	1.00	56	1	1.00
10	21	**3**	0.95	30	2	**0.98**	55	2	**0.98**
11	21	**3**	0.94	30	1	1.00	55	1	1.00

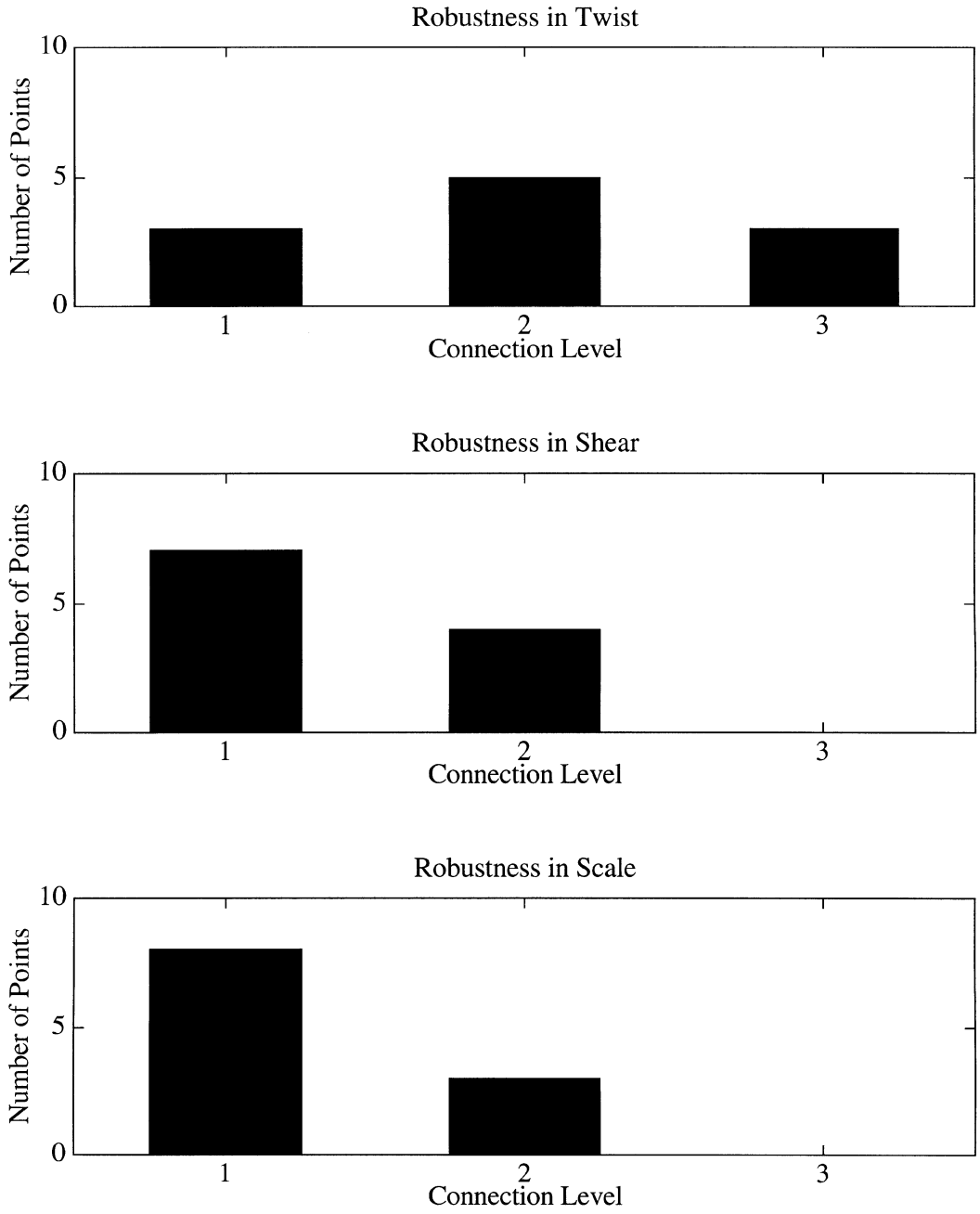

FIGURE 2.4: Histogram of distribution of connection levels of most influential observations for HOACS2D network.

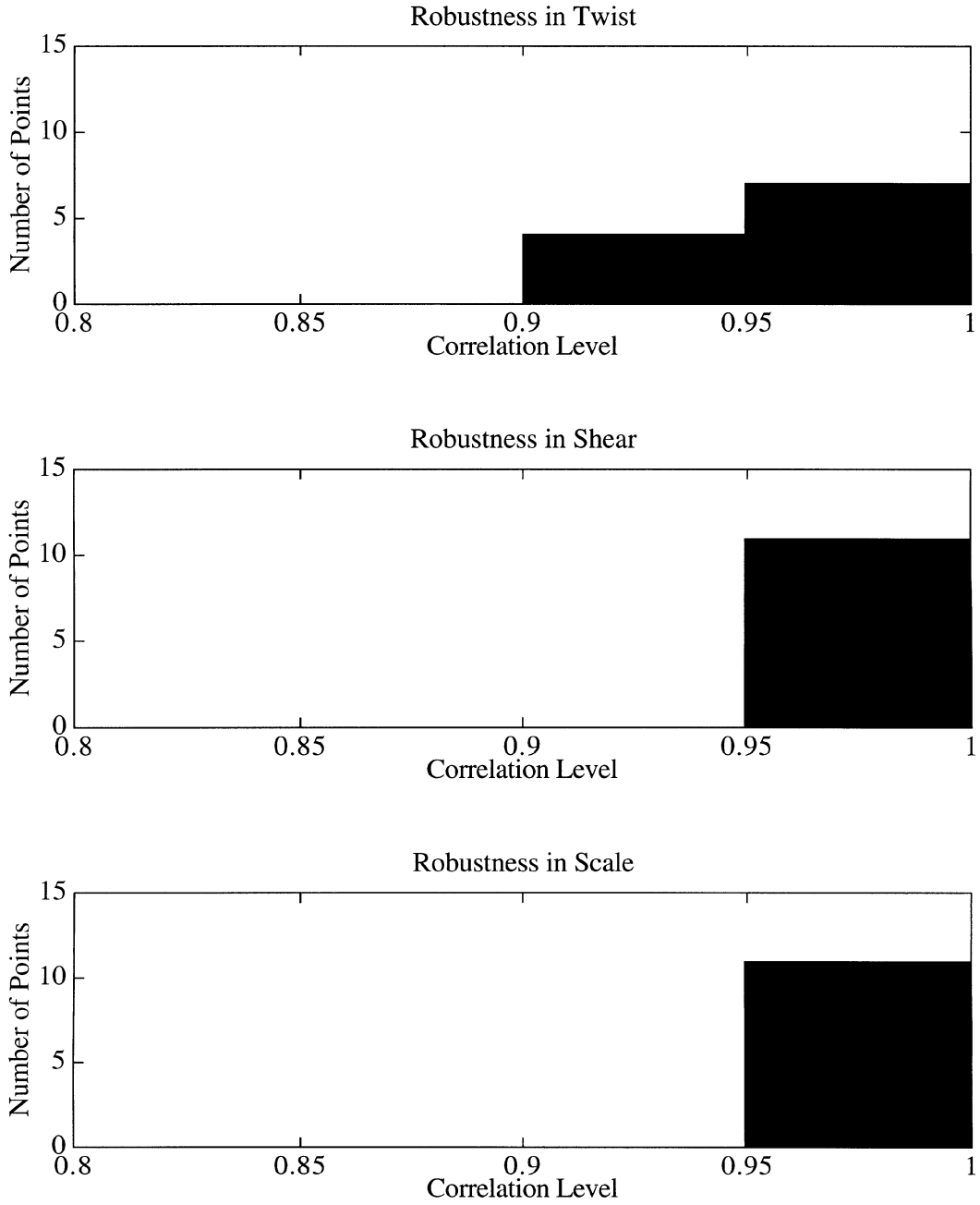

FIGURE 2.5: Histogram of distribution of correlation levels of most influential observations for HOACS2D network.

2.3 REALNET Network

The REALNET network, shown in Figure 2.6, is an example of a real horizontal terrestrial network in southern Quebec consisting of 58 points with 307 direction, 125 distance and 1 azimuth (constraint) observations. The total degrees of freedom of the adjustment is 242.

The correct robustness measures, computed using the network-wide search for the most influential observations, are given in Table 2.3. Note that 4 points (#19, 23, 25, 55) have undefined robustness measures (denoted as N/A in the Table). This is a result of the current strain computation algorithm which is unable to handle the single geometrical ties to these points. A method of handling this situation has been proposed by Krakiwsky et al. (1993) but has yet to be implemented in NETAN.

In Table 2.4, the most influential observation producing the maximum robustness in twist, shear and scale at each point is given together with the number of connections from the point of interest. The largest correlation between each point of interest and the points associated with the most influential observation, is also listed in this Table. Histograms of the distribution of the connection and correlation levels for all the most influential observations are given in Figures 2.7 and 2.8, respectively.

From Table 2.4 and Figure 2.7 we see that it is necessary to search up to only the third connection (for robustness in twist and scale) in order to find the correct "most influential observations". When limiting the search to the 3rd connection level, we find that it is required to search a total of 12404 observations, as compared to 25114 when searching the entire network; a reduction of 51%.

For the correlation method, we see from Table 2.4 and Figure 2.8 that it is necessary to search those points that have a correlation level of at least 78% (for all robustness measures at point #10). This requires searching a total of 24313 observations, as compared to 25114 for the network-wide search; a minor computational savings of only 3%.

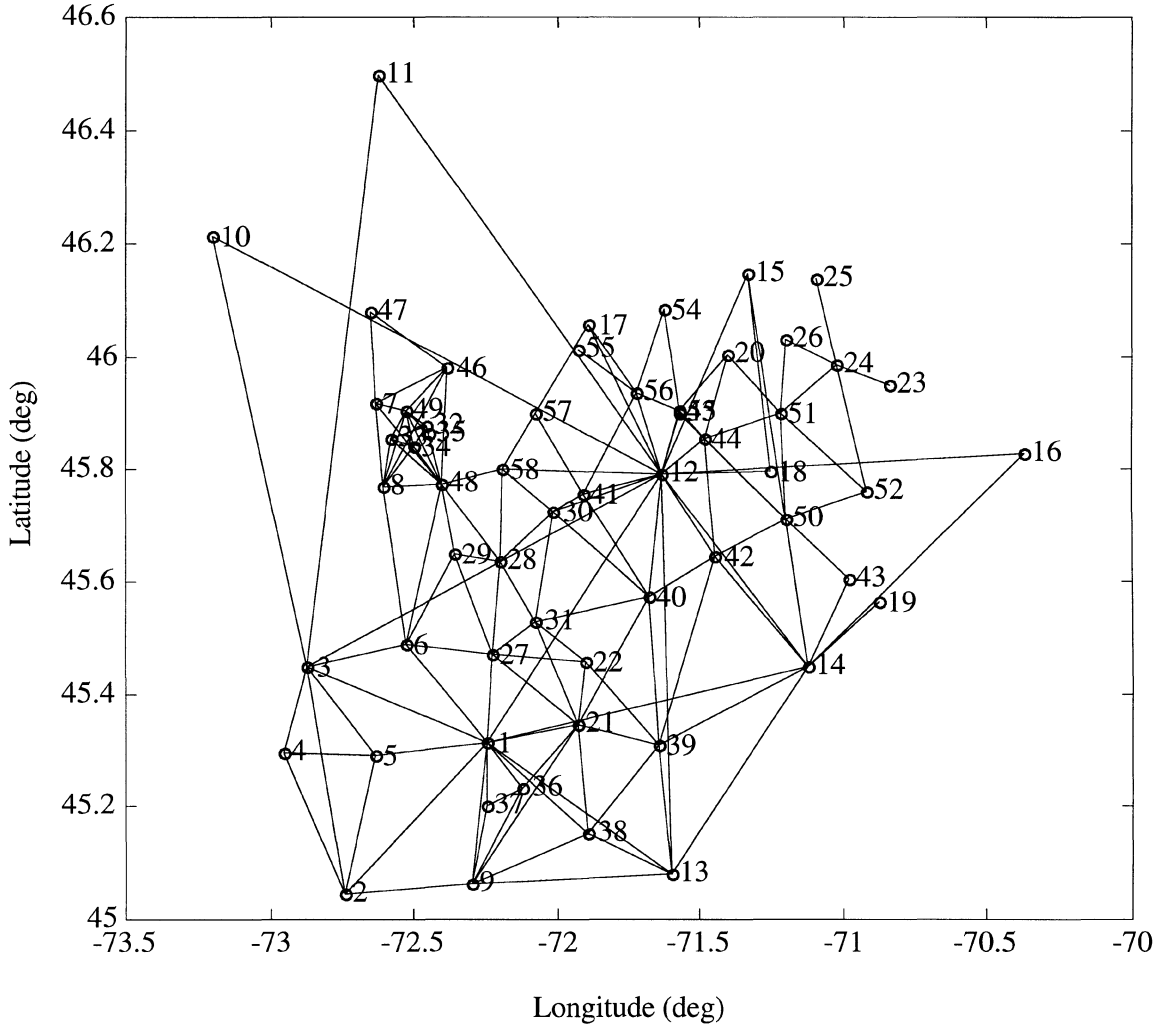

FIGURE 2.6: REALNET real 2D horizontal network with observations ties.

TABLE 2.3: Robustness measures (ppm) for REALNET network.

Point	Twist	Shear	Scale
1	2.3	0.7	1.8
2	1.8	1.9	4.7
3	2.5	3.2	7.1
4	5.1	3.4	6.0
5	-1.9	1.9	4.1
6	3.0	2.6	4.8
7	7.9	9.5	15.0
8	7.7	2.6	4.1
9	2.6	1.6	2.7
10	3.2	4.1	7.7
11	2.4	4.6	9.7
12	2.5	2.2	4.7
13	3.0	0.6	1.3
14	2.9	4.1	7.0
15	-8.5	9.3	19.4
16	3.1	5.4	11.0
17	12.2	16.2	34.6
18	-20.3	18.2	29.1
19	N/A	N/A	N/A
20	-5.7	8.0	9.9
21	2.8	0.8	1.3
22	3.2	2.5	4.7
23	N/A	N/A	N/A
24	-8.1	5.9	9.9
25	N/A	N/A	N/A
26	-12.6	10.0	20.6
27	4.2	1.3	1.9
28	4.5	4.1	9.1
29	5.7	4.4	7.5
30	3.5	2.3	4.1
31	3.3	1.5	2.7
32	8.1	2.3	4.8
33	7.9	1.4	4.0
34	7.9	1.4	4.0
35	**33.8**	**39.6**	**57.5**
36	3.2	1.8	3.0
37	-4.0	4.0	5.8
38	2.9	1.4	2.1
39	3.0	1.3	2.4
40	2.9	1.2	2.7
41	-6.5	4.5	5.2
42	3.0	1.5	3.2
43	-10.9	13.8	20.5
44	3.0	2.4	3.4
45	-8.7	8.8	13.3
46	7.9	9.5	15.0
47	-11.4	21.8	39.2
48	5.6	4.9	9.6
49	7.9	1.3	2.6
50	-4.3	4.9	5.4
51	-5.5	4.1	6.5
52	-9.4	8.2	11.4
53	-5.5	9.3	20.6
54	-7.5	15.4	38.4
55	N/A	N/A	N/A
56	6.5	9.3	18.7
57	16.6	14.3	24.0
58	-6.7	8.7	16.2

TABLE 2.4: Most influential observations for REALNET network.

	Robustness in Twist			Robustness in Shear			Robustness in Scale		
Point	Obs	Conn	Corr	Obs	Conn	Corr	Obs	Conn	Corr
1	216	1	1.00	408	1	1.00	408	1	1.00
2	406	2	0.95	408	2	0.93	408	2	0.93
3	225	1	1.00	224	1	1.00	224	1	1.00
4	204	2	0.96	202	1	1.00	409	1	1.00
5	221	2	0.96	293	2	0.96	408	1	1.00
6	417	2	0.90	310	2	0.91	310	2	0.91
7	417	2	0.99	401	1	1.00	401	1	1.00
8	417	2	1.00	9	1	1.00	310	2	1.00
9	216	2	0.93	215	2	0.92	408	2	0.90
10	225	2	**0.78**	224	2	**0.78**	224	2	**0.78**
11	225	2	0.87	224	2	0.87	224	2	0.87
12	216	2	0.93	224	1	1.00	224	1	1.00
13	216	2	0.94	109	1	1.00	393	**3**	0.96
14	216	2	0.94	226	2	0.98	375	2	0.98
15	226	1	1.00	226	1	1.00	375	1	1.00
16	216	**3**	0.88	229	2	0.92	229	2	0.92
17	412	1	1.00	412	1	1.00	412	1	1.00
18	228	1	1.00	228	1	1.00	422	1	1.00
19					N/A				
20	136	1	1.00	156	1	1.00	156	1	1.00
21	216	2	0.91	88	1	1.00	338	2	0.90
22	47	**3**	0.90	83	1	1.00	358	1	1.00
23					N/A				
24	152	1	1.00	158	1	1.00	158	1	1.00
25					N/A				
26	151	1	1.00	151	1	1.00	395	1	1.00
27	47	2	0.90	58	2	0.95	308	2	0.95
28	47	**3**	0.93	417	2	0.97	417	2	0.97
29	47	2	0.93	310	1	1.00	310	1	1.00
30	47	**3**	0.93	416	2	0.98	416	2	0.98
31	47	**3**	0.91	75	1	1.00	350	2	0.97
32	11	2	0.99	317	1	1.00	317	1	1.00
33	417	2	0.99	317	2	1.00	317	2	1.00
34	417	2	1.00	317	2	1.00	317	2	1.00
35	323	1	1.00	323	1	1.00	323	1	1.00
36	48	2	0.80	366	2	0.83	366	2	0.83
37	53	2	0.82	53	2	0.82	365	1	1.00
38	216	2	0.91	109	2	0.97	330	2	0.97
39	216	**3**	0.94	108	1	1.00	393	2	0.98
40	47	**3**	0.92	393	1	1.00	393	1	1.00
41	418	2	0.96	418	2	0.96	412	2	0.97
42	216	**3**	0.94	393	1	1.00	393	1	1.00
43	277	1	1.00	277	1	1.00	277	1	1.00
44	216	**3**	0.93	136	1	1.00	384	2	1.00
45	141	1	1.00	121	1	1.00	378	1	1.00
46	417	2	0.98	401	2	1.00	401	2	1.00
47	401	1	1.00	401	1	1.00	401	1	1.00
48	47	2	0.93	417	1	1.00	417	1	1.00
49	417	2	0.99	400	1	1.00	400	1	1.00
50	146	1	1.00	146	1	1.00	386	1	1.00
51	146	2	0.99	151	1	1.00	151	1	1.00
52	146	1	1.00	146	1	1.00	146	1	1.00
53	383	1	1.00	383	1	1.00	383	1	1.00
54	245	1	1.00	383	1	1.00	383	1	1.00
55					N/A				
56	383	2	0.99	412	1	1.00	412	1	1.00
57	412	2	0.95	412	2	0.95	244	2	0.95
58	418	1	1.00	418	1	1.00	418	1	1.00

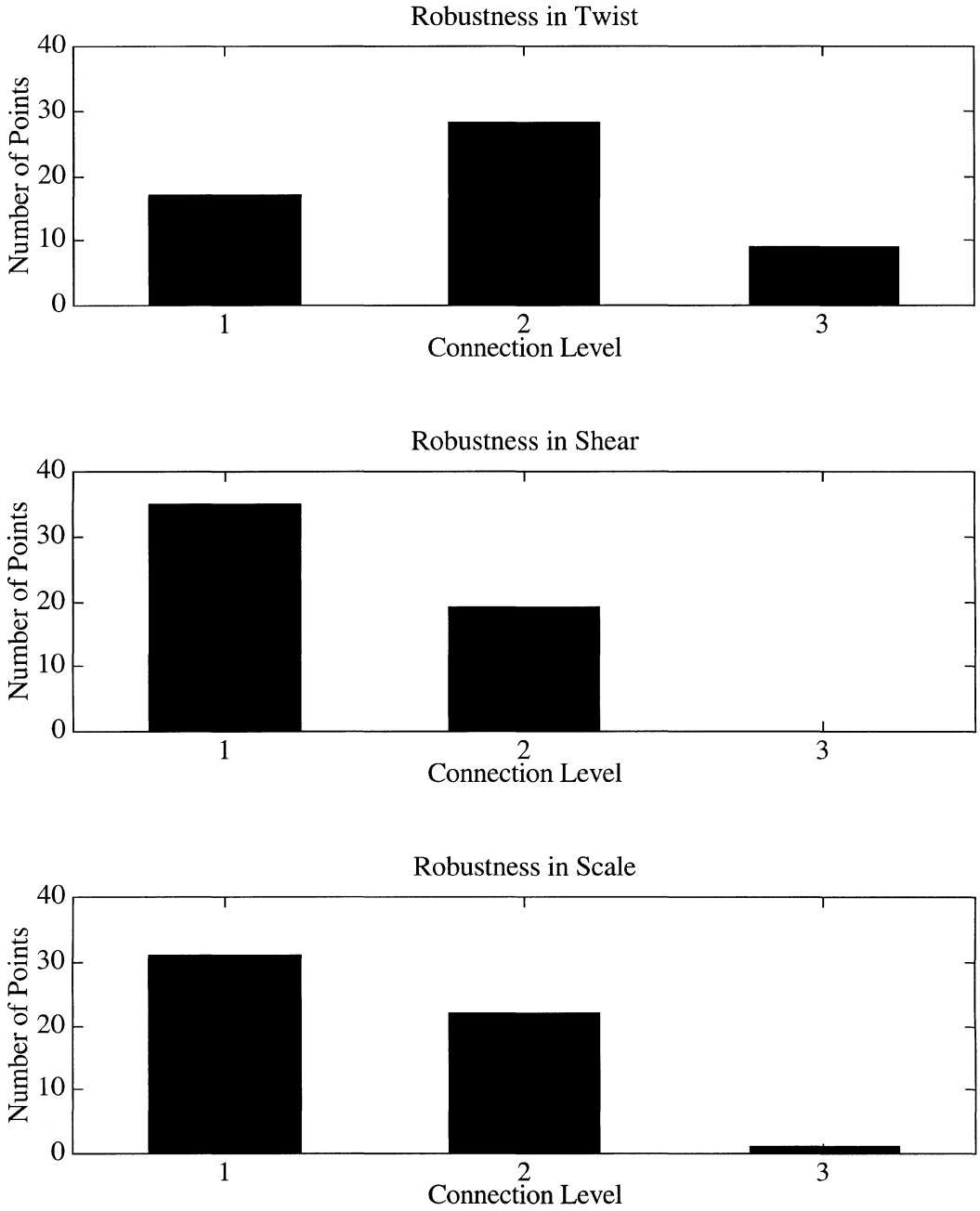

FIGURE 2.7: Histogram of distribution of connection levels of most influential observations for REALNET network.

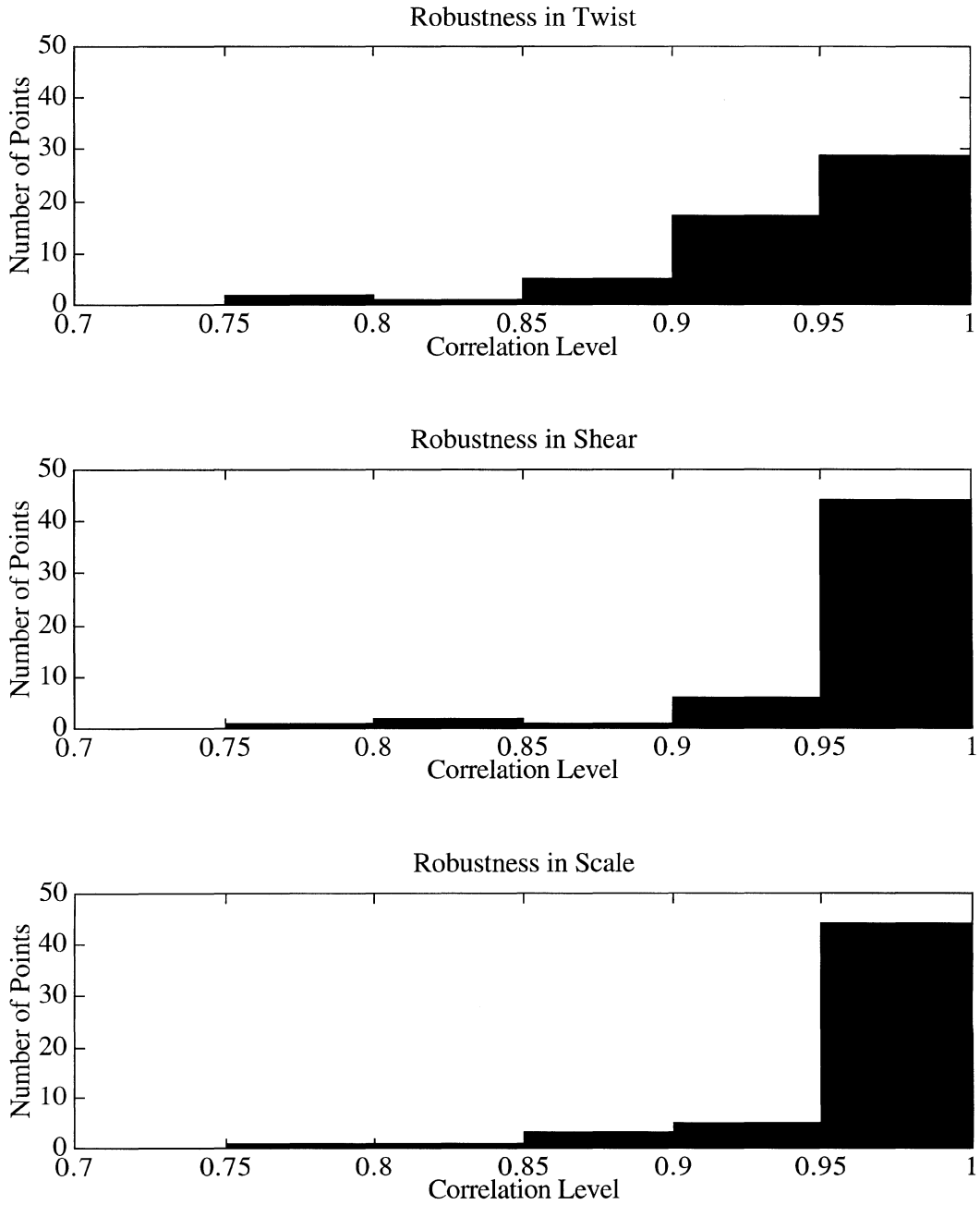

FIGURE 2.8: Histogram of distribution of correlation levels of most influential observations for REALNET network.

2.4 MCEGPS Network

The MCEGPS network, shown in Figure 2.9, is a real example of a 3D GPS network consisting of 91 points with 1 distance, 1 azimuth and 1289 coordinate difference observations. The total degrees of freedom of the adjustment is 1122. We note that only the 2D projection of the network on the reference ellipsoid is analysed here.

The correct robustness measures, computed using the network-wide search for the most influential observations, is given in Table 2.5. Note that robustness is undefined at points #57 and #59 due to the singular geometry, i.e., single geometrical ties to these points. Largest robustness values, highlighted in the table, indicate the weakest parts (largest deformations) of the network. It is interesting to note that compared to the terrestrial networks we have analysed above, the robustness parameters here are significantly smaller. Not surprisingly, the GPS observations, when properly configured, produce a more robust network than terrestrial observations.

In Table 2.6, the most influential observation producing the maximum robustness measures in twist, shear and scale (i.e., minimum robustness at each point) is given together with the number of connection levels from the point of interest and the correlation level. Histograms of the distribution of the connection and correlation levels for all the most influential observations are given in Figures 2.10 and 2.11, respectively.

From Table 2.6 and Figure 2.10 we again see that it is necessary to search up to only the third connection in order to find the correct "most influential observations" (for all robustness measures). When limiting the search to the 3rd connection level, it is required to search a total of only 12591 observations, as compared to 42315 when searching the entire network; a reduction of 70%. This illustrates the point made earlier, that the saving grows with the size of the network, as expected.

For the correlation method, we find from Table 2.6 and Figure 2.11 that it is necessary to search points that have a correlation level of at least 16% (for robustness in shear and scale at point #80). Limiting the search for influential observations to this level results in searching a total of 29471 observations; a computational savings of 30%.

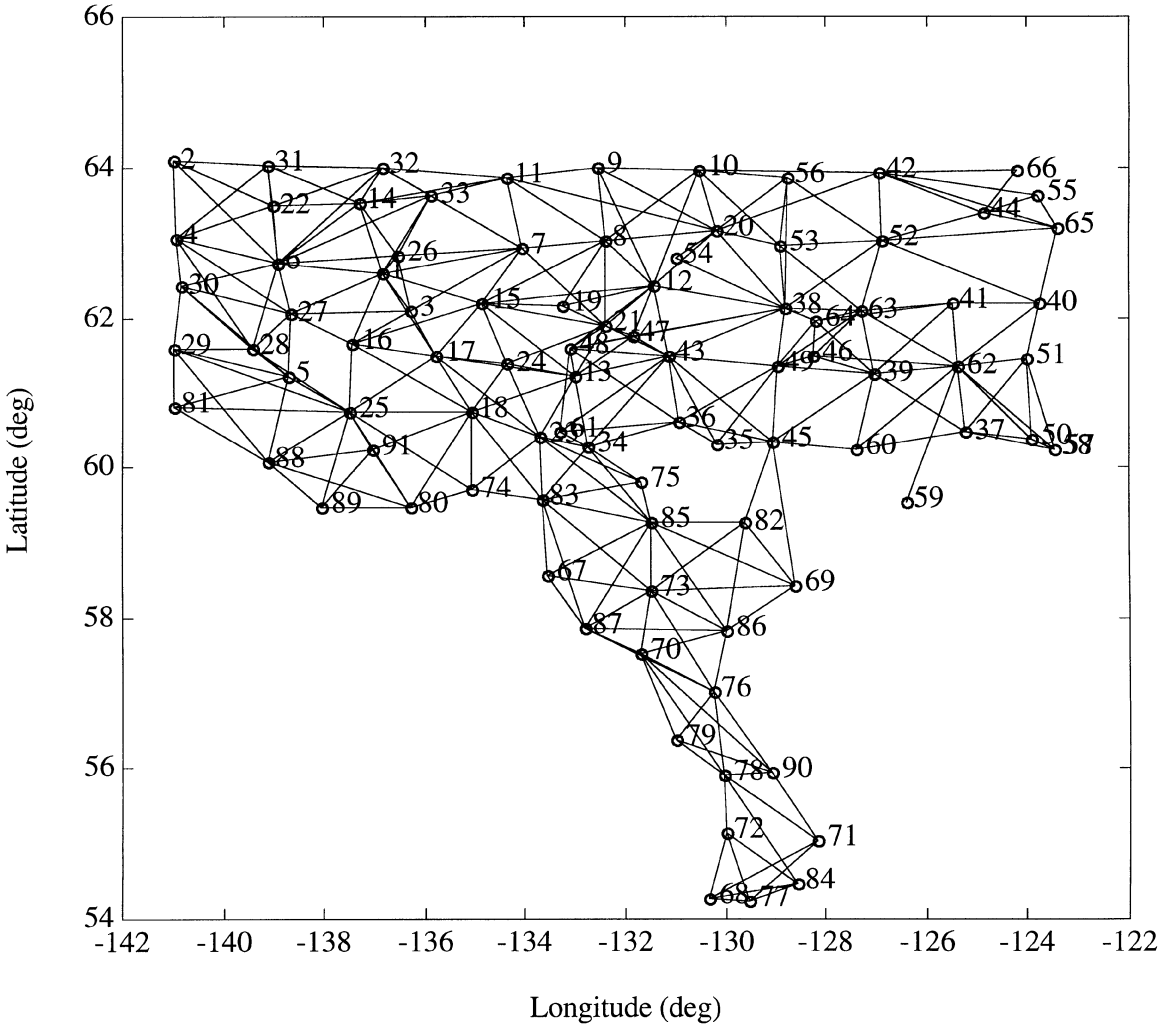

FIGURE 2.9: MCEGPS real 3D GPS network in the Yukon and Northwest Territories with observations ties.

TABLE 2.5: Robustness measures (ppm) for MCEGPS network.

Point	Twist	Shear	Scale
1	-0.2	0.5	0.6
2	0.5	0.6	0.6
3	-0.7	0.9	1.1
4	0.7	0.7	0.8
5	-1.9	2.8	1.6
6	0.3	0.3	0.5
7	-0.2	0.2	0.4
8	-0.2	0.3	0.4
9	0.4	0.4	0.8
10	0.2	0.2	0.5
11	-0.2	0.3	0.5
12	-0.2	0.3	0.4
13	-0.4	0.3	0.5
14	0.4	0.4	0.4
15	-0.2	0.5	0.4
16	-0.8	0.6	0.9
17	-0.3	0.3	0.6
18	0.2	0.3	0.6
19	-0.3	0.5	1.0
20	0.2	0.3	0.5
21	-0.4	0.7	0.7
22	0.4	0.4	0.4
23	-0.3	0.3	0.6
24	-0.4	0.3	0.5
25	-1.0	1.2	0.8
26	0.3	0.4	0.7
27	0.3	0.4	0.9
28	0.5	0.9	1.5
29	-2.3	**3.6**	1.4
30	0.8	1.0	1.6
31	0.4	0.4	0.4
32	0.2	0.3	0.3
33	0.3	0.4	0.4
34	-0.2	0.4	0.8
35	-0.7	0.6	1.0
36	-0.3	0.6	1.1
37	0.2	0.4	0.7
38	0.2	0.3	0.5
39	-0.2	0.3	0.6
40	0.6	0.4	0.5
41	0.6	0.6	1.1
42	0.3	0.4	0.6
43	-0.2	0.4	0.7
44	0.5	0.6	0.8
45	-0.7	1.4	2.6
46	-0.4	0.6	1.2
47	-0.2	0.6	0.6
48	-0.2	0.6	1.2
49	-0.3	0.4	0.6
50	0.4	0.4	0.7
51	0.4	0.7	1.3
52	0.4	0.3	0.5
53	0.4	0.5	1.1
54	1.8	2.0	2.8
55	1.0	2.3	4.3
56	0.4	0.6	1.1
57	N/A	N/A	N/A
58	0.5	0.5	0.7
59	N/A	N/A	N/A
60	0.2	0.5	1.0

TABLE 2.5 Con't.

Point	Twist	Shear	Scale
61	-0.5	0.9	1.7
62	-0.3	0.4	0.4
63	0.2	0.3	0.6
64	0.3	0.6	1.1
65	0.3	0.7	1.0
66	0.8	1.0	0.5
67	-0.4	0.4	0.6
68	-1.2	1.6	3.5
69	-2.8	2.7	3.0
70	0.9	1.3	2.5
71	0.9	1.3	2.1
72	-1.7	1.8	1.9
73	-1.1	1.2	1.3
74	0.3	0.5	0.8
75	-0.4	0.6	1.0
76	0.9	1.3	2.5
77	-1.1	1.6	3.5
78	1.3	1.9	2.2
79	3.0	3.4	**5.9**
80	-0.8	1.2	2.1
81	-2.3	3.5	2.4
82	-2.8	2.8	3.1
83	-0.2	0.2	0.3
84	-1.7	1.8	1.9
85	-1.1	1.1	0.9
86	-1.8	1.8	1.4
87	0.2	0.3	0.3
88	-2.0	2.7	1.6
89	-1.5	1.9	3.1
90	**3.2**	3.5	5.8
91	-0.8	1.6	2.8

TABLE 2.6: Most influential observations for MCEGPS network.

	Robustness in								
	Twist			Shear			Scale		
Point	Obs	Conn	Corr	Obs	Conn	Corr	Obs	Conn	Corr
1	21	1	1.00	273	2	0.00	39	2	0.00
2	306	1	1.00	306	1	1.00	306	1	1.00
3	273	2	0.28	273	2	0.28	39	1	1.00
4	273	2	0.59	273	2	0.59	273	2	0.59
5	1128	1	1.00	1128	1	1.00	273	1	1.00
6	333	2	0.72	273	2	0.78	240	1	1.00
7	21	2	0.39	354	2	0.43	378	2	0.32
8	69	1	1.00	108	2	0.72	75	1	1.00
9	354	2	0.52	660	2	0.93	660	2	0.93
10	594	1	1.00	729	2	0.79	729	2	0.79
11	21	**3**	0.32	354	1	1.00	129	2	0.52
12	108	2	0.67	108	2	0.67	75	2	0.84
13	72	2	0.89	72	2	0.89	804	**3**	0.74
14	333	1	1.00	381	1	1.00	378	2	0.48
15	21	1	1.00	72	2	0.63	63	2	0.55
16	273	2	0.33	273	2	0.33	273	2	0.33
17	21	2	0.31	273	**3**	0.35	273	**3**	0.35
18	78	2	0.42	72	2	0.40	72	2	0.40
19	108	1	1.00	75	2	0.91	75	2	0.91
20	675	1	1.00	729	2	0.88	729	2	0.88
21	72	1	1.00	72	1	1.00	63	2	0.89
22	333	1	1.00	333	1	1.00	333	1	1.00
23	72	2	0.48	72	2	0.48	72	2	0.48
24	72	1	1.00	78	2	0.46	804	**3**	0.34
25	1128	2	0.88	1128	2	0.88	1191	2	0.25
26	273	**3**	0.28	39	1	1.00	39	1	1.00
27	267	2	0.64	240	2	0.58	273	1	1.00
28	273	2	0.96	273	2	0.96	273	2	0.96
29	1128	2	0.52	1128	2	0.52	1146	2	0.36
30	273	2	0.85	273	2	0.85	273	2	0.85
31	333	2	0.97	333	2	0.97	333	2	0.97
32	333	2	0.60	333	2	0.60	273	**3**	0.37
33	273	**3**	0.27	381	2	0.48	378	1	1.00
34	840	2	0.90	804	1	1.00	804	1	1.00
35	507	2	0.64	507	2	0.64	801	1	1.00
36	507	2	0.83	831	1	1.00	831	1	1.00
37	699	1	1.00	420	2	0.97	420	2	0.97
38	585	2	0.89	729	1	1.00	729	1	1.00
39	885	2	0.94	705	1	1.00	705	1	1.00
40	819	1	1.00	819	1	1.00	558	2	0.76
41	819	1	1.00	819	1	1.00	438	1	1.00
42	558	2	0.98	558	2	0.98	660	2	0.83
43	507	1	1.00	831	2	0.92	831	2	0.92
44	558	1	1.00	558	1	1.00	558	1	1.00
45	1335	2	**0.24**	1335	2	0.24	1335	2	0.24
46	885	1	1.00	486	2	0.73	486	2	0.73
47	744	2	0.66	78	2	0.80	744	2	0.66
48	831	1	1.00	831	1	1.00	831	1	1.00
49	507	1	1.00	507	1	1.00	801	2	0.66
50	519	1	1.00	519	1	1.00	420	2	0.90
51	819	2	0.68	819	2	0.68	819	2	0.68
52	819	2	0.80	729	2	0.89	729	2	0.89
53	675	2	0.82	729	2	0.87	729	2	0.87
54	624	1	1.00	624	1	1.00	624	1	1.00
55	450	1	1.00	450	1	1.00	450	1	1.00
56	594	1	1.00	729	1	1.00	729	1	1.00
57					N/A				
58	519	1	1.00	519	1	1.00	420	2	0.79
59					N/A				

TABLE 2.6 Con't.

	Robustness in								
	Twist			Shear			Scale		
Point	Obs	Conn	Corr	Obs	Conn	Corr	Obs	Conn	Corr
60	543	1	1.00	705	2	0.97	705	2	0.97
61	840	1	1.00	831	2	0.63	831	2	0.63
62	885	1	1.00	885	1	1.00	885	1	1.00
63	438	1	1.00	885	2	0.74	486	2	0.97
64	438	2	0.93	486	2	0.83	486	2	0.83
65	558	2	0.87	819	2	0.66	558	2	0.87
66	558	2	0.77	558	2	0.77	558	2	0.77
67	1023	1	1.00	1023	1	1.00	1032	1	1.00
68	1251	2	0.90	1290	1	1.00	1290	1	1.00
69	1335	1	1.00	1335	1	1.00	1335	1	1.00
70	1218	2	0.71	1218	2	0.71	1218	2	0.71
71	1275	1	1.00	1275	1	1.00	1275	1	1.00
72	1278	2	0.90	1278	2	0.90	1275	2	0.90
73	1335	2	0.56	1335	2	0.56	1329	2	0.85
74	963	1	1.00	1176	2	0.42	963	1	1.00
75	1002	1	1.00	1002	1	1.00	981	1	1.00
76	1218	1	1.00	1218	1	1.00	1218	1	1.00
77	1251	2	0.90	1290	2	0.94	1290	2	0.94
78	1218	2	0.69	1251	1	1.00	1275	2	0.92
79	1218	1	1.00	1218	1	1.00	1218	1	1.00
80	1194	2	0.38	1191	2	**0.16**	1191	2	**0.16**
81	1128	1	1.00	1128	1	1.00	1146	2	0.32
82	1335	1	1.00	1335	1	1.00	1335	1	1.00
83	804	2	0.47	1002	1	1.00	981	2	0.78
84	1278	2	0.98	1278	2	0.98	1275	2	0.98
85	1335	2	0.43	1335	2	0.43	1329	2	0.63
86	1335	2	0.65	1335	2	0.65	1329	1	1.00
87	1080	1	1.00	1023	2	0.72	1032	1	1.00
88	1128	2	0.32	1128	2	0.32	1191	1	1.00
89	1194	1	1.00	1191	1	1.00	1191	1	1.00
90	1218	2	0.69	1218	2	0.69	1218	2	0.69
91	1203	2	0.38	1191	2	0.22	1191	2	0.22

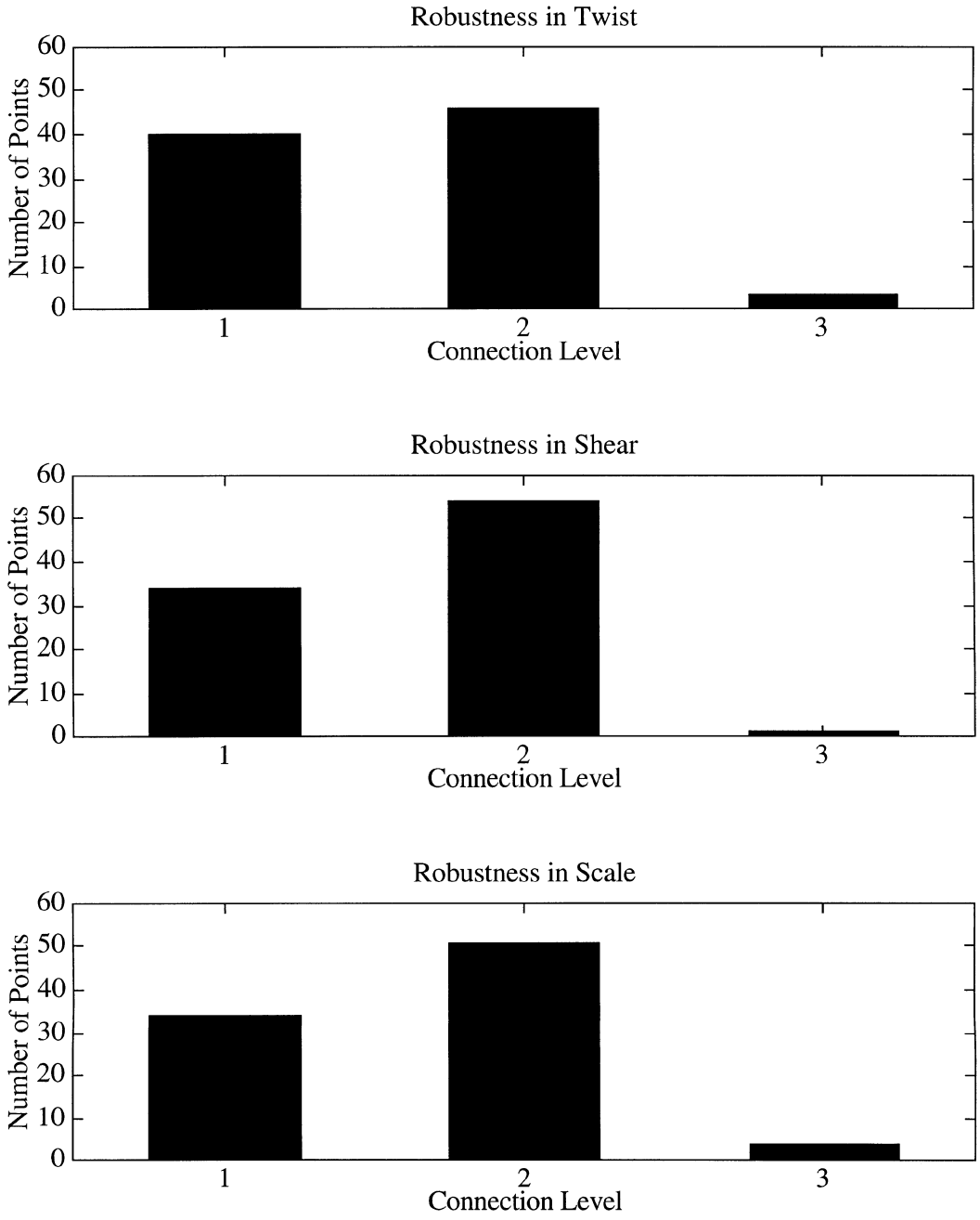

FIGURE 2.10: Histogram of distribution of connection levels of most influential observations for MCEGPS network.

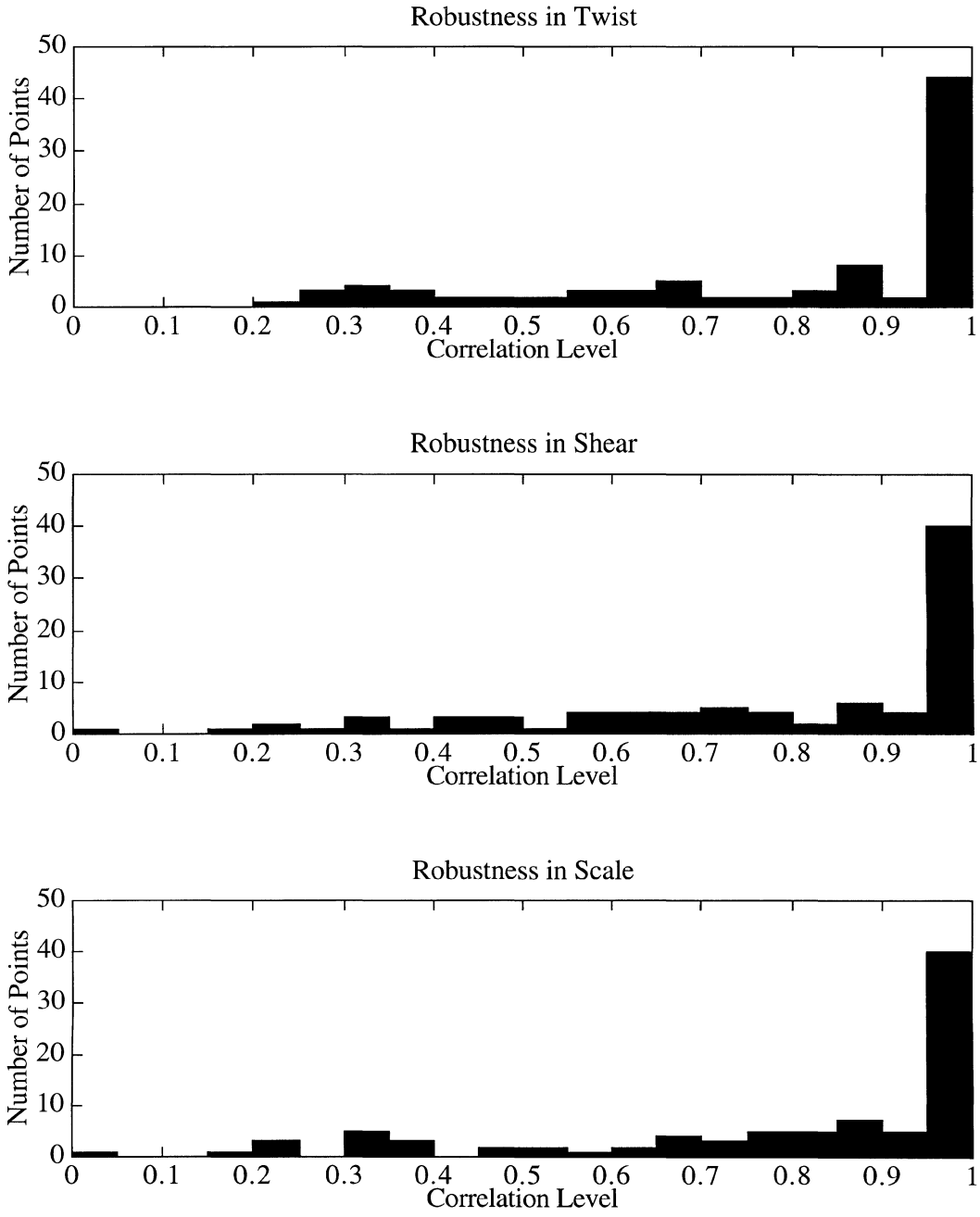

FIGURE 2.11: Histogram of distribution of correlation levels of most influential observations for MCEGPS network.

2.5 NFLDGPS Network

The NFLDGPS network, shown in Figure 2.12, is another example of a real 3D GPS network consisting of 104 points with 786 coordinate difference observations. The total degrees of freedom of the adjustment is 477. Again, only the horizontal projection of the network was analysed.

The correct robustness measures, computed using the network-wide search for the most influential observations, is given in Table 2.7 and in Figure 2.13. Note that robustness is undefined at points #11, 69 and 70 due to the single geometrical ties to these points. The network is again quite robust with the exception of a few points.

In Table 2.8, the most influential observation producing the maximum robustness in twist, shear and scale at each point is given together with the number of connection levels from the point of interest and also the correlation levels. Histograms of the distribution of the connection and correlation levels for all the most influential observations are given in Figures 2.14 and 2.15, respectively.

From Table 2.8 and Figure 2.14 we see that it is necessary to search up to the third connection level in order to find the correct "most influential observations"; for robustness in scale at point #52, the search went up to the 5th level, but the robustness measures at this point are so small that stopping at the 3rd level would not make much of a difference! For all other points the most influential observation is within three connection levels. When limiting the search to the 5th connection level, it is required to search a total of only 9862 observations, as compared to 27248 when searching the entire network; a reduction of 64%. If the search is limited to only the third connection level, there is only one slight error in robustness; at point #52 the error in robustness in scale is only 0.03 ppm (observation number 490 is selected as the most influential observation instead of the correct 499). This results in searching a total of only 4127 observations; a reduction of 84% compared to the network-wide search!

For the correlation method, we find from Table 2.8 and Figure 2.15 that it is necessary to search observations that have a correlation level of at least 56% (for all robustness measures at point #24). Limiting the search for influential observations to this level results in searching a total of 9953 observations, a computational savings of 63% relative to the network-wide search (the same as for limiting the search to the 5th connection level).

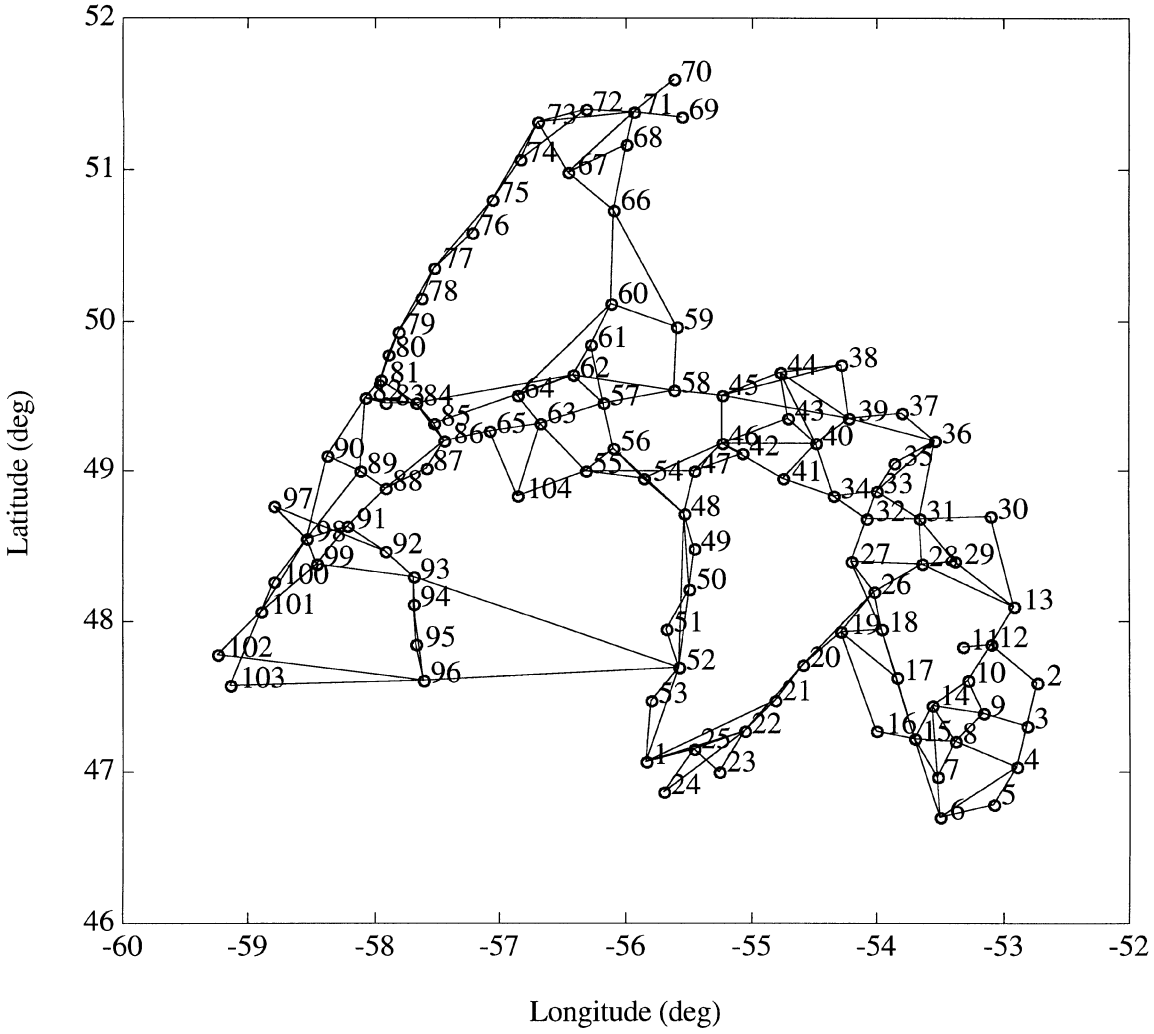

FIGURE 2.12: NFLDGPS real 3D GPS network in Newfoundland with observations ties.

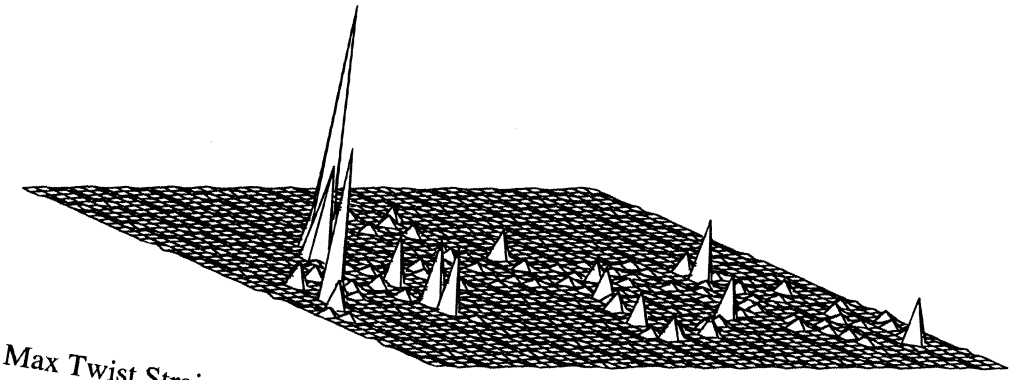

Max Twist Strain = 25.69 ppm, Point # 78

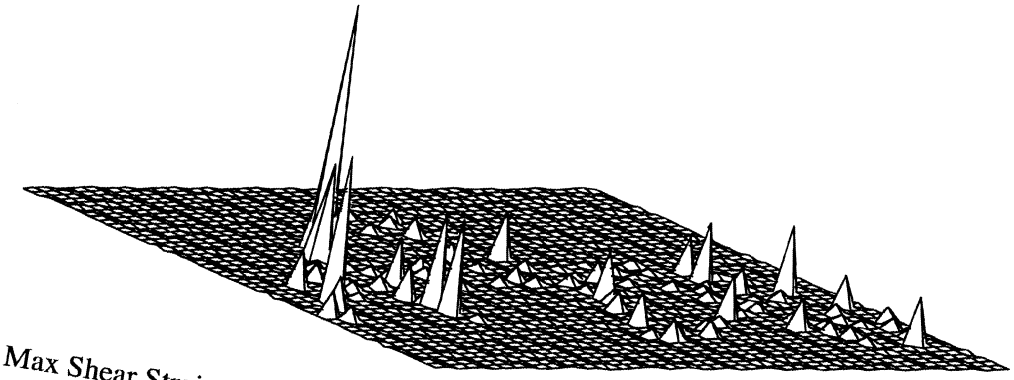

Max Shear Strain = 27.77 ppm, Point # 78

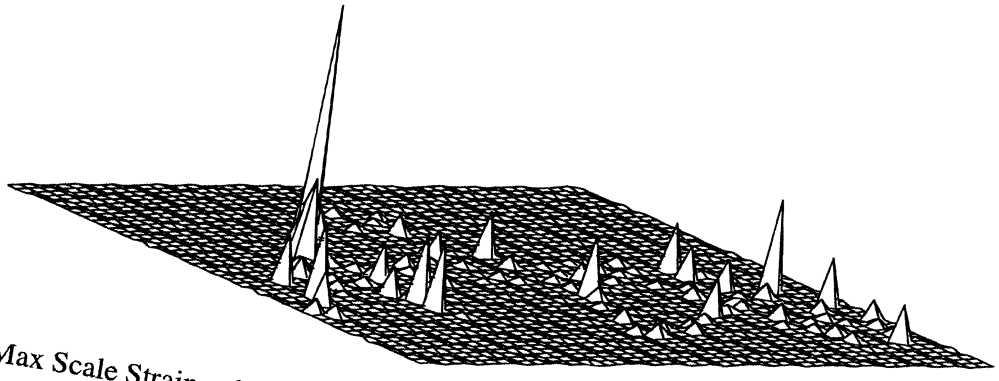

Max Scale Strain = 38.51 ppm, Point # 78

FIGURE 2.13: Surface plots of robustness in twist (top), shear (middle) and scale (bottom) for NFLDGPS network. View is from SW.

TABLE 2.7: Robustness measures (ppm) for NFLDGPS network.

Point	Twist	Shear	Scale
1	-0.8	0.8	1.0
2	1.0	1.6	2.9
3	-1.0	1.2	1.5
4	0.8	1.0	1.5
5	4.7	5.2	5.6
6	0.6	0.9	1.5
7	-0.7	1.1	1.4
8	0.6	0.7	0.9
9	0.5	0.5	0.9
10	0.7	0.8	1.1
11	N/A	N/A	N/A
12	1.0	1.1	2.1
13	-0.8	3.8	7.2
14	-0.5	0.6	1.0
15	-0.7	1.2	1.0
16	-1.1	3.3	1.0
17	-0.7	1.4	2.7
18	-0.6	0.9	1.2
19	0.6	0.6	1.0
20	4.5	4.9	5.9
21	-1.0	1.0	1.3
22	1.0	1.0	1.1
23	1.9	1.9	1.6
24	-2.3	2.3	2.2
25	-1.1	1.2	1.2
26	-0.8	0.8	0.9
27	-0.4	0.9	1.8
28	0.4	0.5	0.8
29	0.5	1.2	2.2
30	1.1	7.3	14.2
31	1.1	2.6	4.8
32	0.5	0.8	1.1
33	0.7	0.7	0.9
34	-0.4	0.8	1.0
35	-6.3	6.5	5.4
36	-0.5	0.6	1.0
37	-2.3	4.2	7.6
38	0.5	0.7	1.3
39	-0.3	0.4	0.7
40	0.4	0.4	0.6
41	0.7	0.8	0.9
42	1.9	2.1	2.5
43	-0.6	0.7	1.1
44	0.3	0.4	0.8
45	0.4	0.4	0.6
46	-0.4	0.4	0.6
47	-0.8	0.9	1.1
48	0.4	0.7	0.9
49	3.2	5.4	9.7
50	-1.0	1.4	1.9
51	-1.7	2.1	1.0
52	-0.2	0.5	0.4
53	-3.6	3.9	2.3
54	0.5	0.8	0.9
55	0.4	0.8	0.4
56	0.4	1.5	1.2
57	0.6	0.7	0.9
58	-1.0	1.2	1.8
59	-3.0	5.2	6.9
60	1.0	1.0	1.2

TABLE 2.7 Con't.

Point	Twist	Shear	Scale
61	1.5	2.2	4.4
62	0.5	0.6	0.9
63	0.6	0.7	0.6
64	-1.2	1.3	2.2
65	0.8	1.0	1.1
66	-1.1	2.1	3.1
67	0.9	1.0	1.0
68	-1.1	1.1	0.8
69	N/A	N/A	N/A
70	N/A	N/A	N/A
71	1.5	1.5	1.3
72	-0.9	1.1	1.5
73	1.6	1.7	2.0
74	1.4	1.5	2.4
75	-3.4	3.7	4.1
76	12.1	12.3	14.3
77	-4.9	5.2	4.1
78	**25.7**	**27.8**	**38.5**
79	5.5	6.0	8.6
80	-9.9	11.2	12.4
81	0.5	0.6	0.9
82	0.6	0.7	1.2
83	-0.7	1.2	2.3
84	-0.5	0.6	0.7
85	-0.8	0.9	1.2
86	0.6	0.8	1.4
87	5.0	5.1	6.0
88	-1.3	1.3	1.2
89	-0.5	0.6	1.0
90	-1.5	1.9	3.0
91	-1.1	1.1	1.1
92	0.9	3.7	4.6
93	-0.5	1.2	1.1
94	-6.7	10.7	10.6
95	-6.7	10.6	10.6
96	-0.5	0.8	0.8
97	-2.5	4.3	7.7
98	-1.2	1.4	1.1
99	-0.7	0.7	0.8
100	-15.9	16.4	12.3
101	2.9	3.6	5.3
102	-0.9	2.8	1.9
103	-0.7	1.5	1.9
104	0.8	0.9	1.0

TABLE 2.8: Most influential observations for NFLDGPS network.

	Robustness in								
	Twist			Shear			Scale		
Point	Obs	Conn	Corr	Obs	Conn	Corr	Obs	Conn	Corr
1	559	1	1.00	559	1	1.00	559	1	1.00
2	55	1	1.00	55	1	1.00	55	1	1.00
3	619	1	1.00	619	1	1.00	616	1	1.00
4	10	2	0.84	10	2	0.84	10	2	0.84
5	10	1	1.00	10	1	1.00	10	1	1.00
6	46	1	1.00	10	1	1.00	613	2	0.79
7	775	2	0.88	775	2	0.88	22	2	0.82
8	613	2	0.78	613	2	0.78	613	2	0.78
9	55	3	0.85	55	3	0.85	769	1	1.00
10	70	2	0.92	70	2	0.92	70	2	0.92
11					N/A				
12	55	1	1.00	610	1	1.00	610	1	1.00
13	130	2	0.60	130	2	0.60	130	2	0.60
14	775	2	0.88	70	1	1.00	70	1	1.00
15	43	1	1.00	43	1	1.00	40	1	1.00
16	43	1	1.00	43	1	1.00	61	2	0.75
17	97	2	0.77	34	2	0.77	34	2	0.77
18	97	1	1.00	97	1	1.00	61	2	0.77
19	67	1	1.00	64	1	1.00	61	1	1.00
20	106	2	0.68	64	1	1.00	106	2	0.68
21	601	2	0.67	601	2	0.67	601	2	0.67
22	583	2	0.57	586	2	0.57	583	2	0.57
23	583	1	1.00	583	1	1.00	583	1	1.00
24	592	2	**0.56**	592	2	**0.56**	592	2	**0.56**
25	586	1	1.00	586	1	1.00	586	1	1.00
26	91	2	0.73	91	2	0.73	91	2	0.73
27	91	1	1.00	103	2	0.80	103	2	0.80
28	610	2	0.70	139	2	0.80	745	1	1.00
29	610	2	0.72	103	2	0.80	745	2	0.80
30	127	2	0.79	130	1	1.00	130	1	1.00
31	130	1	1.00	130	1	1.00	130	1	1.00
32	196	2	0.84	139	1	1.00	745	2	0.84
33	196	1	1.00	196	1	1.00	133	2	0.84
34	214	1	1.00	730	2	0.81	217	1	1.00
35	154	1	1.00	154	1	1.00	199	1	1.00
36	157	1	1.00	157	1	1.00	133	1	1.00
37	148	1	1.00	148	1	1.00	148	1	1.00
38	718	2	0.86	715	1	1.00	715	1	1.00
39	169	1	1.00	715	2	0.86	715	2	0.86
40	187	2	0.83	727	1	1.00	202	2	0.87
41	187	1	1.00	727	2	0.83	202	2	0.75
42	205	1	1.00	205	1	1.00	544	1	1.00
43	166	2	0.81	166	2	0.81	202	1	1.00
44	718	2	0.81	715	2	0.84	715	2	0.84
45	718	1	1.00	193	1	1.00	715	1	1.00
46	178	2	0.76	178	2	0.76	202	1	1.00
47	700	2	0.72	547	1	1.00	544	1	1.00
48	697	1	1.00	256	2	0.73	697	1	1.00
49	706	1	1.00	532	1	1.00	532	1	1.00
50	529	2	0.86	538	1	1.00	532	1	1.00
51	529	1	1.00	529	1	1.00	541	2	0.87
52	514	1	1.00	514	1	1.00	499	**5**	0.56
53	562	1	1.00	526	1	1.00	562	1	1.00
54	697	2	0.84	547	2	0.84	544	3	0.79
55	235	2	0.84	700	1	1.00	682	2	0.84
56	697	1	1.00	700	1	1.00	238	2	0.76
57	256	1	1.00	256	1	1.00	259	1	1.00
58	241	1	1.00	241	1	1.00	241	1	1.00
59	358	2	0.90	358	2	0.90	367	1	1.00

TABLE 2.8 Con't.

	Robustness in								
	Twist			Shear			Scale		
Point	Obs	Conn	Corr	Obs	Conn	Corr	Obs	Conn	Corr
60	367	2	0.90	367	2	0.90	367	2	0.90
61	685	2	0.87	358	2	0.82	358	2	0.82
62	685	1	1.00	685	1	1.00	268	2	0.87
63	700	2	0.70	700	2	0.70	700	2	0.70
64	358	2	0.81	358	2	0.81	358	2	0.81
65	226	2	0.73	235	2	0.83	274	1	1.00
66	358	1	1.00	358	1	1.00	367	1	1.00
67	409	1	1.00	409	1	1.00	409	1	1.00
68	361	2	0.98	361	2	0.98	361	2	0.98
69					N/A				
70					N/A				
71	409	2	0.90	409	2	0.90	409	2	0.90
72	346	2	0.93	340	2	0.92	346	2	0.93
73	409	1	1.00	409	1	1.00	409	1	1.00
74	400	2	0.95	352	1	1.00	352	1	1.00
75	343	1	1.00	343	1	1.00	331	2	0.95
76	331	1	1.00	331	1	1.00	331	1	1.00
77	343	1	1.00	343	1	1.00	337	2	0.94
78	334	1	1.00	334	1	1.00	334	1	1.00
79	334	2	0.88	334	2	0.88	334	2	0.88
80	283	1	1.00	283	1	1.00	412	1	1.00
81	637	1	1.00	640	1	1.00	652	2	0.96
82	424	2	0.76	427	2	0.75	499	3	0.87
83	646	1	1.00	646	1	1.00	646	1	1.00
84	676	1	1.00	676	1	1.00	676	1	1.00
85	676	2	0.95	676	2	0.95	676	2	0.95
86	274	1	1.00	274	1	1.00	499	1	1.00
87	496	1	1.00	496	1	1.00	496	1	1.00
88	316	1	1.00	316	1	1.00	316	1	1.00
89	427	2	0.93	424	1	1.00	424	1	1.00
90	658	1	1.00	658	1	1.00	661	2	0.93
91	490	1	1.00	490	1	1.00	490	1	1.00
92	487	1	1.00	442	2	0.88	490	1	1.00
93	520	1	1.00	514	2	0.95	520	1	1.00
94	472	2	0.96	472	2	0.96	445	2	0.96
95	472	1	1.00	472	1	1.00	445	1	1.00
96	466	1	1.00	463	1	1.00	466	1	1.00
97	442	1	1.00	442	1	1.00	442	1	1.00
98	442	1	1.00	442	1	1.00	436	1	1.00
99	490	2	0.92	439	2	0.96	436	2	0.96
100	433	1	1.00	433	1	1.00	433	1	1.00
101	463	2	0.84	463	2	0.84	463	2	0.84
102	463	2	0.90	460	1	1.00	439	2	0.87
103	466	2	0.90	463	1	1.00	466	2	0.90
104	700	2	0.84	235	1	1.00	229	2	0.84

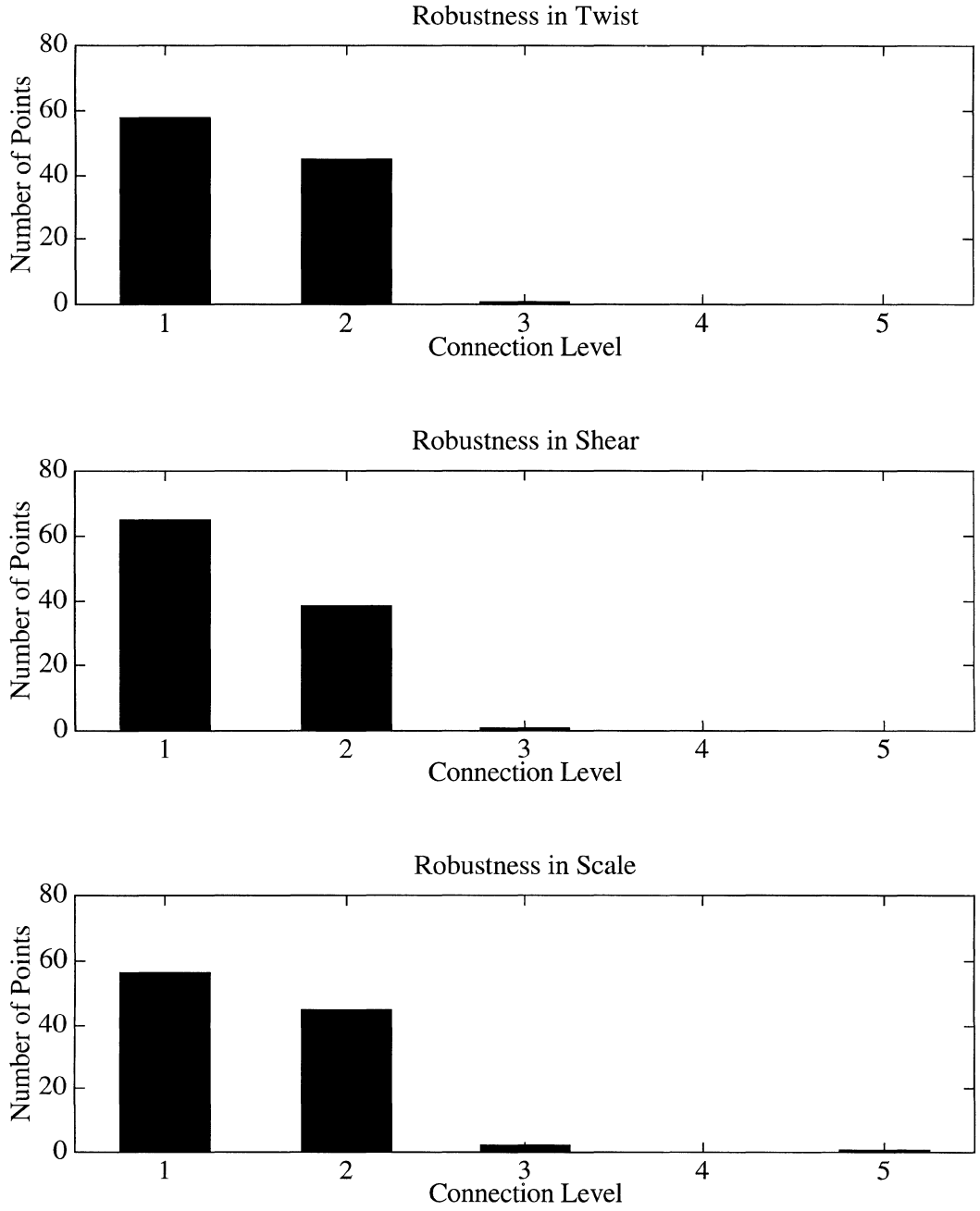

FIGURE 2.14: Histogram of distribution of connection levels of most influential observations for the NFLDGPS network.

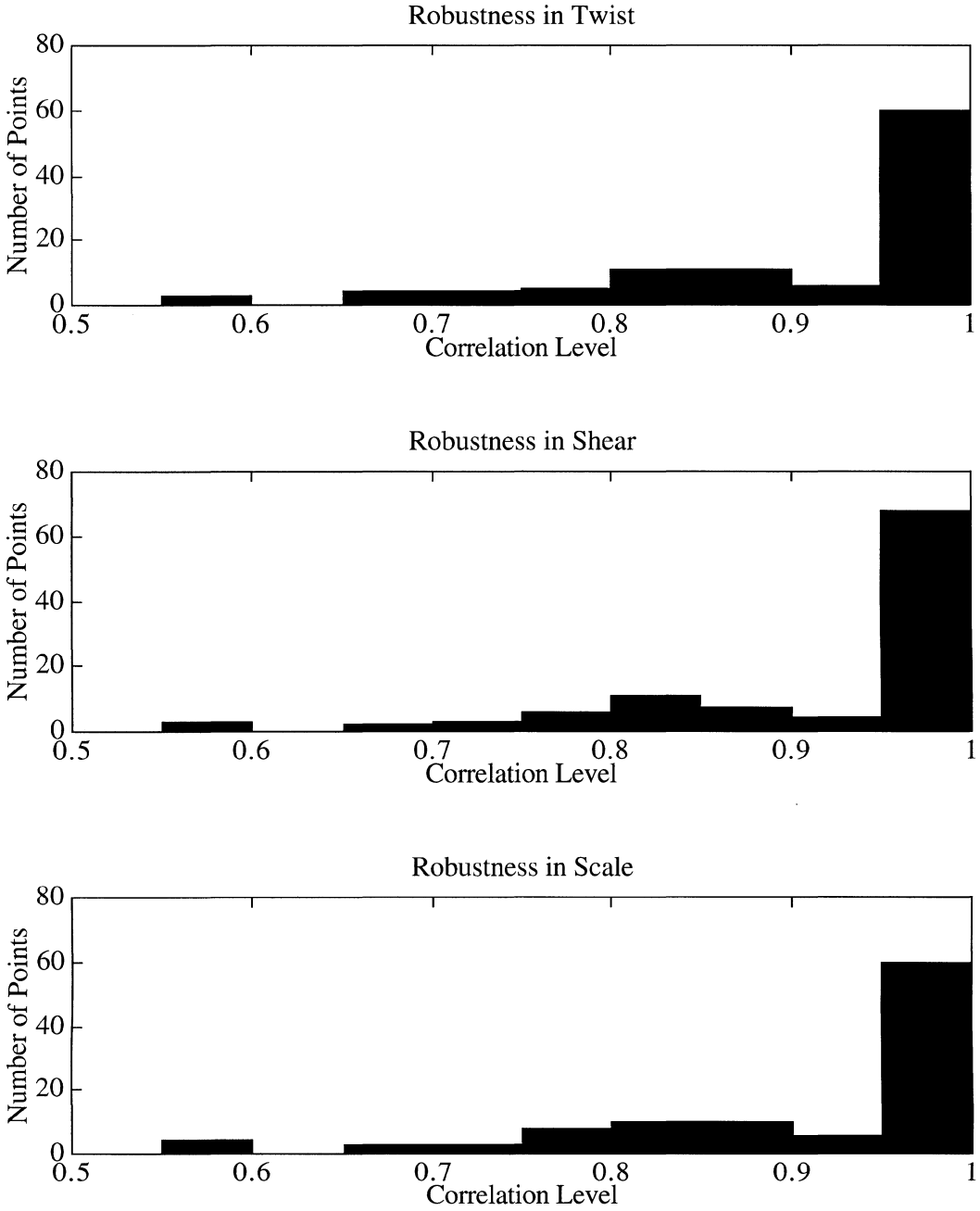

FIGURE 2.15: Histogram of distribution of correlation levels of most influential observations for the NFLDGPS network.

2.6 Discussion

We have demonstrated on the five representative examples shown above that the search for the most influential observations affecting the robustness parameters can be limited to the third connection level. As stated in the Introduction, this does not constitute a firm proof - pathological cases may cause the results from the limited search to be somewhat different. But we are convinced that such pathological cases will be, in all probability, associated with anomalously poor robustness and will thus require a special treatment anyway.

The only other differences encountered are the ones in twist. As explained earlier, the twist values obtained from the limited search approach are affected by any network-wide rotations induced by the biased observation. It is debatable, whether these new twist values are worse indicators of weaknesses in twist than the original ones. It is our conviction that the twist values from the limited search approach can be used equally well for assessing a network.

To check the differences in results for the networks tested, a comparison was made with and without removing the network-wide rotations. Table 2.9 summarizes these results, giving the minimum, maximum, mean and standard deviation of the differences in the twist measure. The differences are much larger for the smaller networks than for the larger ones, as could be expected.

The implementation of the limited search algorithm resulted in a considerable reduction of computational effort. The computation saving is a function of the size of the network and number of observations – the larger the network, the greater the saving. Table 2.10 summarizes the networks we have considered with a limited search to the 3rd connection level. As expected, the relative savings increase with increasing size of network and illustrated in Figure 2.16. Note that the computational effort is given here in terms of the total number of points that need to be searched for all of the observations, instead of actual processing time. This is because the latter varies greatly as a function of user load on Geodetic Survey's multi-user HP9000 computer.

The results for the alternative search algorithm, based on the maximum correlation between the point of interest and the points directly connected by the biased observation, display no uniform level of minimum correlation suitable for general use. The smallest of the maximum correlations for the most influential observations varies from as low as 0.16 to as high as 0.99! Thus it is impossible to determine a priorily what minimum correlation level should be used for any particular network to guarantee correct results. This makes the technique nearly impossible to apply in practice. We have thus to recommend the universal adoption of the "3rd connection level" algorithm.

TABLE 2.9: Summary of differences in robustness in twist (ppm) with and without removing the network-wide rotations.

Network	Minimum	Maximum	Mean	Std. Deviation
HOACS2D	–0.5	13.0	6.8	4.8
REALNET	–0.6	6.0	1.5	1.9
MCEGPS	–1.7	0.2	0.6	0.4
NFLDGPS	–0.9	2.0	0.7	0.2

TABLE 2.10: Summary of computational savings with limited search to 3rd connection level.

Network	No. Points	Total Number Points Searched		Rel. Savings
		Network-Wide	3rd Conn. Level	
HOACS2D	11	638	515	19%
REALNET	58	25114	12404	51%
MCEGPS	91	42315	12591	70%
NFLDGPS	104	27248	4127	85%

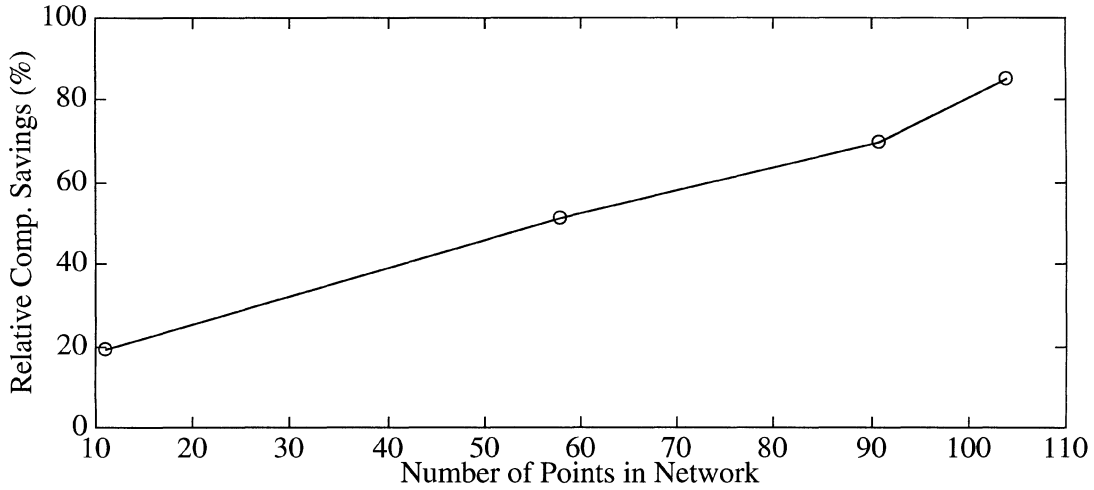

FIGURE 2.16: Trend of relative computational savings using limited search to 3rd connection level with respect to the number of points in network.

3. STRAIN NEIGHBOURHOOD DEFINITION

3.1 Background

The estimation of robustness measures is more fundamentally concerned with the estimation of gradients (i.e., strain) of the coordinate biases induced by a single observation bias. The distribution of coordinate biases can be thought of as a surface represented by point values and the gradients of the surface at each point represent the induced strain deformation. Before estimating the gradient at a point, it is necessary to select a set of points representing the local neighbourhood of the point of interest, to be used in the estimation. The standard approach used in NETAN selects the local neighbourhood as being composed of all the points connected with the point of interest by an observation. As we have pointed out in the Introduction already, strain, being a characterization of local (differential) deformation, calls for the neighbourhood to be as small as possible. This principle may be violated by long observational ties, which frequently occur in GPS networks.

Conventional methods of selecting neighbouring points are based on simple measures, the most common being the distance from the point in question. Figure 3.1 illustrates some of such selection strategies. In Figure 3.1(a) the selection strategy is based on the closest points (in this case the 3 closest ones) while the strategy in Figure 3.1(b) is to use all points within a specified radius (this method is now also available in NETAN). Both methods are adversely affected by an uneven (non-homogenous) distribution of points. In the first method distant points may also exert an excessive influence on the estimated gradients and it is discussed further at the end of this Chapter. The method in Figure 3.1(c) tries to accommodate any ill-distribution of the points by requiring one selected point from each octant around the point of concern. In all these methods, the data from the selected points are usually weighted according to their distance from the point in question. Nevertheless, with these methods, significantly different point selections can result from relatively trivial changes in the coordinates of the points.

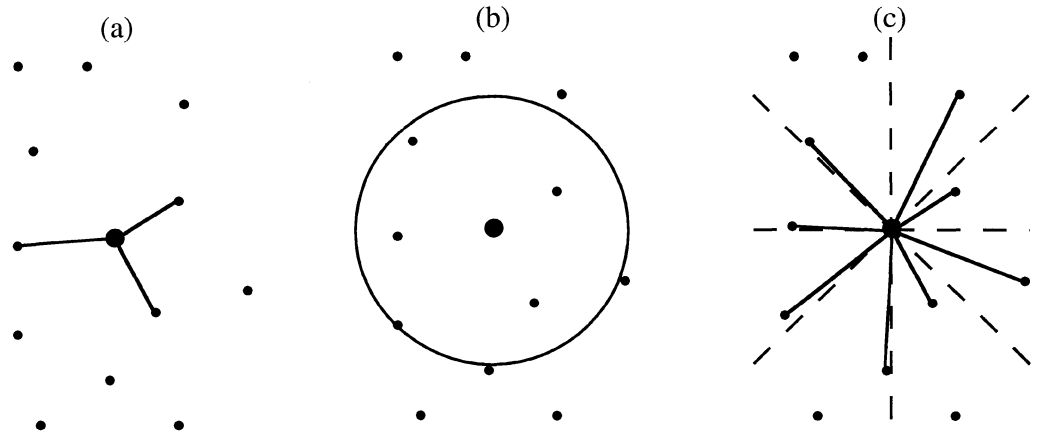

FIGURE 3.1: Traditional neighbourhood definition strategies.

More recently, Voronoi polygons have become one of the most popular ways of representing spatial adjacency in GIS and in cartographic applications such as contouring (Gold, 1989). The Voronoi polygon is not just a mathematical concept, but can be found in nature. Morgan (1967) gives a real world example where, if wicks are put in blotting paper and solvent and ink are added to the wicks, the ink will form a set of convex polygonal "zones of influence" on the blotting paper (see Figure 3.2). The Voronoi diagram or Dirichlet tesselation is the mathematical representation of such convex polygons. Each polygon is associated with a single data point, within which any location is closer to the generating central data point than to any other data point (Sloan, 1987; Gold, 1989). The geometric dual of the Voronoi diagram is the Delaunay triangulation. It is constructed by joining all data points that share a common Voronoi polygon boundary. For the problem at hand, points that share a common polygon boundary (i.e., that are connected by Delaunay triangulation) with the point in question are considered to be adjacent or neighbours; Watson (1992) refers to these are "natural neighbours". Figure 3.3 illustrates the interrelation of both the Voronoi diagram and Delaunay triangulation of a few points.

Delaunay triangulation has some very important properties that make it very attractive in its application. The most important is that the triangulation of a given set of points is always unique. Unlike other triangulation schemes, the result is the same no matter where one begins. Delaunay triangulation also avoids forming so-called shallow triangles with small included angles, whenever possible (Sloan, 1987). The exception is on the boundary of the network where convexity is always enforced and can lead to very long, narrow triangles.

Several algorithms for constructing Delaunay triangulations have been proposed. We have used in the NETAN software the algorithm and FORTRAN subroutines taken from Sloan (1987). This implementation has been shown to be one of the most efficient in terms of both speed and memory, and is suitable for both small and large data sets. In our application to robustness, the triangulation is done in 2D in terms of latitude and longitude. It does not take into account convergence of the meridians and is therefore equivalent to a Delaunay triangulation in terms of UTM coordinates. Although it is possible to perform 3D triangulations (see, e.g., Watson, 1981 and Joe, 1991), the algorithms are much less efficient than for the 2D case and are not likely to result in significant differences except perhaps for large networks at high latitudes.

The effect of using Delaunay ties, instead of observational ties, to define the local neighbourhood (of the point of interest) for computing the robustness parameters is shown for only two of the networks examined in the previous chapter. The HOACS2D network will be used to show the effect on a small chain-type network and the NFLDGPS network will be used to illustrate the application to a large network with some long ties. In these tests, no limited search algorithm was used for detecting the most influential observations (the entire network was searched).

As in the previous chapter the examples in this Chapter use the same Type I and Type II error levels corresponding to a noncentrality parameter of λ=3.61, for all networks. Robustness values for other noncentrality parameters can be easily found by simply rescaling them by λ_{new} / 3.61, where λ_{new} is the new noncentrality parameter.

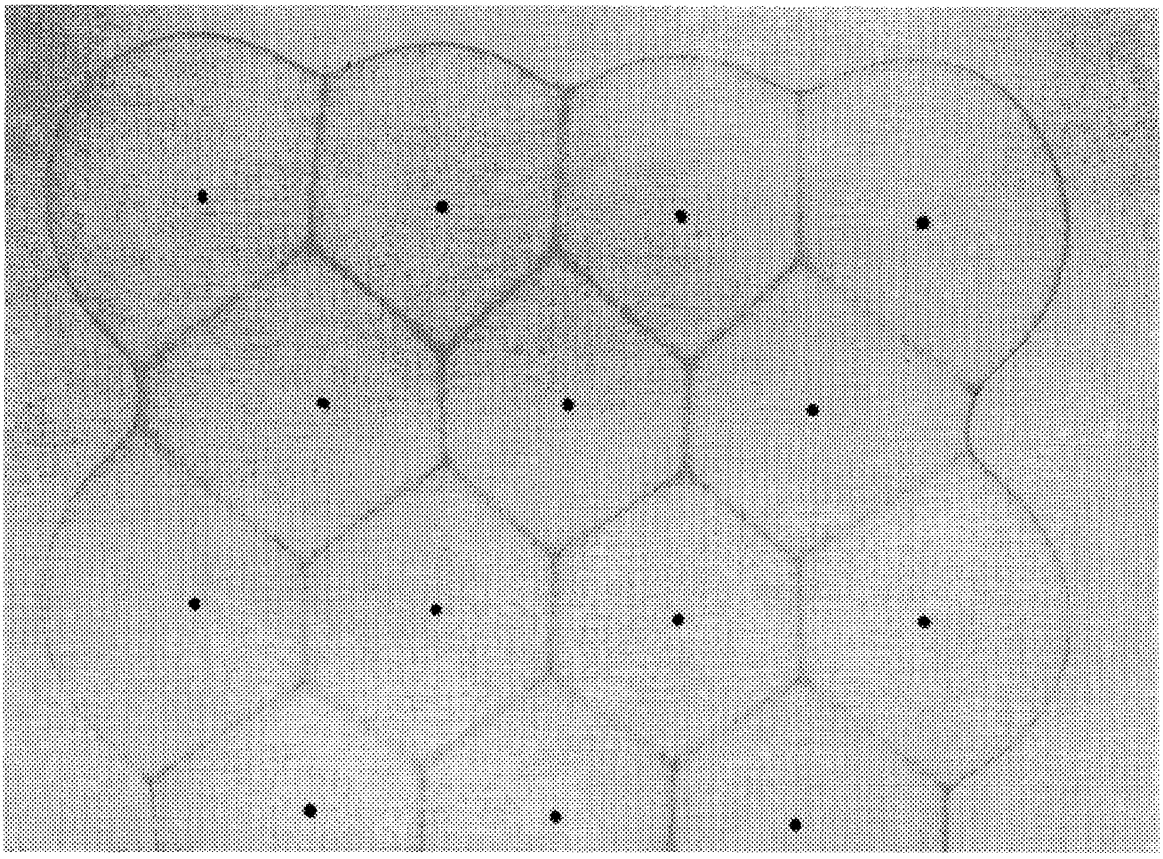

FIGURE 3.2: Voronoi polygons created with blotting paper and wicks (after Morgan, 1967).

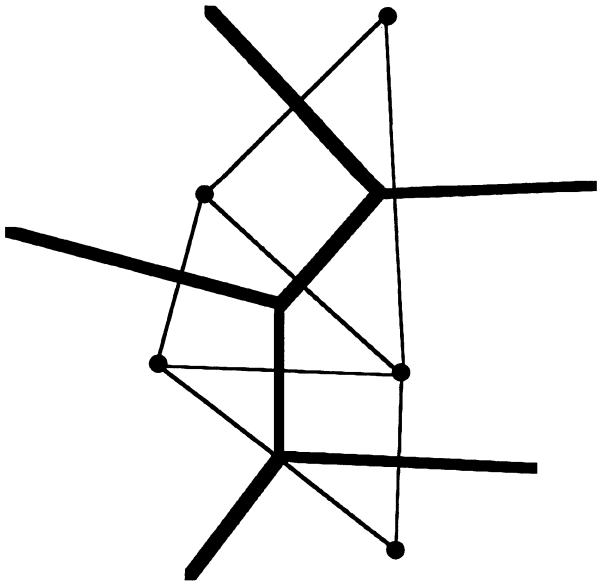

FIGURE 3.3: The Voronoi diagram (bold lines) and Delaunay triangulation (light lines) of a set of 5 points (after Sloan, 1987).

3.2 HOACS2D Network

The observation ties for the HOACS2D network are given in Figure 2.2 of the previous chapter while the Delaunay ties are shown in Figure 3.4 below. We note that the most significant differences between the original network and the Delaunay network are encountered at the peripheral points where the requirement of convexity for Delaunay triangulation manufactures long peripheral ties. We should point out the Delaunay ties between points #2 and 8, 5 and 10, and 6 and 10 in particular.

The resulting robustness measures are given in Table 3.11 and in Figure 3.5, respectively and their comparison with those obtained when using the original observational ties is given in Table 3.12. Inspection of these tables shows that the results are significantly different, the largest differences being at points #1, 5 and 8. The robustness values are different because of the use of different definition of "neighbouring stations" in the their computation. We note that this difference occurs even when the same influential observations are found. However, because the robustness values are computed differently (from differently defined neighbourhood), the selection of the most influential observations producing the largest robustness values will also, in general, be different.

The unwarranted smoothing effect of the long Delaunay ties can be at least partially removed by omitting the long boundary ties. We have omitted all ties outside of the boundary defined by the actual observations (cf. Figure 2.2). Figure 3.6 displays the resulting (modified) Delaunay ties and Table 3.13 and Figure 3.7 give the resulting robustness measures; the differences with respect to those measures based on observation ties are listed in Table 3.14. It can be seen that some of the differences become even worse than when using the long boundary ties. Clearly, the strain computations are very sensitive to the choice of local neighbourhood. Although the best method to use is one which gives both the closest points and a homogenous distribution of points, it is not clear which will be the best one in general, i.e., that based on observation ties or Delaunay ties. The influential observations will not necessarily be the same for neighbourhoods defined by either observation or Delaunay ties. This is because the robustness measures will, in general, be different for each observation bias (they are computed using different neighbourhood points, thus producing different strain measures). Since the robustness measures are different for each observation bias, the largest value will not necessarily be the same, nor will it necessarily occur for the same observation bias.

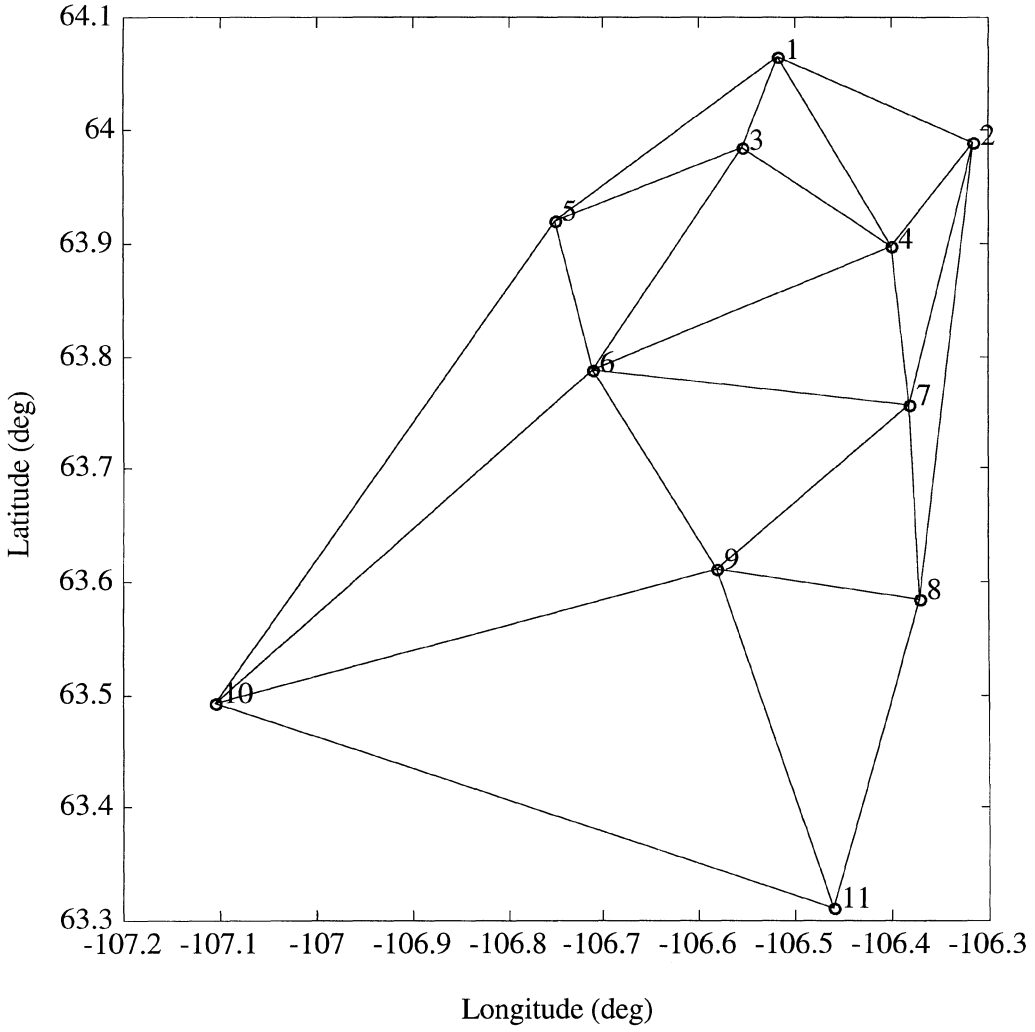

FIGURE 3.4: HOACS2D simulated 2D horizontal network Delaunay triangulation ties.

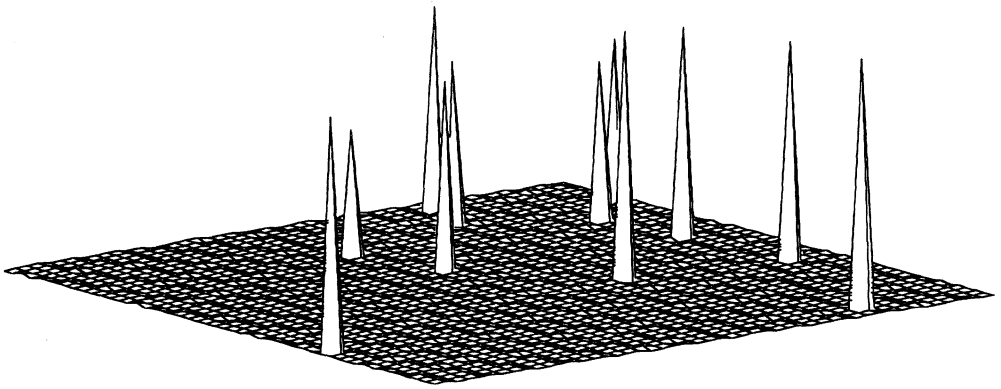

Max Twist Strain = 8.86 ppm, Point # 11

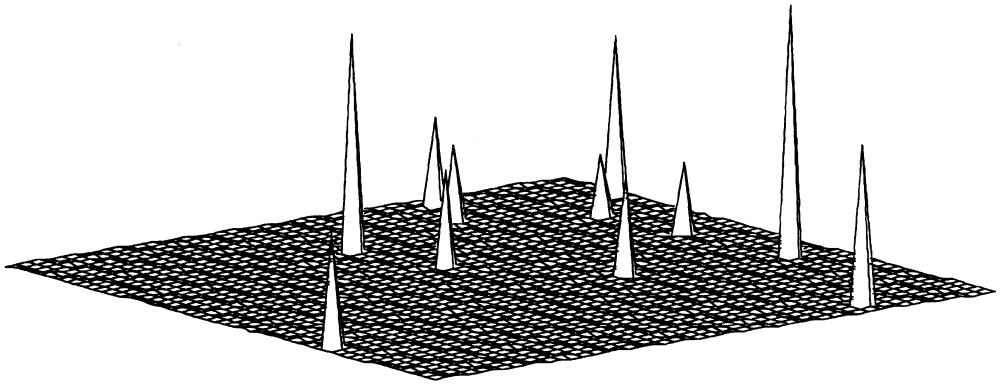

Max Shear Strain = 7.58 ppm, Point # 8

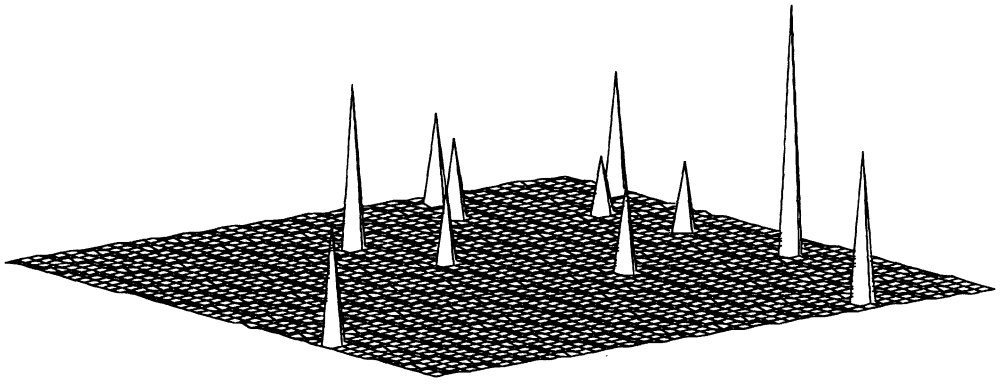

Max Scale Strain = 15.18 ppm, Point # 8

FIGURE 3.5: Surface plots of robustness in twist (top), shear (middle) and scale (bottom) for HOACS2D network with Delaunay ties. View is from SW.

TABLE 3.11: Robustness measures (ppm) for HOACS2D network when using Delaunay ties.

Point	Twist	Shear	Scale
1	7.2	2.7	5.5
2	5.8	4.8	7.5
3	5.8	2.3	4.9
4	5.6	1.8	3.6
5	-4.4	**6.6**	10.1
6	6.7	2.9	4.6
7	7.5	2.1	4.3
8	7.8	7.6	**15.2**
9	8.8	3.0	5.4
10	8.3	3.5	7.5
11	**8.9**	4.8	9.2

TABLE 3.12: Differences in robustness for HOACS2D network when using observation and Delaunay ties respectively. For each robustness measure "Diff" represents the difference in the measure (Delaunay ties minus observation ties), Obs1 the number of the most influential observation based on observation ties, and Obs2 the number of the most influential observation based on Delaunay ties.

	Twist			Shear			Scale		
Point	Diff	Obs1	Obs2	Diff	Obs1	Obs2	Diff	Obs1	Obs2
1	**14.82**	6	17	-3.25	6	44	**-7.14**	40	40
2	-0.78	17	17	1.12	7	3	1.23	41	4
3	-1.44	17	17	-0.41	44	44	-0.66	40	44
4	0.81	17	21	-0.24	45	24	-1.08	45	45
5	**-9.29**	17	48	3.68	48	48	3.81	48	48
6	0.14	21	21	0.87	52	33	0.48	52	56
7	-0.09	21	21	-0.38	22	54	-0.17	52	54
8	-1.05	21	21	**4.59**	34	54	**9.74**	56	54
9	-0.33	21	21	-0.68	32	34	-1.21	56	56
10	-0.51	21	21	-1.33	30	34	-1.72	55	56
11	0.02	21	21	-0.63	30	30	-0.92	55	55

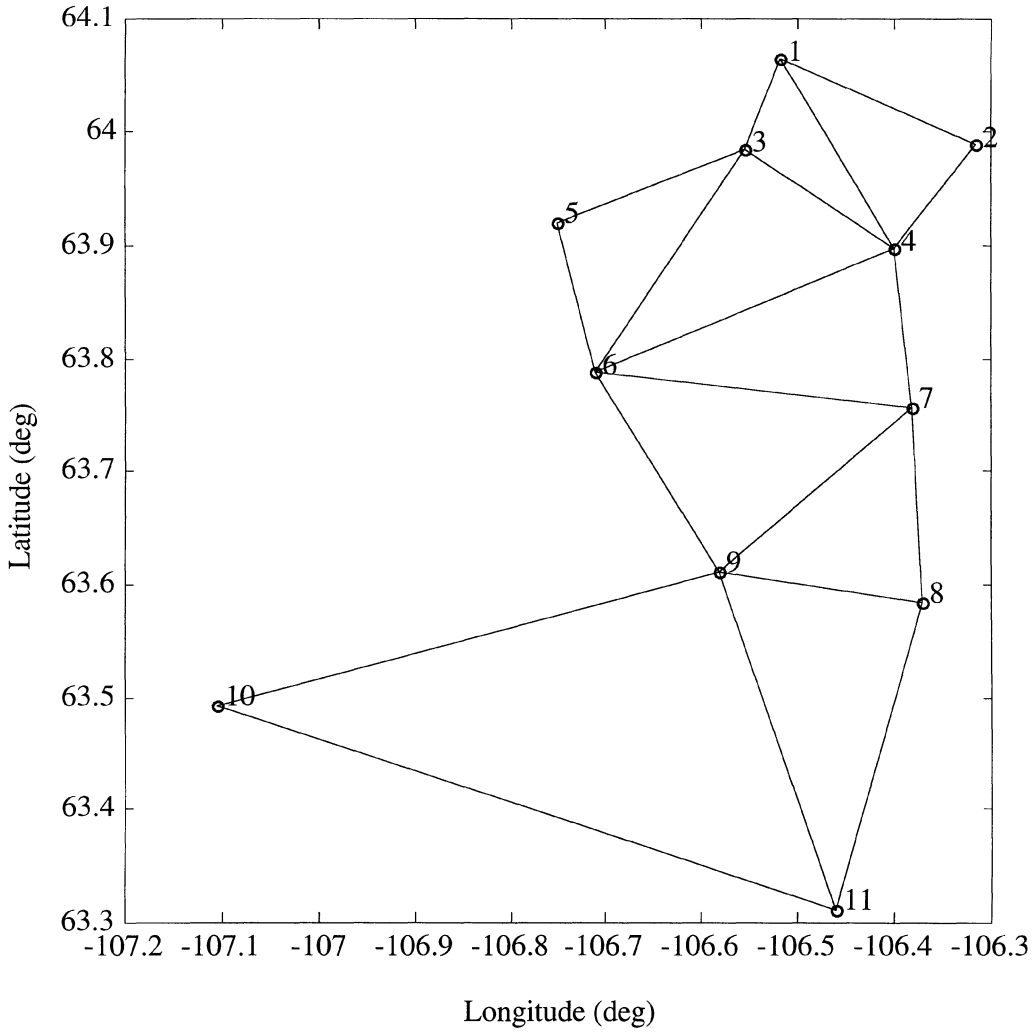

FIGURE 3.6: HOACS2D simulated 2D horizontal network Delaunay triangulation ties within boundary defined by observations ties (cf. Figure 2.2).

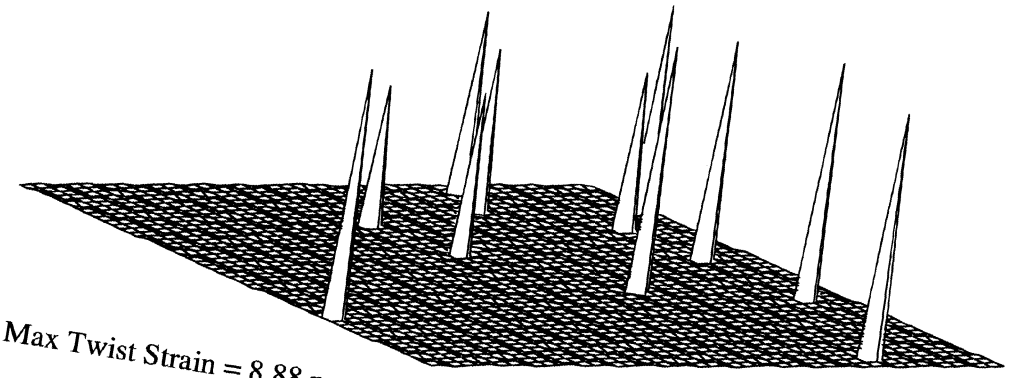

Max Twist Strain = 8.88 ppm, Point # 10

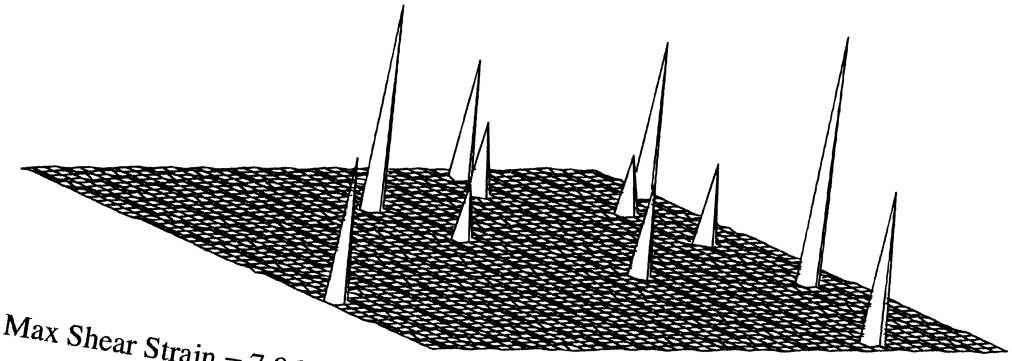

Max Shear Strain = 7.86 ppm, Point # 8

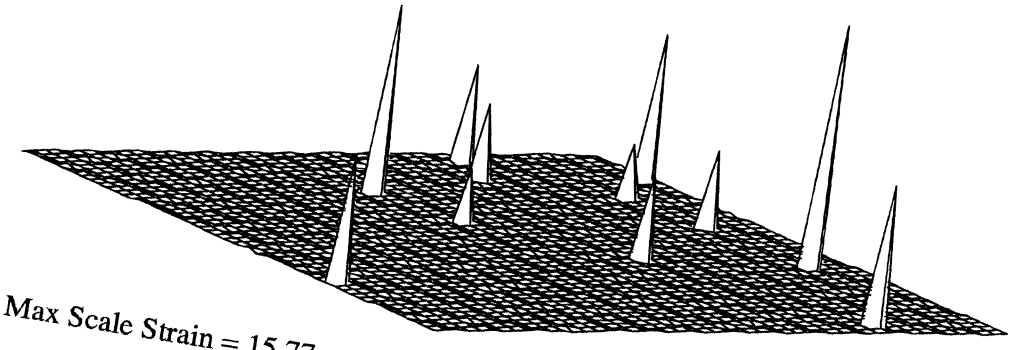

Max Scale Strain = 15.77 ppm, Point # 8

FIGURE 3.7: Surface plots of robustness in twist (top), shear (middle) and scale (bottom) for HOACS2D network with modified Delaunay ties in Figure 20. View is from SW.

TABLE 3.13: Robustness measures (ppm) for HOACS2D network when using modified Delaunay ties in Figure 21.

Point	Twist	Shear	Scale
1	6.5	3.7	6.3
2	-7.4	4.9	9.6
3	5.8	2.3	4.9
4	5.6	1.8	3.6
5	5.0	6.5	12.3
6	5.8	1.8	3.5
7	7.9	2.5	5.0
8	8.6	**7.9**	**15.8**
9	8.8	3.0	5.4
10	**8.9**	4.5	8.3
11	**8.9**	4.8	9.2

TABLE 3.14: Differences in robustness for HOACS2D network when using observation and modified Delaunay ties in Figure 21. For each robustness measure "Diff" represents the difference in the measure (Delaunay ties minus observation ties), Obs1 the number of the correct most influential observation based on observation ties, and Obs2 the number of the most influential observation based on Delaunay ties.

	Twist			Shear			Scale		
Point	Diff	Obs1	Obs2	Diff	Obs1	Obs2	Diff	Obs1	Obs2
1	**14.13**	6	17	-2.24	6	7	**-6.35**	40	41
2	**-13.96**	17	14	1.24	7	4	3.24	41	41
3	-1.44	17	17	-0.41	44	44	-0.66	40	44
4	0.81	17	21	-0.24	45	24	-1.08	45	45
5	0.18	17	17	3.65	48	44	6.00	48	44
6	-0.70	21	21	-0.27	52	25	-0.68	52	44
7	0.31	21	21	0.02	22	54	0.53	52	54
8	-0.26	21	21	**4.87**	34	54	**10.33**	56	54
9	-0.33	21	21	-0.68	32	34	-1.21	56	56
10	0.02	21	21	-0.27	30	34	-0.84	55	55
11	0.02	21	21	-0.63	30	30	-0.92	55	55

3.3 NFLDGPS Network

The observation ties for the 3D NFLDGPS network are given in Figure 2.12 of the previous chapter while the Delaunay ties are shown in Figure 3.8. We note again the considerable change in the geometry of the network along the periphery and the very long ties introduced by Delaunay algorithm. Again we note that the most significant differences between the original network and Delaunay network are encountered at the peripheral points where very long ties are introduced by the Delaunay triangulation. We point out the ties between points #24 and 103, 36 and 69, and 77 and 97 in particular.

The resulting robustness measures are given in Table 3.15 and Figure 3.9, and their comparison with those obtained when using the original observational ties is shown in Table 3.16. Table 3.17 summarizes the differences. Inspection of these tables show that the results are very significantly different, the largest differences (in absolute value) being up to 38 ppm at point #78 as compared to the largest measures which are all smaller than 10. The robustness values are different because of the use of different neighbouring stations in their computation (e.g., for point #78 the Delaunay method uses point #64 far to the east, while the observation method uses only points along the NE traverse line). As for the HOACS2D network, the differences are large even when the same influential observations are found. But, because the robustness values are different, the selection of the most influential observations producing the largest robustness values will also, in general, be different.

The smoothing effect of the long Delaunay ties can be removed by omitting the long boundary ties. As for the HOACS2D example, we have omitted all ties outside of the boundary approximately defined by the actual observations (cf. Figure 2.12). Figure 3.10 displays the resulting (modified) Delaunay ties, Table 3.18 and Figure 3.11 give the resulting robustness measures and the differences with respect to those based on observation ties are shown in Table 3.19 and summarized in Table 3.20. From Table 3.20 it can be seen that omitting the long ties doesn't affect the overall picture. Clearly, the strain computations are very sensitive to the choice of local neighbourhood.

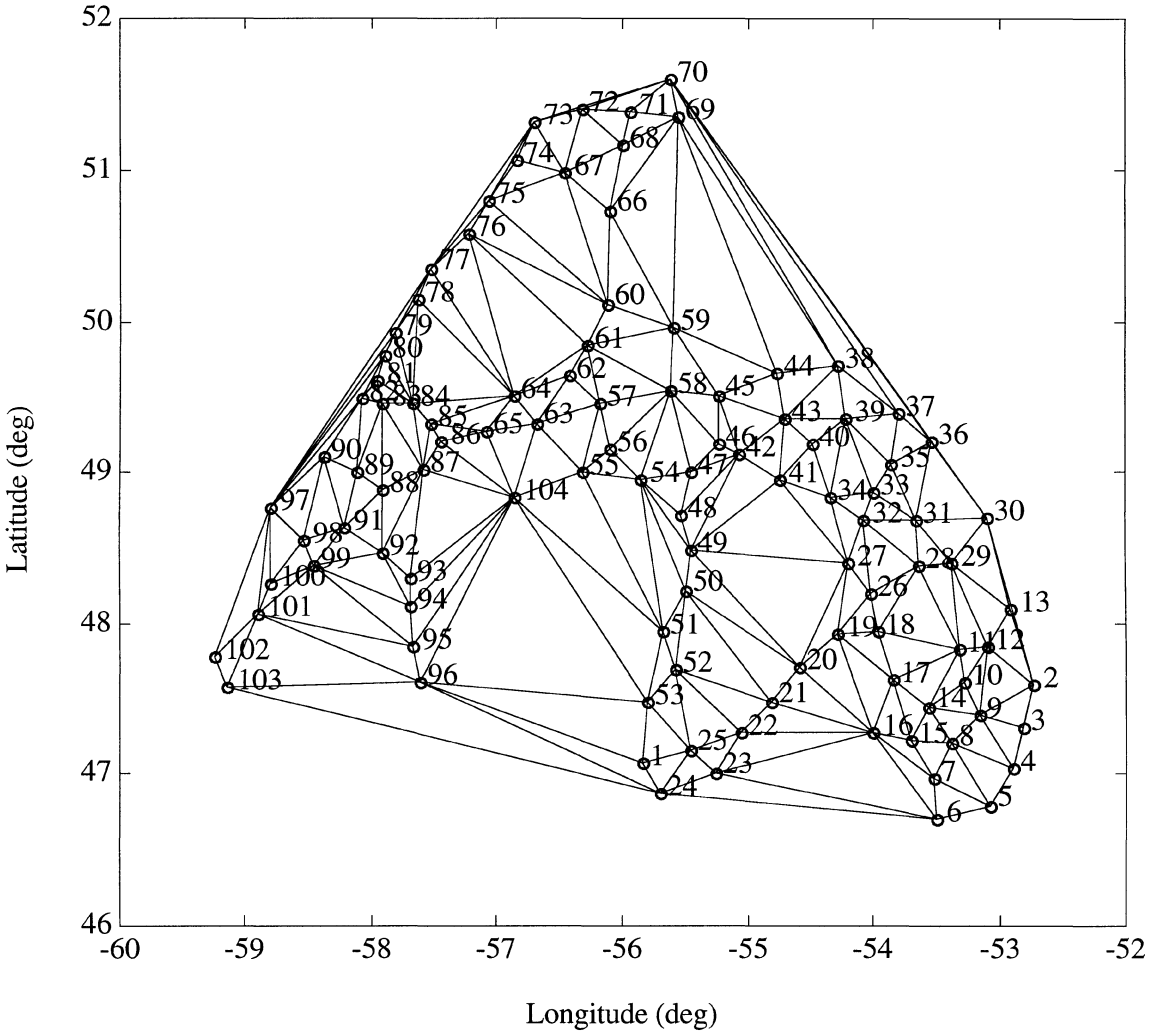

FIGURE 3.8: NFLDGPS 3D network Delaunay triangulation ties.

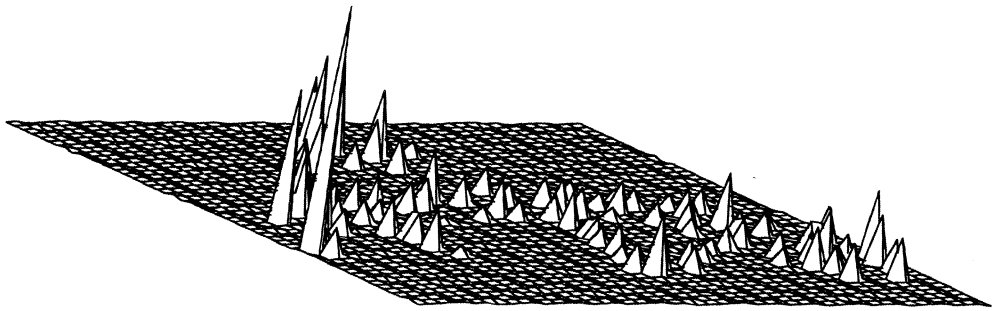

Max Twist Strain = -4.78 ppm, Point # 102

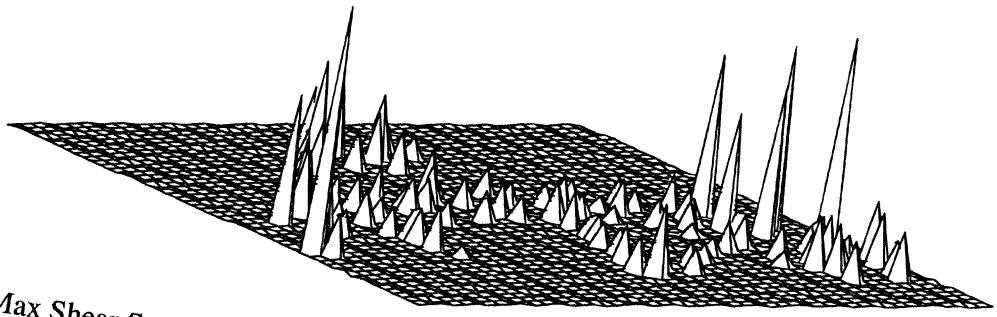

Max Shear Strain = 5.59 ppm, Point # 102

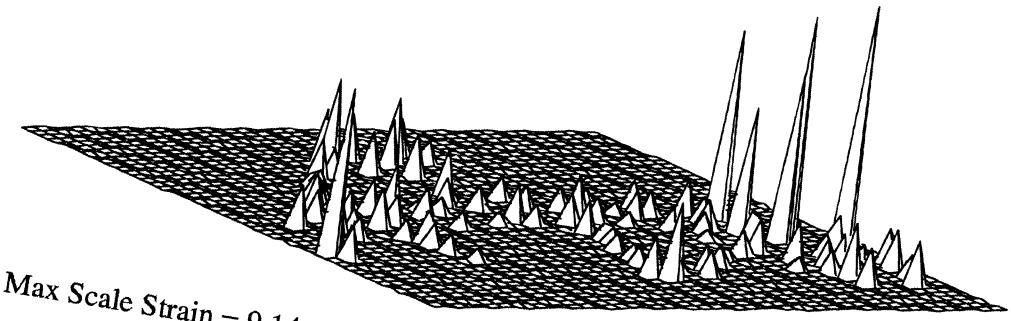

Max Scale Strain = 9.14 ppm, Point # 13

FIGURE 3.9: Surface plots of robustness in twist (top), shear (middle) and scale (bottom) for NFLDGPS network with Delaunay ties. View is from SW.

TABLE 3.15: Robustness measures (ppm) for NFLDGPS network with Delaunay ties.

Point	Twist	Shear	Scale
1	-0.6	0.8	1.5
2	-1.2	1.3	1.4
3	-1.0	1.2	1.5
4	0.6	0.7	0.8
5	0.8	1.1	1.7
6	-0.7	0.9	1.4
7	-0.5	1.1	2.1
8	0.4	0.7	0.9
9	0.5	0.6	0.8
10	-0.9	1.0	1.1
11	-0.5	0.6	0.8
12	0.5	0.8	1.5
13	-0.7	4.7	9.1
14	-0.5	0.7	1.1
15	-0.8	1.2	0.9
16	0.3	0.4	0.5
17	-0.5	0.8	1.5
18	0.5	0.7	1.2
19	0.4	0.6	1.0
20	-0.3	0.4	0.4
21	-0.3	0.4	0.8
22	-0.5	0.6	0.9
23	0.5	0.6	1.0
24	-1.2	1.6	2.9
25	-0.6	0.6	0.8
26	-0.4	0.7	1.4
27	-0.3	0.3	0.4
28	0.5	0.5	0.9
29	-0.4	3.3	6.3
30	0.3	4.1	**8.2**
31	1.1	2.6	4.8
32	0.5	0.6	0.8
33	-0.4	0.6	1.1
34	-0.4	0.6	0.8
35	-0.5	0.6	1.0
36	0.5	3.6	7.2
37	-0.3	0.8	1.3
38	0.2	0.5	1.0
39	-0.4	0.5	0.9
40	0.6	0.8	1.0
41	-0.2	0.3	0.5
42	0.5	0.6	0.9
43	0.3	0.3	0.5
44	-0.4	0.5	0.7
45	-0.5	0.5	0.9
46	-0.6	0.9	1.6
47	-0.5	0.9	1.2
48	-0.7	0.8	1.2
49	-0.3	0.4	0.7
50	-0.4	0.6	0.6
51	-0.4	0.6	0.6
52	-0.5	0.6	0.6
53	-0.3	0.8	0.7
54	-0.3	0.6	0.8
55	-0.3	0.7	0.5
56	0.7	0.8	1.4
57	0.6	0.6	0.9
58	-0.4	0.5	0.9
59	-0.5	0.6	0.9

TABLE 3.15 Con't.

Point	Twist	Shear	Scale
60	-0.3	0.9	1.8
61	0.4	0.5	0.6
62	1.0	0.9	1.1
63	0.6	0.7	0.6
64	0.3	0.5	0.4
65	0.6	0.8	1.1
66	-0.7	0.9	1.7
67	0.5	0.9	1.5
68	0.8	1.1	1.8
69	-0.3	0.5	0.8
70	0.3	0.7	1.4
71	1.3	1.4	2.4
72	1.8	1.8	1.7
73	1.5	1.6	2.0
74	2.1	2.4	3.5
75	1.1	1.1	1.1
76	0.7	1.1	1.6
77	-0.3	0.4	0.5
78	0.3	0.5	0.8
79	-0.6	1.0	0.9
80	0.5	0.8	0.8
81	0.5	0.8	1.0
82	-1.1	1.5	1.4
83	-0.5	0.6	1.1
84	-0.3	0.4	0.7
85	-0.6	0.8	1.3
86	0.7	1.1	2.0
87	0.4	0.6	1.1
88	-0.5	0.8	1.4
89	-0.7	1.0	1.2
90	-1.2	1.6	1.1
91	-0.5	0.6	0.8
92	-0.7	0.7	0.7
93	-0.5	0.7	1.2
94	0.5	0.8	0.8
95	0.8	1.0	0.7
96	-0.2	0.3	0.5
97	-2.6	2.9	1.6
98	-1.2	1.5	1.4
99	0.5	0.6	0.8
100	-1.9	2.0	1.6
101	0.5	0.7	0.9
102	**-4.8**	**5.6**	6.3
103	-0.5	1.0	1.3
104	-0.1	0.5	0.6

TABLE 3.16: Differences in robustness for NFLDGPS network when using observation and Delaunay ties. For each robustness measure "Diff" represents the difference in the measure (Delaunay ties minus observation ties), Obs1 the number of the correct most influential observation based on observation ties, and Obs2 the number of the most influential observation based on Delaunay ties.

	Twist			Shear			Scale		
Point	Diff	Obs1	Obs2	Diff	Obs1	Obs2	Diff	Obs1	Obs2
1	0.22	559	514	0.02	559	562	0.49	559	562
2	-2.23	55	130	-0.32	55	130	-1.54	55	55
3	0.00	619	619	0.00	619	619	0.00	616	616
4	-0.17	10	10	-0.28	10	10	-0.63	10	55
5	-3.96	10	25	-4.09	10	10	-3.90	10	10
6	-1.28	46	43	0.01	10	43	-0.11	613	43
7	0.22	775	43	0.00	775	10	0.64	22	10
8	-0.15	613	10	0.01	613	10	-0.05	613	613
9	0.02	55	55	0.05	55	55	-0.05	769	55
10	-1.60	70	607	0.21	70	607	-0.05	70	766
11	-0.52	0	34	0.59	0	34	0.82	0	40
12	-0.52	55	55	-0.33	610	610	-0.63	610	610
13	0.09	130	79	0.87	130	130	1.92	130	130
14	-0.03	775	37	0.09	70	37	0.03	70	607
15	-0.09	43	43	0.02	43	43	-0.03	40	40
16	1.35	43	67	-2.96	43	64	-0.55	61	601
17	0.24	97	34	-0.64	34	607	-1.24	34	607
18	1.16	97	607	-0.19	97	607	-0.01	61	607
19	-0.14	67	67	-0.01	64	64	0.00	61	61
20	-4.73	106	559	-4.56	64	112	-5.44	106	601
21	0.65	601	559	-0.62	601	67	-0.57	601	67
22	-1.47	583	559	-0.46	586	559	-0.15	583	67
23	-1.37	583	46	-1.35	583	43	-0.59	583	43
24	1.11	592	514	-0.69	592	514	0.70	592	514
25	0.52	586	562	-0.57	586	562	-0.38	586	559
26	0.34	91	91	-0.07	91	103	0.48	91	103
27	0.13	91	559	-0.66	103	559	-1.42	103	187
28	0.09	610	607	-0.01	139	34	0.06	745	91
29	-0.89	610	79	2.09	103	130	4.07	745	130
30	-0.87	127	130	-3.19	130	130	-5.98	130	130
31	0.01	130	130	-0.01	130	130	0.01	130	130
32	-0.06	196	139	-0.13	139	139	-0.22	745	745
33	-1.12	196	157	-0.12	196	154	0.19	133	154
34	0.04	214	214	-0.20	730	730	-0.16	217	724
35	5.75	154	157	-5.84	154	157	-4.36	199	133
36	1.01	157	130	2.95	157	130	6.15	133	130
37	1.97	148	157	-3.34	148	157	-6.33	148	160
38	-0.24	718	148	-0.15	715	160	-0.25	715	160
39	-0.08	169	157	0.12	715	160	0.17	715	160
40	0.23	187	727	0.40	727	727	0.44	202	724
41	-0.90	187	559	-0.46	727	547	-0.39	202	202
42	-1.40	205	187	-1.50	205	187	-1.61	544	187
43	0.92	166	718	-0.33	166	730	-0.59	202	715
44	-0.72	718	241	0.12	715	241	-0.05	715	382
45	-0.94	718	241	0.11	193	241	0.27	715	202
46	-0.19	178	712	0.47	178	544	0.96	202	544
47	0.32	700	712	-0.04	547	547	0.14	544	544
48	-1.09	697	703	0.20	256	547	0.34	697	544
49	-3.48	706	559	-4.97	532	547	-9.09	532	544
50	0.62	529	559	-0.83	538	559	-1.35	532	553
51	1.36	529	700	-1.51	529	700	-0.35	541	694
52	-0.33	514	559	0.13	514	562	0.15	499	553

TABLE 3.16 Con't.

	Twist			Shear			Scale		
Point	Diff	Obs1	Obs2	Diff	Obs1	Obs2	Diff	Obs1	Obs2
53	3.31	562	514	-3.09	526	514	-1.64	562	520
54	-0.79	697	700	-0.27	547	700	-0.08	544	259
55	-0.69	235	700	-0.15	700	700	0.07	682	238
56	0.31	697	694	-0.76	700	700	0.14	238	259
57	-0.05	256	256	-0.10	256	256	-0.04	259	259
58	0.61	241	241	-0.70	241	358	-0.90	241	367
59	2.44	358	358	-4.60	358	358	-6.02	367	367
60	-1.30	367	310	-0.07	367	409	0.57	367	409
61	-1.13	685	367	-1.72	358	262	-3.86	358	241
62	0.46	685	685	0.29	685	685	0.19	268	268
63	-0.03	700	700	-0.01	700	700	0.00	700	700
64	1.46	358	274	-0.89	358	310	-1.74	358	274
65	-0.16	226	226	-0.22	235	310	-0.06	274	274
66	0.45	358	409	-1.21	358	367	-1.41	367	382
67	-0.41	409	358	-0.11	409	409	0.49	409	409
68	1.85	361	409	0.01	361	382	1.01	361	382
69	-0.31	0	241	0.48	0	241	0.83	0	382
70	0.27	0	130	0.68	0	394	1.36	0	394
71	-0.17	409	409	-0.09	409	394	1.14	409	394
72	2.70	346	409	0.70	340	409	0.21	346	409
73	-0.11	409	409	-0.14	409	409	-0.07	409	409
74	0.70	400	409	0.88	352	409	1.04	352	409
75	4.50	343	358	-2.51	343	358	-3.00	331	358
76	-11.39	331	358	-11.22	331	358	-12.72	331	358
77	4.58	343	310	-4.74	343	310	-3.63	337	307
78	**-25.35**	**334**	**307**	**-27.23**	**334**	**310**	**-37.71**	**334**	**307**
79	-6.10	334	442	-5.05	334	442	-7.71	334	499
80	10.43	283	280	-10.40	283	442	-11.69	412	499
81	0.00	637	637	0.18	640	640	0.07	652	634
82	-1.70	424	442	0.76	427	442	0.21	499	424
83	0.22	646	499	-0.63	646	316	-1.23	646	319
84	0.18	676	676	-0.13	676	310	0.00	676	307
85	0.25	676	676	-0.15	676	274	0.16	676	274
86	0.10	274	235	0.21	274	274	0.60	499	274
87	-4.63	496	226	-4.57	496	499	-4.88	496	499
88	0.85	316	490	-0.54	316	496	0.25	316	496
89	-0.26	427	427	0.44	424	427	0.21	424	661
90	0.34	658	442	-0.28	658	442	-1.85	661	436
91	0.59	490	478	-0.54	490	478	-0.27	490	424
92	-1.55	487	490	-3.07	442	490	-3.88	490	496
93	-0.03	520	496	-0.51	514	235	0.08	520	235
94	7.24	472	514	-9.91	472	514	-9.83	445	235
95	7.47	472	514	-9.67	472	514	-9.90	445	514
96	0.33	466	700	-0.55	463	463	-0.32	466	226
97	-0.10	442	442	-1.42	442	442	-6.12	442	442
98	0.00	442	442	0.07	442	442	0.32	436	436
99	1.13	490	514	-0.16	439	514	0.02	436	436
100	13.95	433	442	-14.45	433	442	-10.66	433	451
101	-2.40	463	514	-2.88	463	514	-4.35	463	514
102	-3.90	463	460	2.79	460	460	4.41	439	463
103	0.20	466	514	-0.52	463	460	-0.59	466	514
104	-0.93	700	514	-0.42	235	514	-0.35	229	499

TABLE 3.17: Summary statistics of differences in robustness for NFLDGPS network when using observation and Delaunay ties (cf. Table 3.16). Note: "mean" denotes average of absolute values of robustness measures. All values in ppm.

	Minimum	Maximum	Mean	St.Dev.
Diff. in Twist	-25.4	14.0	1.7	3.4
Diff. in Shear	-27.2	3.0	1.8	3.6
Diff. in Scale	-37.7	6.1	2.2	4.5

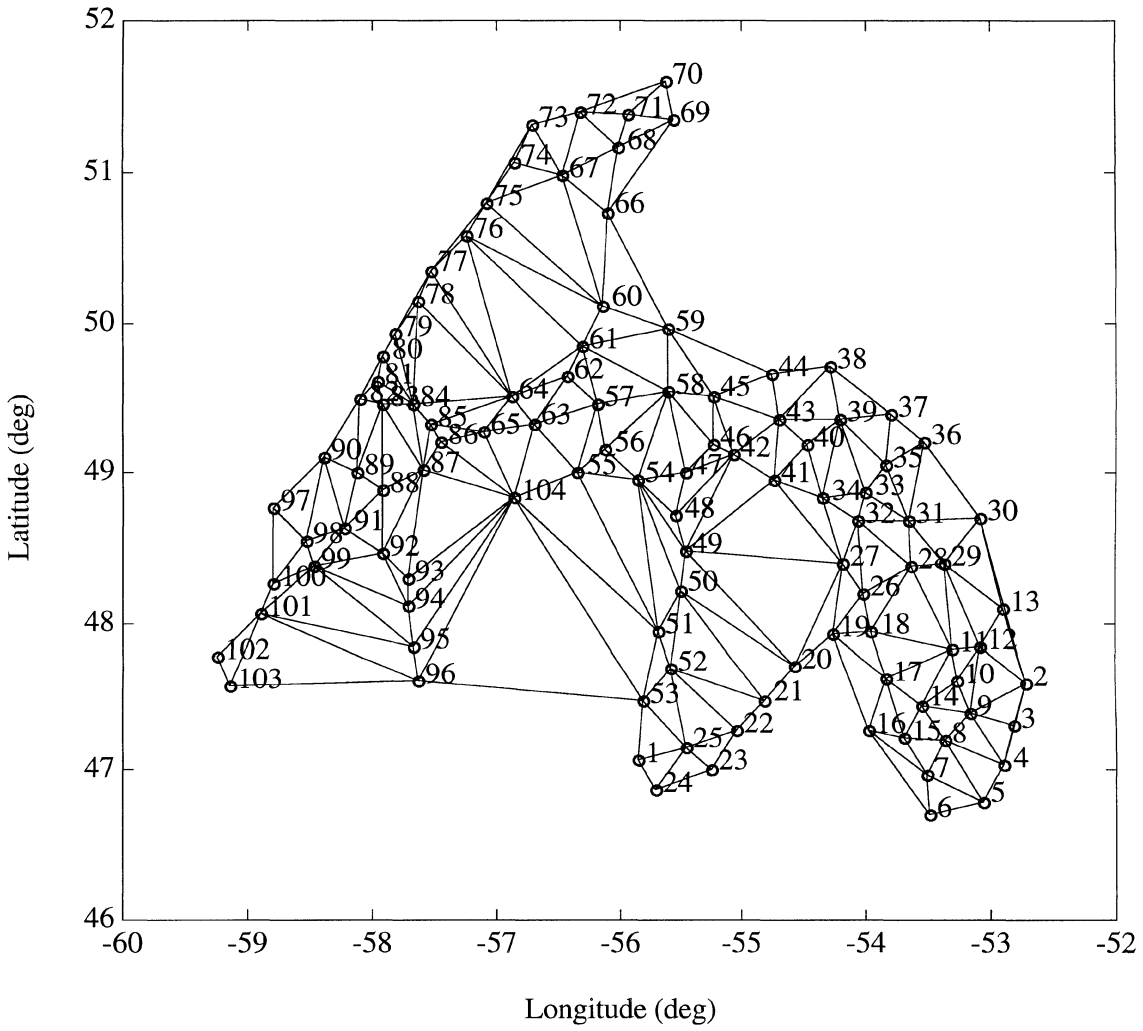

FIGURE 3.10: NFLDGPS 3D network Delaunay triangulation ties within boundary approximately defined by observations ties (cf. Figure 2.12).

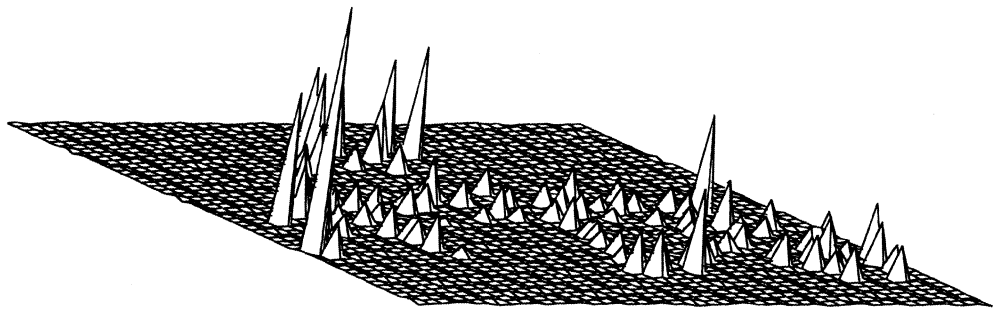

Max Twist Strain = -5.68 ppm, Point # 102

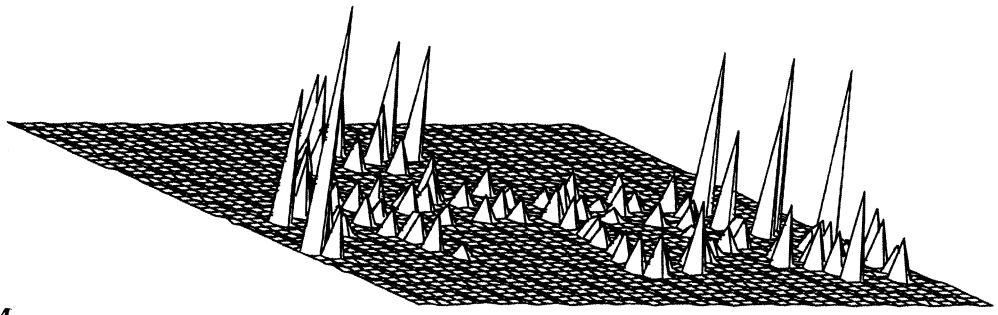

Max Shear Strain = 6.58 ppm, Point # 102

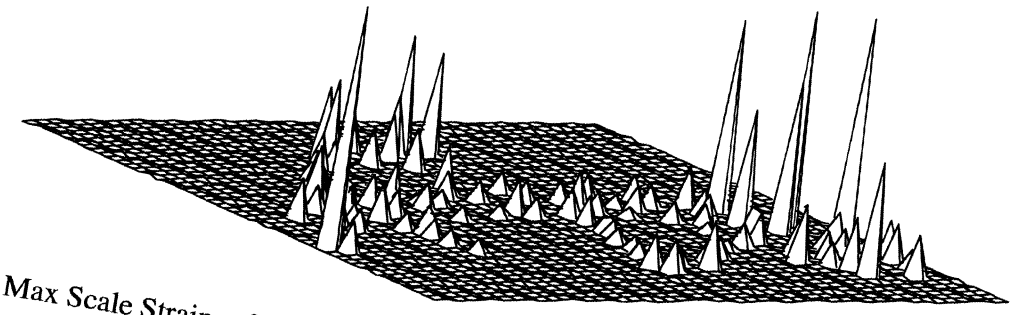

Max Scale Strain = 9.99 ppm, Point # 102

FIGURE 3.11: Surface plots of robustness in twist (top), shear (middle) and scale (bottom) for NFLDGPS network with modified Delaunay ties in Figure 20. View is from SW.

TABLE 3.18: Robustness measures (ppm) for NFLDGPS network with modified Delaunay ties in Figure 3.10.

Point	Twist	Shear	Scale
1	-1.0	1.0	1.4
2	-1.2	1.3	1.4
3	-1.0	1.2	1.5
4	0.6	0.7	0.8
5	0.8	1.1	1.7
6	-0.7	2.4	4.7
7	-0.5	1.1	2.1
8	0.4	0.7	0.9
9	0.5	0.6	0.8
10	-0.9	1.0	1.1
11	-0.5	0.6	0.8
12	0.5	0.8	1.5
13	-0.7	4.7	9.1
14	-0.5	0.7	1.1
15	-0.8	1.2	0.9
16	-0.8	1.6	2.3
17	-0.5	0.8	1.5
18	0.5	0.7	1.2
19	0.4	0.6	1.0
20	-0.4	0.4	0.4
21	-0.6	0.6	0.7
22	-0.8	0.8	0.8
23	1.9	1.9	2.0
24	-1.1	1.1	1.4
25	-0.6	0.6	0.8
26	-0.4	0.7	1.4
27	-0.3	0.3	0.4
28	0.5	0.5	0.9
29	-0.4	3.3	6.3
30	0.6	4.5	8.8
31	1.1	2.6	4.8
32	0.5	0.6	0.8
33	-0.4	0.6	1.1
34	-0.4	0.6	0.8
35	-0.5	0.6	1.0
36	2.3	4.3	7.8
37	-0.5	1.0	1.6
38	0.5	0.8	1.0
39	-0.4	0.5	0.9
40	0.6	0.8	1.0
41	-0.2	0.3	0.5
42	0.5	0.6	0.9
43	0.3	0.3	0.5
44	-0.8	0.8	1.1
45	-0.5	0.5	0.9
46	-0.6	0.9	1.6
47	-0.5	0.9	1.2
48	-0.7	0.8	1.2
49	-0.3	0.4	0.7
50	-0.4	0.6	0.6
51	-0.4	0.6	0.6
52	-0.5	0.6	0.6
53	-0.3	0.8	0.7
54	-0.3	0.6	0.8
55	-0.3	0.7	0.5
56	0.7	0.8	1.4
57	0.6	0.6	0.9
58	-0.4	0.5	0.9

TABLE 3.18 Con't.

Point	Twist	Shear	Scale
59	-0.6	0.7	0.8
60	-0.3	0.9	1.8
61	0.4	0.5	0.6
62	1.0	0.9	1.1
63	0.6	0.7	0.6
64	0.3	0.5	0.4
65	0.6	0.8	1.1
66	-0.7	0.9	1.7
67	0.5	0.9	1.5
68	0.8	1.1	1.8
69	2.5	2.9	4.3
70	-2.1	2.9	4.6
71	1.3	1.4	2.4
72	1.8	1.8	1.7
73	2.0	2.2	2.8
74	2.1	2.4	3.5
75	1.1	1.1	1.1
76	0.7	1.1	1.6
77	0.3	0.5	0.7
78	0.3	0.5	0.8
79	0.6	0.9	1.6
80	0.6	0.7	0.9
81	0.5	0.8	1.0
82	-1.3	1.6	2.3
83	-0.5	0.6	1.1
84	-0.3	0.4	0.7
85	-0.6	0.8	1.3
86	0.7	1.1	2.0
87	0.4	0.6	1.1
88	-0.5	0.8	1.4
89	-0.7	1.0	1.2
90	-1.2	1.6	1.1
91	-0.5	0.6	0.8
92	-0.7	0.7	0.7
93	-0.5	0.7	1.2
94	0.5	0.8	0.8
95	0.8	1.0	0.7
96	-0.2	0.3	0.5
97	-3.0	3.6	1.7
98	-1.2	1.5	1.4
99	0.5	0.6	0.8
100	-1.9	2.0	1.6
101	0.6	0.8	0.9
102	-5.7	6.6	10.0
103	-0.8	1.3	1.2
104	-0.1	0.5	0.6

TABLE 3.19: Differences in robustness for NFLDGPS network when using observation and modified Delaunay ties in Figure 3.10. For each robustness measure "Diff" represents the difference in the measure (Delaunay ties minus observation ties), Obs1 the number of the correct most influential observation based on observation ties, and Obs2 the number of the most influential observation based on Delaunay ties.

	Twist			Shear			Scale		
Point	Diff	Obs1	Obs2	Diff	Obs1	Obs2	Diff	Obs1	Obs2
1	-0.20	559	562	0.18	559	562	0.39	559	592
2	-2.23	55	130	-0.32	55	130	-1.54	55	55
3	0.00	619	619	0.00	619	619	0.00	616	616
4	-0.17	10	10	-0.28	10	10	-0.63	10	55
5	-3.96	10	25	-4.09	10	10	-3.90	10	10
6	-1.33	46	43	1.51	10	10	3.20	613	10
7	0.22	775	43	0.00	775	10	0.64	22	10
8	-0.15	613	10	0.01	613	10	-0.05	613	613
9	0.02	55	55	0.05	55	55	-0.05	769	55
10	-1.60	70	607	0.21	70	607	-0.05	70	766
11	-0.52	0	34	0.59	0	34	0.82	0	40
12	-0.52	55	55	-0.33	610	610	-0.63	610	610
13	0.09	130	79	0.87	130	130	1.92	130	130
14	-0.03	775	37	0.09	70	37	0.03	70	607
15	-0.09	43	43	0.02	43	43	-0.03	40	40
16	0.31	43	43	-1.74	43	43	1.29	61	61
17	0.24	97	34	-0.64	34	607	-1.24	34	607
18	1.16	97	607	-0.19	97	607	-0.01	61	607
19	-0.14	67	67	-0.01	64	64	0.00	61	61
20	-4.85	106	559	-4.52	64	559	-5.44	106	601
21	0.42	601	559	-0.42	601	559	-0.60	601	601
22	-1.76	583	559	-0.26	586	559	-0.32	583	598
23	0.01	583	583	-0.06	583	583	0.42	583	583
24	1.21	592	586	-1.19	592	586	-0.86	592	583
25	0.52	586	562	-0.57	586	562	-0.38	586	559
26	0.34	91	91	-0.07	91	103	0.48	91	103
27	0.13	91	559	-0.66	103	559	-1.42	103	187
28	0.09	610	607	-0.01	139	34	0.06	745	91
29	-0.89	610	79	2.09	103	130	4.07	745	130
30	-0.52	127	130	-2.79	130	130	-5.38	130	130
31	0.01	130	130	-0.01	130	130	0.01	130	130
32	-0.06	196	139	-0.13	139	139	-0.22	745	745
33	-1.12	196	157	-0.12	196	154	0.19	133	154
34	0.04	214	214	-0.20	730	730	-0.16	217	724
35	5.75	154	157	-5.84	154	157	-4.36	199	133
36	2.81	157	130	3.64	157	130	6.85	133	130
37	1.72	148	157	-3.19	148	154	-6.02	148	148
38	0.03	718	160	0.08	715	181	-0.31	715	175
39	-0.08	169	157	0.12	715	160	0.17	715	160
40	0.23	187	727	0.40	727	727	0.44	202	724
41	-0.90	187	559	-0.46	727	547	-0.39	202	202
42	-1.40	205	187	-1.50	205	187	-1.61	544	187
43	0.92	166	718	-0.33	166	730	-0.59	202	715
44	-1.13	718	241	0.44	715	241	0.27	715	241
45	-0.94	718	241	0.11	193	241	0.27	715	202
46	-0.19	178	712	0.47	178	544	0.96	202	544
47	0.32	700	712	-0.04	547	547	0.14	544	544
48	-1.09	697	703	0.20	256	547	0.34	697	544
49	-3.48	706	559	-4.97	532	547	-9.09	532	544
50	0.62	529	559	-0.83	538	559	-1.35	532	553
51	1.36	529	700	-1.51	529	700	-0.35	541	694
52	-0.33	514	559	0.13	514	562	0.15	499	553

TABLE 3.19 Con't.

	Twist			Shear			Scale		
Point	Diff	Obs1	Obs2	Diff	Obs1	Obs2	Diff	Obs1	Obs2
53	3.31	562	514	-3.09	526	514	-1.64	562	520
54	-0.79	697	700	-0.27	547	700	-0.08	544	259
55	-0.69	235	700	-0.15	700	700	0.07	682	238
56	0.31	697	694	-0.76	700	700	0.14	238	259
57	-0.05	256	256	-0.10	256	256	-0.04	259	259
58	0.61	241	241	-0.70	241	358	-0.90	241	367
59	2.38	358	358	-4.50	358	358	-6.05	367	367
60	-1.30	367	310	-0.07	367	409	0.57	367	409
61	-1.13	685	367	-1.72	358	262	-3.86	358	241
62	0.46	685	685	0.29	685	685	0.19	268	268
63	-0.03	700	700	-0.01	700	700	0.00	700	700
64	1.46	358	274	-0.89	358	310	-1.74	358	274
65	-0.16	226	226	-0.22	235	310	-0.06	274	274
66	0.45	358	409	-1.21	358	367	-1.41	367	382
67	-0.41	409	358	-0.11	409	409	0.49	409	409
68	1.85	361	409	0.01	361	382	1.01	361	382
69	2.55	0	382	2.94	0	382	4.27	0	382
70	-2.10	0	394	2.89	0	394	4.64	0	394
71	-0.17	409	409	-0.09	409	394	1.14	409	394
72	2.70	346	409	0.70	340	409	0.21	346	409
73	0.41	409	409	0.46	409	409	0.75	409	409
74	0.70	400	409	0.88	352	409	1.04	352	409
75	4.50	343	358	-2.51	343	358	-3.00	331	358
76	-11.39	331	358	-11.22	331	358	-12.72	331	358
77	5.27	343	307	-4.66	343	334	-3.44	337	325
78	**-25.35**	**334**	**307**	**-27.23**	**334**	**310**	**-37.71**	**334**	**307**
79	-4.84	334	280	-5.09	334	328	-6.98	334	508
80	10.48	283	637	-10.50	283	640	-11.50	412	643
81	0.00	637	637	0.18	640	640	0.07	652	634
82	-1.84	424	658	0.82	427	427	1.10	499	661
83	0.22	646	499	-0.63	646	316	-1.23	646	319
84	0.18	676	676	-0.13	676	310	0.00	676	307
85	0.25	676	676	-0.15	676	274	0.16	676	274
86	0.10	274	235	0.21	274	274	0.60	499	274
87	-4.63	496	226	-4.57	496	499	-4.88	496	499
88	0.85	316	490	-0.54	316	496	0.25	316	496
89	-0.26	427	427	0.44	424	427	0.21	424	661
90	0.34	658	442	-0.28	658	442	-1.85	661	436
91	0.59	490	478	-0.54	490	478	-0.27	490	424
92	-1.55	487	490	-3.07	442	490	-3.88	490	496
93	-0.03	520	496	-0.51	514	235	0.08	520	235
94	7.24	472	514	-9.91	472	514	-9.83	445	235
95	7.47	472	514	-9.67	472	514	-9.90	445	514
96	0.27	466	700	-0.48	463	514	-0.24	466	226
97	-0.55	442	442	-0.75	442	442	-6.00	442	442
98	0.00	442	442	0.07	442	442	0.32	436	436
99	1.13	490	514	-0.16	439	514	0.02	436	436
100	13.95	433	442	-14.45	433	442	-10.66	433	451
101	-2.29	463	514	-2.77	463	514	-4.35	463	514
102	-4.80	463	460	3.78	460	460	8.08	439	463
103	-0.03	466	466	-0.26	463	463	-0.62	466	466
104	-0.93	700	514	-0.42	235	514	-0.35	229	499

TABLE 3.20: Summary statistics of differences in robustness for NFLDGPS network when using observation and modified Delaunay ties (cf. Table 3.19). Note: "mean" denotes average of absolute values of robustness measures. All values in ppm.

	Minimum	Maximum	Mean	St.Dev.
Diff. in Twist	-25.4	14.0	1.8	3.4
Diff. in Shear	-27.2	3.8	1.8	3.6
Diff. in Scale	-37.7	8.1	2.3	4.5

3.4 Discussion

The estimation of strain parameters for irregularly spaced data should be regarded as two separate problems: the selection of the local neighbourhood points used in the strain (gradient) computation at each point, and the method of gradient computation itself. We have investigated only the first problem in this contract, but the second problem should also be examined since both problems are somewhat interlinked.

For the first problem, the conventional approach to selecting a local neighbourhood for strain (i.e., gradient) estimation is to select either the nearest fixed number of points, or all the data within a fixed radius. However, these methods are adversely affected by uneven data distribution (e.g., too few or too many points are often selected). More recently, "Delaunay neighbours" have been used almost exclusively to define local neighbourhoods with much better results. However, as we have seen in our examples, long ties can arise in geodetic networks, especially on the periphery. This situation is not different from the observation-defined neighbourhood, where longer ties from the observations may be also introduced. Such long ties can significantly and adversely affect the computed strain as shown above. One method of reducing the affect of long ties is to use an inverse distance weighting function in the strain computations (see below). The advantage of this approach is that the closer points have the greatest influence on the determination of strain. This can be used with methods that also give a more homogenous distribution of points in the neighbourhood.

Although outside the scope of this contract, there are many ways in which to compute the strain (gradient) of a surface using the selected neighbourhood points (see Watson, 1992, Chapter 2.4). The least squares plane fitting is the most popular and arguably the most reliable approach. It is the method we use in NETAN, mainly due to its low computational requirements. The problem with this method though is that more distant points can excessively influence (smooth) the robustness parameter surfaces as we have already discovered. To avoid this problem, a variety of distance-based weighting schemes may be employed (ibid.). It is strongly recommended to investigate the applicability of these methods for robustness analysis. For example, one simple type of weighting function for the observation-based neighbourhood would be a step function that goes from one to zero at some critical distance, say two times the average length of the observation ties to the point of interest. The median should be used here for the average value because it is less affected by long anomalous ties. Other weighting functions that don't completely omit such long ties should be also investigated, even though they would probably require some additional computational effort.

Higher-order surfaces have also been used, but these are generally not very reliable for unevenly distributed data because exaggerated peaks and valleys can occur as a result of pathological point distributions. Splines may be the most reliable method of avoiding pathological situations, but the computational burden involved is probably too great for application to the robustness analysis of large geodetic networks.

4. CRITERIA FOR THE CLASSIFICATION OF ROBUSTNESS

4.1 Concepts of Precision and Accuracy

Traditionally, errors in observations are classified as being either random or systematic (see Figure 4.1). Random errors are assumed to follow a normal or Gaussian distribution about the true value. Systematic errors, on the other hand, cause a shift or bias of the entire distribution of the random errors (see Figure 4.2). The random observation errors are propagated into the parameter (coordinate) estimates and portrayed in the form of confidence regions which are measures of precision. On the other hand, biases in the observations result in a systematic shift in the estimates of coordinates. The smaller the shift, the more accurate is the solution.

Different combinations of random and systematic errors are illustrated in Figure 4.3, where the dot marks the true value and the ellipse is the confidence ellipse centred at the estimated value. The bias vector is the shift of the estimated value from the true one. The best situation is (1), where the confidence ellipse is small (precise) and centred at the true value (good accuracy); i.e., when there is no bias. The worst case, in terms of precision and accuracy, is (4), where the confidence ellipse is large (imprecise) and shifted far from the true value (inaccurate); i.e., the bias vector is large. However, the most potentially dangerous case is (3), where the confidence region is small (precise) but shifted far from the true value (inaccurate). Clearly, using only a precision estimate (confidence ellipse) to represent the acceptable error would lead to an incorrect conclusion in this case. This could be very dangerous in a very real sense if, e.g., the dots represented land mines and accuracy and precision represent the user's error in estimating the positions of the mines. Using only precision estimates would lead to a false sense of security as to where the mines are actually located.

Biases are traditionally detected using statistical test for outliers among the estimated observation residuals as described in Vaníček and Krakiwsky (1986, pp.237-239). With this test it is possible to commit two kinds of errors. Rejecting an unbiased observation as one that is biased is called a Type I error. The probability of such an error is α, called the significance level, and the probability of correctly accepting an unbiased observation is $1-\alpha$, called the confidence level. On the other hand, accepting a biased observation as an unbiased one is called a Type II error. The probability of this error is β and the probability of correctly rejecting such biased observations is $1-\beta$, referred to as the "power of the (outlier) test". These probabilities are illustrated in Figure 4.2.

Clearly, there is a need to quantify the maximum size of potential observation bias that is not detectable by the outlier tests for a given network design. This quantification is related to the "strength" of the network: the stronger the network the smaller the maximum undetectable bias becomes, while the weaker the network the larger it becomes. The resulting maximum undetectable potential coordinate biases can thus be used as a measure of the strength of the network, or of the accuracy of the given solution for the coordinates. This quantification can be done in terms of reliability or robustness measures such as distortions in orientation, shape and scale (Vaníček et al., 1993). Other alternatives are discussed later in this Chapter.

It is important to emphasize that in practice one does not know if any observation biases are actually present. Through the use of reliability and robustness analysis it is only possible to provide a measure of the maximum size of any potential observation bias that may be undetectable by the outlier tests on the observation residuals (cf. Vaníček et al., 1990).

The values to use for α and β are not easy to define. The problems associated with this issue are discussed in Krakiwsky et al.(1994). Clearly, a network that has to support a litigation for

detecting a possible movement of points would require high levels of both confidence and power, while say a control network for photogrammetry need not have such high levels. Note that higher confidence and power levels would lead to a larger noncentrality parameter and thus require better network design and redundancy to achieve the same accuracy. This in turn leads to higher costs that may render the survey uneconomical. Thus, the particular selection of the confidence and power levels are left up to the professional judgment of the geodesist; they clearly must relate to the particular context within which the coordinates are to be used.

The related issue of out-of-context and in-context testing and confidence regions for both the observations and parameters have been reported upon in Krakiwsky et al. (1994). Only the salient features are discussed within this report as they relate to the issue of classification criteria.

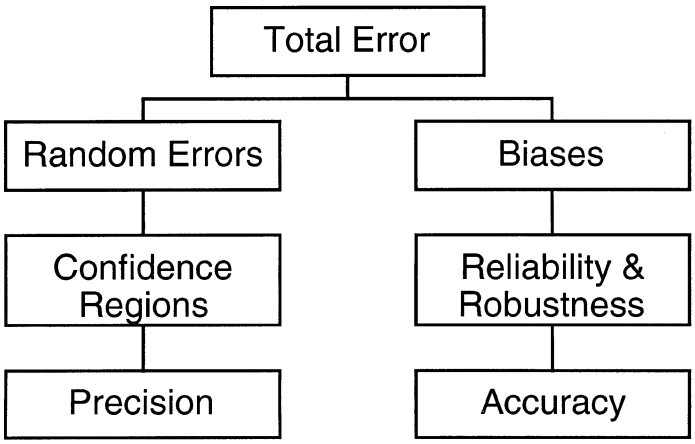

FIGURE 4.1: Classification of total error in terms of random errors and biases.

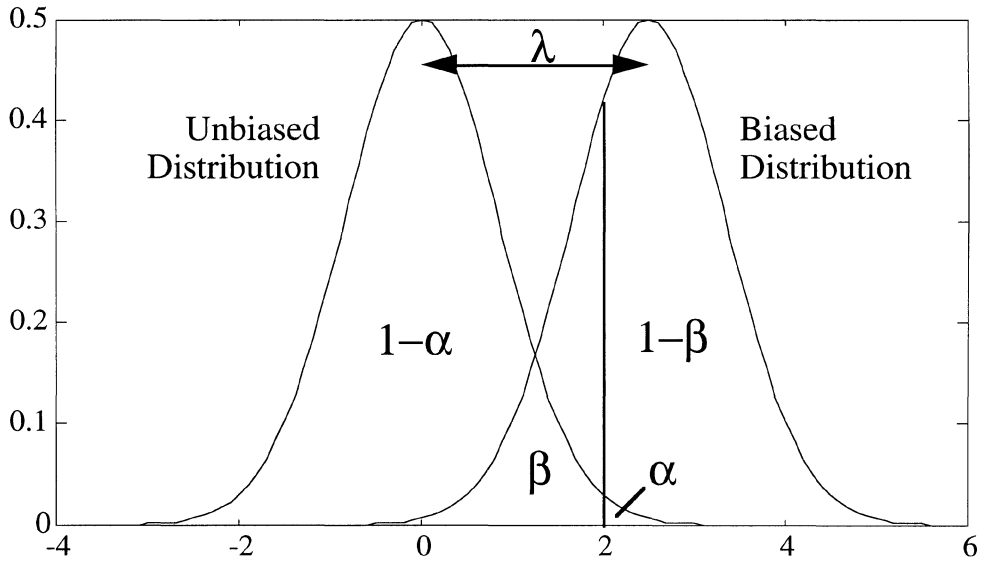

FIGURE 4.2: Unbiased and biased error distributions and probability levels.

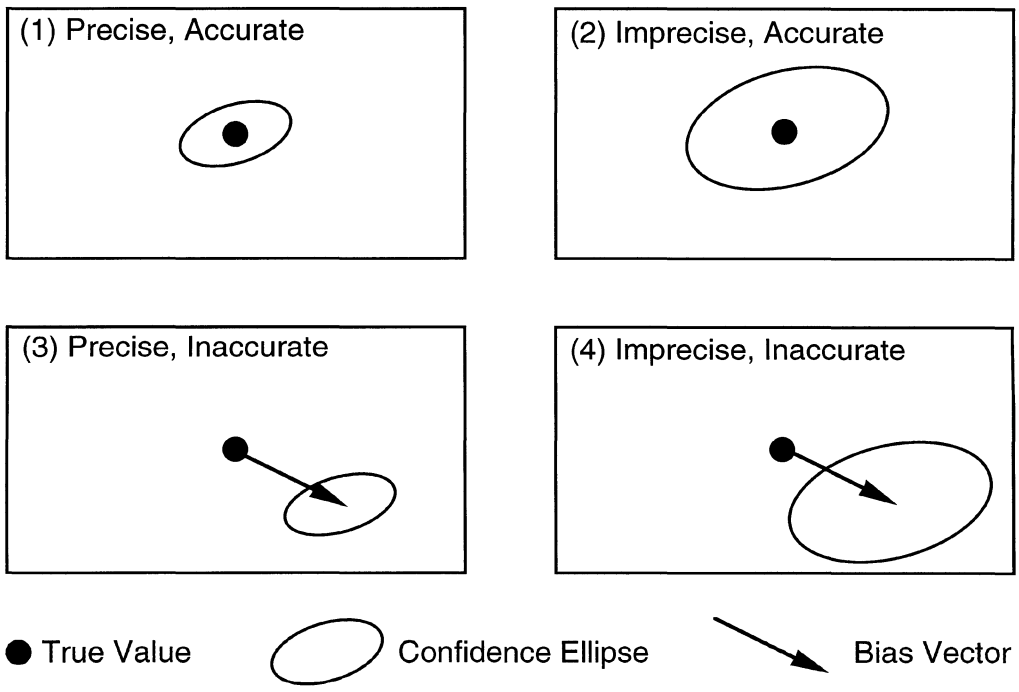

FIGURE 4.3: Illustrations of different combinations of precision and accuracy.

4.2 Characterization of Precision (Random Errors)

Although not explicitly part of the present contract, we have also reviewed and examined the methods of characterizing and classifying precision measures. The purpose here is to try to use analogous measures for accuracy whenever possible, or vice versa. This will provide a consistent approach for both precision and accuracy which hopefully users will find easier to comprehend.

In the traditional treatment of random errors, confidence regions (intervals, ellipses and ellipsoids) are widely used in assessing and classifying the precision of a set of determined coordinates. Confidence regions can be computed in an absolute sense for the positions of points in a network (absolute confidence regions) or in a relative sense for the position differences between pairs of points (relative confidence regions). The confidence regions are obtained from the covariance matrix of the least squares estimates for the coordinates.

Any measure of precision should ideally be independent of the choice of minimum constraints (datum) used in the solution. This makes classification and inter-comparison possible as the measures would be free of subjective definitions of the choice of datum. The problem is that some precision measures are inherently datum dependent. This issue will be discussed for each of the proposed measures.

In this discussion of classification of precision, it is assumed that each point is taken out-of-context of any others in the network. If it is required to classify a set of points simultaneously, then the confidence regions should be computed using the in-context significance level. This applies to both absolute and relative confidence regions. For more information on in-context testing, see Vaníček and Krakiwsky (1986, pp.229-231,240-241) and Krakiwsky et al.(1994).

Finally, it is important to emphasize that these measures represent only random errors or precision. They do not provide any information about the presence of biases or blunders in the observations. They therefore cannot be used to guarantee the accuracy or total repeatability of the results.

Measures of Absolute Precision

In 1D (vertical) positioning the precision of an estimated position is defined by a absolute confidence interval, in 2D (horizontal) positioning by an absolute confidence ellipse, and in 3D positioning by an absolute confidence ellipsoid. In the sequel, we shall concentrate on the 2D case only, as the 2D (horizontal) networks are the ones we are supposed to deal with in this report. The confidence region defines the region within which the true position is expected to fall with a specified level of probability (confidence level). This assumes that all observations are free of blunders and systematic errors; i.e., that only random errors exist in the observations. Figure 4.4 depicts an absolute confidence ellipse with major semi-axis of length a and azimuth α (not to be confused with the confidence level α), and minor semi-axis of length b. The size and orientation of confidence regions are affected by the precision of the measurements (encoded in the observation covariance matrix), design of the network (e.g., total number, type and the number of redundant of observations), and chosen confidence level. A solution is called acceptably precise if its confidence region (major semi-axis) lies fully within the specified acceptable tolerance at the required confidence level.

The problem with such absolute measures of precision is that they are inherently datum dependent, i.e., their values depend on the chosen datum constraints. Here we refer to the sizes of the absolute confidence regions, which depend not only on the definition of the scale, but also on the choice of the point held fixed in the adjustment. Although datum independent measures should be preferred over those that are not, the exception may be acceptable in cases where the datum

definition is well established and does not change from adjustment to adjustment. An example of such a case may be network integration using weighted constraints (weighted positions of the known points) which inherently represent the fixed datum of the higher-order network. All absolute measures would then refer to the same higher-order datum constraints, thereby allowing for inter-comparison and classification of precision among all solutions based on the same datum definition.

Measures of Relative Precision

If one is interested in the relative precision between pairs of points, then relative confidence regions corresponding to coordinate differences need to be computed. A relative confidence region is a direct function of the covariance sub-matrix pertaining to the pair of points of interest. From the covariance sub-matrix of the two points, the relative confidence region can be computed in a similar way as an absolute confidence region is computed from the covariance sub-matrix of the single point of interest.

Individual Relative Confidence Region between Points. Traditionally, relative precision is classified in terms of the length of the semi-major axis of the relative confidence region for each pair of points. However, this may be impractical for large networks as it calls for too much information that cannot be presented in an easily digestible form. What is needed in these cases, especially for classification purposes, are measures that characterize the relative precision in the local neighbourhood around each point. A variety of mainly ad hoc methods have been used to achieve this. All are concerned with determining some representative measure characterizing the relative confidence regions in the neighbourhood of the point of interest.

The neighbourhood of a point can also be defined in different ways. We have already discussed some of the more popular methods in Chapter 3 in the context of an application to robustness analysis. Exactly the same methods can be applied equally well here too. The most common definitions of a neighbourhood in practice include the n-closest points, all points within a circle centered on the point of interest, all points directly connected by observations, as well as various combinations of these. In addition, the neighbourhood should also be restricted to the highest hierarchy of the network to which the point belongs. This is discussed further in the next section.

Maximum Relative Confidence Region at a Point. The simplest measure to use here is the largest major semi-axis length of the relative confidence regions between the point of interest and all the others in the neighbourhood. However, this only provides a measure of the worst case precision and may not be suitable for general classification purposes.

Average Relative Confidence Region at a Point. An average measure of relative precision in the neighbourhood of each point may be a better choice for classification. Most such measures are based on some kind of averaging of the lengths of the major semi-axes of relative confidence regions. The average measures can be represented in a variety of ways. For example, Papo and Stelzer (1985) have used the mean of the relative precision in scale and orientation at the point of interest with respect to the others in the neighbourhood. The precision in scale is defined as the random error along a connecting line (divided by distance) while the precision in orientation is defined as the random error perpendicular to the connecting line (divided by distance and converted to angular units). The neighbourhood is defined as a circle with its radius equal to the average inter-station distance for the entire network. Alternatively, other approaches, such as those discussed in the next section in the context of classifying biases, can be used equally well here. These include the mean, median, linear trend with respect to distance, and surface fitting (see the next section).

Note that a popular method of representing the size of a relative confidence region is to express it as the relative error in the interstation distance, which can also be viewed as the strain in the

connection between the two points. However, this implicitly assumes there is no constant observational error present. For many networks established with modern positioning systems, such as GPS, this does not correctly reflect the actual propagation of error which contains both constant and distance-dependent components. If both constant and distance dependent errors are present in the observation tie between the two points then the relative error between the two points must also have both a constant component and another inversely proportionate to the distance.

The relative precision measures discussed above may or may not be independent of the choice of minimum constraints (datum) used in the adjustment. For example, the direction of the vector representing the major semi-axis is datum dependent; it depends on the location of the fixed point and the orientation constraint. Consequently, most analysts use the length of the major semi-axis of the relative confidence region, which depends only on the definition of scale. If a minimum constraint adjustment is employed (as we always assume), then the scale is provided by the observations themselves (e.g., distances) and the length of the major axis is datum independent, as are those measures derived from it.

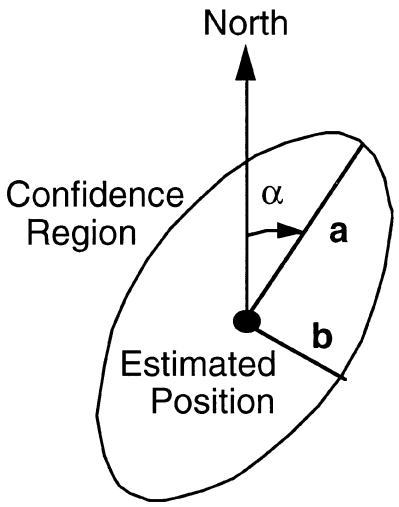

Figure 4.4: Absolute confidence ellipse representing precision of an estimated position.

4.3 Characterization of Accuracy (Biases)

If an undetectable systematic error or bias exists in an observation, the estimated position will be biased, i.e., the position will be shifted from the correct one as illustrated in Figure 4.5. The objective of this section is to identify possible ways of quantifying such potential biases that could remain undetectable. As well, the conditions for and circumstances under which the discussed quantifiers should be used is discussed.

The quantification of the maximum size of bias that cannot be detected in a given network is synonymous with the quantification of strength or robustness of the solution. The smaller the robustness measure the stronger the solution in terms of detecting potential biases and the greater the likelihood that the biased (shifted) solution will still be within some required specified tolerance limit.

As for the precision measures, accuracy measures should also be datum independent whenever possible in order to allow us to make an objective classification. However, the problem is again that absolute measures are inherently datum dependent, being dependent on the chosen datum constraints. On the other hand, some measures of relative accuracy are datum independent and should be preferred over those that are not. The only exception may be in cases where the datum definition does not change, such as the example of network integration discussed in the previous section in the context of random errors.

Whenever possible, we attempt to parallel the treatment traditionally used in characterizing random errors, namely, the use of absolute (point) and relative precision measures. The approach suggested here is to use some simple measures for general classification and more meaningful measures, such as scale, shear and twist robustness discussed in chapters 2 and 3, for detailed pre- and post-analyses. For the classification of precision only the maximum size of the absolute and relative regions in some area are generally used as we have discussed above. For the classification of accuracy we will be looking for analogous measures to represent the absolute and relative accuracy. Specifically, we will seek a single measure representing the maximum possible deformation in both absolute and relative senses. We believe that such an approach would be essential if the majority of users are to easily and properly understand accuracy classification.

Measures of Absolute Accuracy

Absolute accuracy may be represented by the potential coordinate bias vector at each point in the network. Such bias vectors are caused by the maximum potential undetectable biases in observations. In Baarda's terminology used in his theory of reliability, the maximum undetectable bias (or minimally detectable blunder) represents the "internal reliability" of the network. Its interpretation is the largest potential measurement bias that can be detected through the statistical outlier testing of the estimated residuals at a specified confidence level. In other words, if one makes an error in a given measurement which is slightly smaller than the maximum potential bias, there is a β-level probability that it will not be detected in the outlier testing and thus will remain in the solution and bias the estimated coordinates.

In Baarda's terminology, the resulting vectors of coordinate biases for each potential observation bias represents the "external reliability" of the network. This results in a set of n potential coordinate bias vectors at each point in the network, where n is the total number of observations. Clearly, it would be impractical to present all these values to the user. The conventional way of dealing with this preponderance of information in reliability theory is to use one quadratic form of all the point bias vectors in the network produced by a single potential observation bias. This gives n quadratic forms, one for each of the n observation biases. (We note that this treatment should

not be understood as being statistically equivalent to the formally similar treatment of observation residuals, or coordinate differences because there exists no statistical interpretation for these external reliability quadratic forms.) This is often referred to as the global external reliability measure. However, we concentrate here on obtaining values of accuracy measures for each point in the network, which are needed for point classification purpose.

The simplest method of providing a single point measure of absolute accuracy, is to take the magnitude of the largest bias vector at each point, noting which observation biases are responsible for them. In terms of reliability theory, this might be referred to as the maximum local external reliability. It represents the largest potential bias at the point, in the same way that the maximum size (i.e., the major semi-axis) of confidence regions are used to represent point precision. Unfortunately, this quantity is dependent on the choice of datum constraints; specifically, on the choice of orientation and fixed point. On the other hand, it is independent of datum scale for all practical purposes (i.e., a small scale error times a small bias vector is an insignificantly small vector). One might also consider using as a measure the average of the magnitudes of the bias vectors at each point. However, for classification purposes it is usually more desirable to use the worst case measures instead (i.e., the maximum magnitude). This is analogous to the treatment of random errors where we use the major semi-axis instead of, say, the average of the major and minor semi-axes.

Measures of Relative Accuracy

Measures of relative accuracy can be represented by the potential relative bias vector which is defined as the potential bias in the coordinate difference vector between a pair of points. It is evaluated by taking the vector difference between the absolute bias vectors for the two points, i.e.,

$$\Delta\nabla\mathbf{x}(\nabla l)_{ij} = \nabla\mathbf{x}(\nabla l)_j - \nabla\mathbf{x}(\nabla l)_i ,$$

where $\nabla\mathbf{x}(\nabla l)$ are the bias vectors at each point i and j produced by observation bias ∇l. Only the magnitude of $\Delta\nabla\mathbf{x}$ would normally be needed for classification purposes.

As for relative confidence regions, there will be a total of m(m+1)/2 possible (unique) relative bias vectors among the m points in the network for each of the potential observation bias. Thus, for n observation biases there will be a total of n m(m+1)/2 possible relative bias vectors, which would be very difficult to analyse.

Maximum Individual Relative Coordinate Bias between Points. As in the absolute case, the preponderance of relative bias vectors can be reduced by using, for each pair of points, only the largest of the relative biases vectors produced by the potential observation biases. This maximum bias vector for a pair of points is thus defined by

$$(\Delta\nabla\mathbf{x}_{max})_{ij} = \max_{k=1,..n}(\Delta\nabla\mathbf{x}(\nabla l_k)_{ij}) .$$

There is a total of m(m+1)/2 such maximum relative bias vectors for all possible pairs of points. Only the magnitude of this measure would be needed for classification purposes.

For large networks this measure still produces too much information that is not easy to analyse. Moreover, in large networks, there is usually no need to check the relative bias between points that are far apart, because in this case the relative biases behave more like absolute biases.

Maximum Relative Coordinate Bias at a Point. To make the relative bias information more manageable, a representative measure for the neighbourhood around each point is needed. This can be obtained from the maximum relative bias vectors $|\Delta\nabla\mathbf{x}_{max}|$ from the point of concern to the others in the neighbourhood, i.e.,

$$(\Delta\nabla\mathbf{x}_{max})_i = \max_{j \text{ in the neighbourhood of } i}[\ (\Delta\nabla\mathbf{x}_{max})_{ij}\ ] .$$

Note that we are considering here only the maximum relative bias vector $(\Delta\nabla\mathbf{x}_{max})_{ij}$ between each pair of points, i.e., the largest of the relative bias vectors produced by each of the n observation biases. For classification purposes, only the magnitude of this measure would be needed.

This measure is analogous to the maximum relative confidence region in the neighbourhood about a point. It gives a worst case measure of relative accuracy which may be suitable for ensuring that some specified accuracy level is achieved. It is also independent of the chosen datum and only weakly dependent on scale.

Average Relative Coordinate Bias at a Point. In some situations it may be desirable to characterize the typical relative accuracy for the neighbourhood of a point. In this case, an average measure of the magnitudes of the maximum relative bias vectors to all points in the neighbourhood can be used instead of the maximum defined above; i.e.,

$$|\Delta\nabla\mathbf{x}_{ave}|_i = \text{ave}_{j \text{ in the neighbourhood of } i}[\ |\Delta\nabla\mathbf{x}_{max}|_{ij}\ ] ,$$

where "ave" represents some kind of averaging function and $|\bullet|$ is the absolute value.

There are a variety of different averaging functions, including the mean, median, linear trend with respect to distance, and surface fitting. The median is a robust estimator of the mean, which makes it insensitive to outlier values in the neighbourhood that may have a very large or very small (anomalous) relative biases. A linear trend can also be used to model the lengths of the average relative bias vectors in the neighbourhood of a point in terms of constant and distance-dependent components. Surface fitting is similar to the linear trend method, but also takes into account the horizontal distribution of the magnitudes of the relative biases in the neighbourhood. The value of the surface and it largest maximum gradient at the point of interest can be used to represent its average constant and distance-dependent components. Robust estimators of the linear trend and surface can also be used. All of these measures are based on the magnitudes of the relative bias vectors which, for all practical purposes, are independent of the chosen datum constraints.

Robustness Analysis. The robustness analysis technique (Vaníček et al., 1990) is also based on plane fitting but uses separate planes for each coordinate component. The gradients of these planes are converted to strain measures to provide a detailed analysis of the kind of network deformation caused by the observation biases. The most common measures of strain are the ones used the NETAN program that we have dealt with already in chapters 2 and 3. The principal axes of the strain ellipse can also be used in place of shear and dilatation. For classification, however, it may only be necessary to use the average differential rotation and the maximum principal strain (largest axis of the strain ellipse). Reducing this information to one single measure of maximum deformation is a more difficult proposition. One possibility may be to simply use the maximum gradient of the plane for each coordinate bias component. A single measure of the maximum gradient for all coordinate components could be obtained by taking the geometical mean (vector length) of the maximum gradients for each coordinate component. We should re-iterate here that, although the individual components of the relative bias vectors are datum dependent, the strain measures are not.

Discussion

For classification purposes, what is needed is a single measure of the absolute and relative accuracy at each point in terms of the maximum deformation caused by the potential observation biases. The maximum relative coordinate bias in the neighbourhood of each point is probably the best choice in this case because it provides a worst-case measure and is easy to compute.

Nevertheless, systematic comparisons of the different measures should be done before deciding on one for classification purposes. For more descriptive measures, the robustness technique should be used.

As in the random error case, one problem that needs to be addressed is how to define the neighbourhood for each point. This has been discussed already in chapter 3 above. The neighbourhood should also be restricted to the highest hierarchy of network to which the point belongs. Otherwise lower order neighbourhood points will cause the point of interest (of a higher order) to appear to have lower precision and accuracy. The advantage of using observation ties to define the neighbourhood is that this approach relates directly to how the points were established and will avoid using points from different Helmert blocks in a single local neighbourhood. As discussed in the Introduction, this approach may not be suitable, however, if long VLBI or GPS ties are used as they tend to smooth (average) out the information across the network. The inverse-distance weighting scheme suggested in chapter 3 may help here as well. Whatever method is used must also be practical for the use on the entire national network. Two alternative methods of dealing with this problem are described in chapter 2 and they would be equally applicable here. In any case, processing time is probably of not much concern if the analysis only needs to be done once or twice.

Finally, it is again emphasized that one must be cognizant of those measures that are datum (for adjustment) independent and those which are not. Absolute measures are inherently datum dependent, while relative measures may or may not be. In order to have a universal standard for the classification of networks, the relative measures should not depend upon the particular datum used. Otherwise it would make impossible to objectively compare various networks with different datum constraints. On the other hand, when working within the same minimum constraints for the adjustment (e.g., Canadian national network), and having the requirement that the new points are to be integrated into the existing adjusted network, then the use of datum dependent measures may be justified in the absence of datum independent measure.

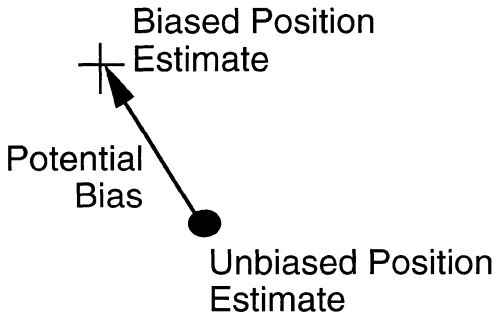

Figure 4.5: Potential bias vector representing accuracy of an estimated position.

4.4 Joint Characterization of Precision and Accuracy

A user of positions usually specifies the required positioning precision and accuracy in terms of a circle (or a sphere in a 3D case) with a specified radius. This value is generally understood by the user as representing both precision and accuracy (i.e., the total error). Geodesists, on the other hand, have traditionally interpreted this as representing only precision where the specified circle is centred at the solution for the coordinates and the confidence ellipse must reside wholly within it to meet the specifications. Clearly this approach does not take into account the presence of systematic errors; i.e., it does not consider the accuracy of the solution at all.

To meet the practical requirement, one should treat both precision and accuracy simultaneously (jointly). We have not found the definitive solution of how jointly to treat precision and accuracy, if any such a solution even exists; what is presented here is only exploratory in nature.

Let us begin by examining the situation when a the solution for the coordinates is potentially biased by a (potential) bias in an observation. First, the confidence region (ellipse in Figure 4.6) shifts to the end of the bias vector: as usual it is centred at the estimated position (coordinates). Secondly, the true coordinates are understood to be at the base of the bias vector. This means that for the user requirement to be met (jointly in precision and accuracy) at any point, one must consider all potential coordinate bias vectors (due to all potential observation biases) together with the error ellipse as shown in Figure 4.6. Clearly, this joint view is somewhat more pessimistic than viewing precision and accuracy separately.

In this joint approach, the total error (bias plus random error) must be examined, rather than considering only the largest bias or only the random error (ellipse). One possibility is to take the radius of the smallest circle that encloses all of the shifted (biased) confidence regions caused by the potential observation biases, i.e., the worst scenario case. This might be more simply represented by the vector sum of the potential bias vector and a vector in the confidence region major semi-axis (see Figure 4.6). Care must be taken to ensure that the direction of the semi-axis (one of two possibilities) is chosen so that the total vector is maximized. Then the magnitude of the largest of these total error vectors for all potential observation biases can be used to represent the measure of the worst total error in the estimated position. Although more work must be done on the joint approach, it appears to be quite promising; it has been used already by one of the authors in the context of GPS kinematic positioning (Abousalem et al., 1994). We have to utter a word of caution here, however: so defined a total error is not datum independent.

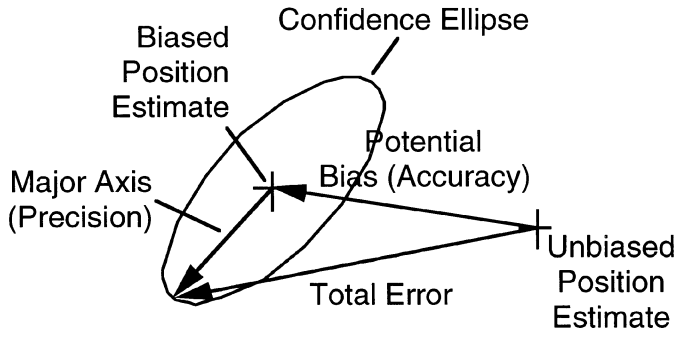

Figure 4.6: Joint characterization of precision and accuracy for an estimated position.

5. CONCLUSIONS AND RECOMMENDATIONS

In this report we have addressed three more or less independent problems: finding a more economical algorithm for searching for the most influential observations (Chapter 2), finding a more satisfactory definition of the neighborhood in which strain measures are evaluated (Chapter 3) and finding a technique for network classification that would take into account both the precision (random error contribution) and accuracy (potential systematic error or bias contribution) of station positions in geodetic networks. Each of these three topics is discussed separately.

5.1 Search for Most Influential Observations

We have conceived and tested the performance of two basically different algorithms which we initially considered equally hopeful. The first algorithm is based on our past experience with robustness analysis that the most influential observation is never too far removed from the point of interest. We have thus limited the search for the most influential observation to those observations that are between points connected with the point of interest by only a few observation ties. Numerical testing with 4 different networks has shown that a search limited to observations that are no more than 3 levels of observation connections from the point of interest yields practically identical results with the algorithm that searches all the observations in the network as far as robustness in scale and shape are concerned. Differences in the performance of these two algorithms may occur in networks with pathological design, however. Such pathological case will require a special treatment in any case, so the possible difference would be inconsequential. Values of the robustness in twist obtained from the "3rd level search" are, however, generally different than those obtained from the complete search for the reason described in Chapter 2. The "3rd level search" algorithm shows a substantial computer time saving as required; the saving is the more significant the larger is the network.

The other algorithm we have tested is based on the a posteriori correlations between point coordinates. The most influential observations are sought amongst the observations linking together points whose coordinates are correlated with the coordinates of the point of interest at a level higher than a prescribed threshold. This algorithm works fine when the appropriate threshold is known and usually as fast as the "3rd level search" algorithm. The problem is that the threshold value changes from network to network and some numerical experimentation is needed to establish the value for any new network. This flaw renders the second algorithm almost useless.

Our conclusion is that the "3rd level search" algorithm satisfies the aim of our investigation and it is this algorithm that we recommend be used routinely in robustness analysis. The way the robustness in twist depends on the adjustment datum definition should be further studied to determine if the degree of dependence is detrimental to the whole analysis.

5.2 Definition of Neighbourhood for Strain Computation

To avoid the recognized problem of unjustified strain smoothing caused by long observation ties—when the neighbourhood is defined through observation ties—we have tested an alternative neighborhood definition based on Delaunay triangulation. Numerical testing with several different networks have shown that Delaunay triangulation has problems of its own. The standard Delaunay triangulation algorithm always produces a convex boundary (hull) which often results in long triangles along the edges of the network, creating unwarranted long ties and a strain smoothing effect not unlike the one we set out to eliminate. Even a manual elimination of the long edge triangles does not bring much improvement as irregular network geometries produce similar long triangles even well within the network. We have thus concluded that the neighbourhood definition based on Delaunay triangulation is not a very helpful alternative to the original definition.

We now think that the most hopeful way of abating the unwanted effect of the long observation ties would be to use some appropriate weighting scheme when the planes for strain computation are fitted to the virtual coordinate displacements in the neighbourhood defined by observation ties. One possibility that should be definitely considered is to use weights inversely proportional to the distance from the point of interest. Another possibility that should be investigated, is to use "cut-off weights", where points within a distance equal to one half of the longest observational tie are given a weight equal to 1 and the other points a weight equal to 0. These schemes were not yet tested by us.

5.3 Classification of Networks According to Their Robustness

When realizing that robustness quantifies potential biases (systematic errors) it is not difficult to see that robustness is really a measure—really a conglomerate of 3 measures for scale, shape and twist—of the accuracy of the analysed network. This is indeed the complementary measure to the precision measure as quantified by the commonly used confidence regions (error ellipses) which reflect the potential effect of random errors on adjusted positions. Both these measures are equally important from the point of view of the user of positions, who probably does not care just where the errors are coming from as long as s/he knows that they are present and that they amount to a specific uncertainty. Thus the obvious remedy seems to be to give the user the total effect of both the accuracy and the precision, the effect that reflects the total error composed of the potential bias and the random error. It is probably this total effect that should be the basis of a modern network classification scheme and it is this total effect that we have tried to address in this report.

The problem with computing the total effect is that the accuracy and precision measures, as they are used now, cannot be simply added together. To understand the underlying problem let us discuss separately the point effects—sometimes called absolute effects—and the relative effects. With the precision measures, these two approaches correspond to the absolute and relative confidence regions. With the accuracy measures, the two approaches correspond to Baarda's "local or point external reliability" measure (a multitude of virtual displacement, or potential bias, vectors at the point) and robustness (the relative measure), respectively. While the absolute measures are intrinsically datum (adjustment) dependent, the relative measures are practically datum independent.

For the point measures one can take any of the potential bias vectors and center the absolute confidence ellipse at the tip of this vector. Every one of the vectors will give a different configuration. The open question is: "which of the vectors should be selected"? One possibility is to represent the confidence ellipse also by a vector coincident with its major semi-axis and add these two vectors together. This can be done for all the potential bias vectors to give us as many vector sums as there are observations. From these we may select either the largest, the average, the median, etc., as being the representative value for the point.

For the relative measures a similar scenario can be suggested, where instead of the n potential bias vectors at a point we consider the n sets of differences of the potential bias vectors for each pair of points and instead of the absolute confidence ellipse we consider the relative confidence ellipse. This assumes that only one observation bias is considered at a time; i.e., that each set of coordinate bias vector differences is determined for only one observation bias at a time.

We note that while the confidence regions are associated with a specific confidence level $1-\alpha$, the virtual displacement vectors are associated with a probability level β. Both these probability levels have to be selected beforehand to get any numerical results. While the selection of the confidence level has been very extensively studied and a standard selection of 95% has been well established, the selection of a standard value of β is still a rather open question.

Finally, we must address the question as to where does the robustness fit into a scheme for classifying the accuracy of adjusted positions in geodetic networks. We have come to the conclusion that for classification purposes, a more simple approach, such as the combined precision/accuracy measure described above, would be more appropriate. On the other hand, robustness analysis would have its place in analysing networks. If this distinction is not acceptable, than there is certainly no problem in defining appropriate thresholds for the 3 robustness measures to be used for classification purposes if the appropriate value of β can be selected (Krakiwsky et al., 1994). Then the a network would be classified separately in precision, robustness in scale, robustness in shape and robustness in twist, where the precision classification would be based on relative confidence regions. Alternatively, the 3 robustness measures could be lumped together in one of the many possible ways and one threshold value used for the lump sum. However, in this approach a network would still have different classifications in precision and in accuracy.

REFERENCES

Abousalem, M.A., J.F. McLellan, E.J. Krakiwksy (1994). A new technique for quality control in GPS kinematic positioning. *Proceedings of the IEEE 1994 Position, Location and Navigation Symposium*, Las Vegas, NV, pp.621-628.

Craymer, M.R., A. Tarvydas, P. Vaníček (1987). NETAN: A Program Package for the Interactive Covariance, Strain and Strength Analysis of Networks. Geodetic Survey of Canada Contract Report 88-003, May.

Gold, C.M. (1989). Surface interpolation, spatial adjacency and GIS. In *Three Dimensional Applications in Geographical Information Systems*, J. Raper, ed., Taylor & Francis, New York.

Joe, B. (1991). Construction of three-dimensional Delaunay triangulations using local transformations. *Computer Aided Geometric Design*, Vol. 8, pp. 123-142.

Krakiwsky, E.J., P. Vaníček, D. Szabo (1993). Further Development and Testing of Robustness Analysis. Geodetic Survey of Canada Contract Report 93-001, March.

Krakiwsky, E.J., D. Szabo, P. Vaníček, M. Craymer (1994). Development and Testing of In-Context Confidence Regions for Geodetic Survey Networks. Geodetic Survey of Canada Contract Report, March, April.

Morgan, M.A. (1967). Hardware models in geography. In *Models in Geography*, R.J. Chorley and P. Haggett, ed., Methuen, London.

Papo, H.B. and D. Stelzer (1985). Relative error analysis of geodetic networks. *Journal of Surveying Engineering*, Vol. 111, No. 2.

Sloan, S.W. (1987). A fast algorithm for constructing Delaunay triangulations in the plane. *Advances in Engineering Software*, Vol. 9, No. 1, pp. 34-55.

Vaníček, P., E.J. Krakiwsky, M.R. Craymer, Y. Gao and P. Ong (1990). Robustness Analysis. Geodetic Survey of Canada Contract Report 91-002, November.

Watson, D.F. (1992). *Contouring: A Guide to the Analysis and Display of Spatial Data.* Pergamon Press, New York.